

PDF hosted at the Radboud Repository of the Radboud University Nijmegen

The following full text is a publisher's version.

For additional information about this publication click this link.

<http://hdl.handle.net/2066/113863>

Please be advised that this information was generated on 2017-03-14 and may be subject to change.

4074

**ENERGY REDISTRIBUTION
IN
PHOTOEXCITED MOLECULES**

Paul Uijt de Haag

**ENERGY REDISTRIBUTION
IN
PHOTOEXCITED MOLECULES**

ENERGY REDISTRIBUTION IN PHOTOEXCITED MOLECULES

EEN WETENSCHAPPELIJKE PROEVE OP HET GEBIED VAN
DE NATUURWETENSCHAPPEN

PROEFSCHRIFT

TER VERKRIJGING VAN DE GRAAD VAN DOCTOR
AAN DE KATHOLIEKE UNIVERSITEIT TE NIJMEGEN,
VOLGENS BESLUIT VAN HET COLLEGE VAN DECANEN
IN HET OPENBAAR TE VERDEDIGEN
OP DONDERDAG 22 NOVEMBER 1990,
DES NAMIDDAGS TE 1.30 UUR PRECIES

door

PAULUS ANTONIUS MARIA UIJT DE HAAG

geboren op 28 december 1960
te Utrecht



1990
Offsetdrukkerij Haveka B.V.,
Alblasserdam

Promotor : Prof. Dr. J. Reuss

Co-promotor : Dr. W.L. Meerts

Gaarne wil ik op deze plaats allen danken die direct of indirect een bijdrage hebben geleverd aan het tot stand komen van dit proefschrift. In het bijzonder wil ik hierbij noemen:

alle (oud-) medewerkers van de afdeling Molekuul- en Laserfysika

Cor Sikkens, John Holtkamp, Frans van Rijn en Eugene van Leeuwen voor de hulp op technisch gebied

Annet van der Heijden voor haar hulp bij het bewerken van de tekst

Willy van Herpen en Johannes Heinze voor de vele nuttige discussies en de experimentele bijdragen

de medewerkers van de verschillende dienstverlenende afdelingen, met name dhr J. Peters voor het vervaardigen van de meeste tekeningen

Maarten Ebben, Rudie Spooren, Marcel Drabbels en Michel Versluis voor hun bijdragen aan de verschillende experimenten

Joop Konings, Lex Sewuster en Erik Zwart met wie ik de kamer heb gedeeld gedurende deze jaren

Finally I like to thank Jon Hougen for his contributions in the interpretation of the spectra and especially for his very stimulating enthusiasm

Contents

1	Introduction	9
1.1	Past, present and future: an absorption spectrum	11
1.2	Experimental set-up	13
	References	16
2	Study of dark states in naphthalene, pyrimidine and pyrazine by detection of phosphorescence after UV laser excitation	18
2.1	Introduction	19
2.2	Experimental	21
2.3	Results	23
	2.3.1 Naphthalene	23
	2.3.2 Pyrazine and pyrimidine	26
2.4	Discussion	28
	References	31
3	Vibrational and rotational effects on the intersystem crossing in pyrazine and pyrimidine	33
3.1	Introduction	34
3.2	Experimental	35
3.3	Results and Analysis	35
	3.3.1 Pyrimidine	35
	3.3.2 Pyrazine	41
3.4	Discussion	43
	References	47
4	Rotational assignments in the $S_1(^1B_{3u})$ state of pyrazine by UV-UV pump-probe laser spectroscopy	49
4.1	Introduction	50
4.2	Experimental	50
4.3	Results and Discussion	52
	References	55
5	A study of the $S_1 6^1(^1A_2'')$ vibronically excited state of sym-triazine by high resolution UV laser spectroscopy	56
5.1	Introduction	57
5.2	Experimental	58
5.3	Results and Analysis	60
	5.3.1 High resolution experiment	60

5.3.2	Life time measurements	69
5.4	Discussion	70
	Appendix: A simple theory of molecular eigenstates	73
	References	75
6	Internal rotation in 1,4-dimethylnaphthalene studied by high resolution laser spectroscopy	77
6.1	Introduction	78
6.2	Experimental	79
6.3	Results and asymmetric rotor analysis	79
6.4	Internal rotation analysis	83
6.5	Summary and conclusion	89
	References	91
	Samenvatting	92
	Curriculum Vitae	95

Chapter 1

Introduction

Atomic and molecular spectroscopy is based on the interaction between electromagnetic radiation and matter, like absorption or scattering. The absorption of a photon in an atom involves a change in the electron configuration of the atom. After absorption the atom is in an (photo-) excited state. However, an excited atom is not able to hold the excess energy. The surplus of energy is released by fluorescence: the emission of photons. On this principle the laser induced fluorescence technique is founded: the fluorescence emitted after the absorption of a photon is detected.

In a molecule a change in the electron configuration can also be induced by the absorption of a photon. However, the situation in a molecule is more complicated compared to an atom as a molecule has also vibrational and rotational degrees of freedom. Different electron configurations (electronic states) may have the same energy because the difference in electronic energy can be compensated by rotational and vibrational energy. In case the potential surfaces belonging to the different electronic states interact an excited electronic state is coupled to several (nearly) iso-energetic rovibronic states. Excitation of the electronic state results then in an energy redistribution over the coupled iso-energetic rovibronic states. An excited isolated molecule still has to release all the absorbed energy by the emission of photons, independent of the nature of the coupled states. The transition dipole moment of these coupled states to the electronic ground state can be very low. In this case the photon yield of the molecules after photon absorption is very low on the time scale of the experiment.

A general model used to describe the coupling between a singlet electronic state and a triplet electronic state is depicted in figure 1.1. The singlet ground state of the molecule is denoted by S_0 and the first excited singlet state by S_1 . The molecule is excited to a rovibrationally excited state $|S\rangle$ of the singlet S_1 state by absorption of a photon. The excited state $|S\rangle$ is radiatively coupled to the ground state with a decay rate k_r . The state $|S\rangle$ is coupled to iso-energetic vibrationally excited states $\{|T\rangle\}$ with coupling matrix elements V_{st} . The radiative transition between the singlet ground state S_0 and the triplet state T_1 is spin forbidden and hence neglected. The triplet states are therefore called dark. The rovibronic states $|S\rangle$ and $\{|T\rangle\}$ are the zero order Born-Oppenheimer states.

The effect of the singlet-triplet coupling depends on the density ρ_T of the triplet states and the average coupling strength. In case of a high density ρ_T and a large coupling strength the excitation energy is redistributed over a large number of coupled dark states. As the recurrence time in this case is much longer than the time scale of the experiment the energy flow is practically irreversible and the non-radiative decay rate k_{nr} is described with the

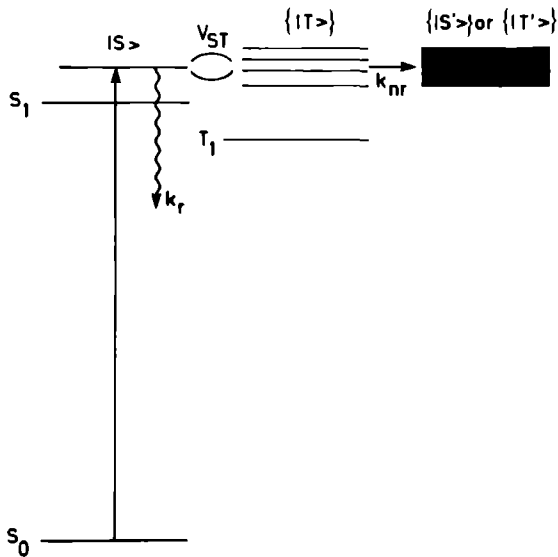


Figure 1.1: Schematic representation of a singlet-triplet coupling scheme.

Fermi golden rule:

$$k_{nr} = \frac{4\pi^2}{h} \rho_T V_{ST}^2$$

The quantum yield measured in an experiment is therefore less than one. An example of such a molecule is naphthalene ($C_{10}H_8$) described in chapter 2.

In case the density of triplet states and/or the coupling strength is low only a few dark states are coupled to the bright singlet state and mixed singlet-triplet states are formed. The singlet absorption strength is distributed over these mixed singlet-triplet states and in the spectrum of the molecule every single rotational transition consists of a number of lines. In the literature these mixed singlet-triplet states are called the molecular eigenstates (MEs). Despite the fact that this denomination is incorrect and confusion is created we too will use the term ME for the mixed singlet-triplet state. As only a very limited number of dark states is coupled the recurrence time is short and the quantum yield is near one.

In a real molecule both cases are often encountered simultaneously. The MEs are coupled to a dense set of dark background states (due to the inappropriate denomination this is a contradiction in terms), either highly excited vibrational states $\{ |S' \rangle \}$ or triplet states $\{ |T' \rangle \}$.

In the literature several molecules are used over the years in the study of different coupling mechanisms between the potential energy surfaces like acetone [1], acetylene [2], benzene [3], formaldehyde [4] and pyrazine [5]. Especially the pyrazine molecule (para- $C_4H_4N_2$)

has become a prototype molecule to study the singlet-triplet coupling since the recording of a spectrum of the individual MEs [6].

We report here the study of the singlet-triplet coupling in several molecules after excitation of the first excited singlet state S_1 . The experimental method used is the laser induced fluorescence spectroscopy. In this technique the fluorescence emitted by the molecules after absorption of laser photons is detected. Visible and UV photons can be detected very efficiently and the method is therefore very sensitive. The use of a tunable single frequency laser and the molecular beam technique provided a spectral resolution better than 10^8 . As a result rotationally resolved spectra are recorded for the molecules considered here and also the individual MEs are resolved. The experimental set-up is described at the end of this chapter.

The results of the experiments on the singlet-triplet coupling in the molecules pyrazine, pyrimidine (meta- $C_4H_4N_2$), sym-triazine (sym- $C_3H_3N_3$) and naphthalene are described in the chapters 2-5. In chapter 6 finally an experimental study is reported on the internal rotation of a methyl group in the 1,4-dimethylnaphthalene molecule. In this also the coupling between the two methyl groups via the electron system of the molecule is considered.

A very rewarding experiment in the research on the singlet-triplet coupling would be the determination of a high resolution ME absorption spectrum. In the next section a survey is given of the efforts in this direction.

1.1 Past, present and future: an absorption spectrum

The ME spectrum of the pyrazine molecule is obtained with the laser induced fluorescence technique. As a consequence the intensities in the high resolution spectrum are the excitation intensities. The analysis of the spectra is usually performed with the procedure of Lawrance and Knight [7]. In this procedure however the absorption intensities are needed. It is demonstrated for the strongest lines in the P(1)-branch in the spectrum of pyrazine that the absorption intensities and the excitation intensities are not identical. Hence there is a quest for the high resolution ME absorption spectrum of pyrazine. Furthermore, a model is proposed which predicts the presence of a strong broad band absorption in the spectrum of pyrazine [8]. A high resolution absorption spectrum with a good signal to noise ratio would validate or reject this model.

Several experimental techniques are used over the years to acquire a high resolution absorption ME spectrum.

- The excitation intensity and the absorption intensity of a single ME are related to each other by the life time of the excited ME. Hence the absorption intensity can be derived from the excitation intensity in case the life time is known. The life time of some selected MEs in the P(1)-branch transition in pyrazine were measured [9]. The result demonstrated the deviation between the excitation intensity and the absorption intensity. However, the experimental technique is quite laborious and only applicable to the strongest lines. Furthermore, the relation which connects the absorption intensity with the excitation intensity is dependent on the model used. Therefore other experimental techniques were applied.
- A different approach is the determination of the amount of energy left in the molecular

beam after the excitation of the molecules. As the quantum yield of pyrazine is known to be low [10] the amount of energy left in the molecular beam resembles the absorbed energy. In case the excited ME decays into a bath of dark triplet states, e.g. the naphthalene molecule, the method of the detection of phosphorescence [11] can be applied. This method is described in detail in chapter 2. In pyrazine however, the excited MEs exhibit a strong non radiative decay into high vibrationally excited states of the singlet ground state. Hence the application of a bolometer to monitor the amount of absorbed energy is obvious [12]. The result of the bolometer detected absorption spectra of pyrazine [13] clearly revealed the differences between the absorption spectra and the excitation spectra. It was also shown that the deviation between the two spectra was not large. The complete absence of a strong broad band absorption in the bolometer spectra gnaws at the fundamentals of the model proposed by Amirav [8]. The signal to noise ratio in the bolometer detected absorption spectra was however low. Therefore different detection techniques were considered.

- A method to determine the absorption intensities of the MEs would be an UV-UV pump-probe experiment analog to the experiment described in chapter 4. It is clear that the hole burnt in the population distribution of the molecules in the molecular beam is proportional to the absorption intensity of the pumped line. Hence a scan of the pump laser with the probe laser fixed to a line results in an absorption spectrum of all the lines with the same rotational ground state as the probed line. The spectra presented in chapter 4 shows that the pump-probe signal is too low to record an absorption spectrum.

- The most direct way to measure an absorption spectrum would be to monitor the diminution of the laser power after crossing the molecular beam [14]. In our present experimental set-up the fractional absorption for the strongest lines in the spectrum of pyrazine is estimated to be 10^{-7} . The power fluctuation of the UV laser amounts to a few per cent. Hence the direct measurement of the absorption is very troublesome. However, the use of slit nozzles and the excitation of the molecules closer to the nozzle with respect to the present situation may result in high resolution absorption spectra with satisfactory signal to noise ratio.

- An alternative approach to measure a high resolution absorption spectrum is the application of (resonantly enhanced) multiphoton ionization spectroscopy (REMPI). In principle single ions can be detected and thus REMPI is a very sensitive technique used in many spectroscopic applications [15]. In the study of the predissociation of complexes REMPI is very useful especially in case the fluorescence is quenched [16]. The mass selectivity in the detection of ions is very rewarding in the spectroscopy of complexes [17]. As the vibrational energy of the excited molecule is not transferred to the ion REMPI can be used in the study of dynamical processes in the molecule like intersystem crossing [18].

We can apply the REMPI technique to detect the absorption spectrum of MEs of pyrazine. Molecules are excited to a single well-defined ME by the cw radiation field of the single frequency UV laser. Ionization from the excited ME is performed by a second laser. The cross section for ionization is normally low [16, 19] and high laser powers are required. Therefore a pulsed laser is used for the ionization step. As a consequence a few orders of magnitude in detection sensitivity is lost with respect to cw laser induced fluorescence due to the low duty cycle. The number of ions generated in this way is directly

proportional to the number of excited molecules. Thus the ion signal is a direct measure of the absorption intensity of the excited ME.

The ionization potential of pyrazine is measured by 1 + 1 REMPI with the S_1 state as intermediate state and is 74915 cm^{-1} [20]. Therefore a photon energy of at least 44040 cm^{-1} is required in case of ionization from the singlet S_1 state, whereas for ionization from the triplet T_1 state a photon energy of 48100 cm^{-1} is required. As a result the application of a laser with a photon energy between 44040 cm^{-1} and 48100 cm^{-1} allows us to measure directly the amount of singlet character in an excited ME and the result is independent of the model used.

We have performed a preliminary 1 + 1 REMPI experiment on pyrazine in our molecular beam machine. At a distance of 60 cm from the nozzle orifice the pyrazine molecules are excited to a ME by the single mode UV laser. A tunable excimer laser operating on ArF (output power 50 mJ per pulse at 193 nm) was used as the ionization source. As ionization takes only place from the excited ME the two lasers were spatially overlapping. The first ionization potential in pyrazine is due to the ionization of the non-bonding electron [20]. The electronic transition $S_1 \leftarrow S_0$ in pyrazine is a $n\pi^*$ transition, i.e. the excitation of the non-bonding electron. Therefore the cross section for ionization from the S_1 and T_1 state is expected to be relatively large [16, 19] and a substantial fraction of the excited state molecules is expected to be ionized. The ions were detected with a particle multiplier connected to a gated detector. With the use of a repeller plate a crude mass selection of the ions is obtained due to differences in time of flight. The detection system was tested by the measurement of the multiphoton ionization spectra of the hydrogen molecule and of the krypton atom in the frequency range of the ArF laser [21]. A constant background appeared to be present. The background is ascribed to fragmentation and ionization of oil products.

Application of the 1 + 1 REMPI technique to pyrazine did not result in a detectable pyrazine ion signal. We have made an estimation of the expected ion signal to noise ratio based on the results of this experiment and the laser induced fluorescence spectrum. In the calculation rate equations were used and the ionization yield of the excited molecules was estimated to be 10 %. The ion signal is calculated to be near the detection limit in the present experimental set-up. However, several experimental improvements can be made. As the ionization laser is pulsed in the experiment, the use of a pulsed valve does no longer affect the duty cycle of the experiment. The number of molecules in the beam can however be increased with two orders of magnitude in this way. Also excitation near the nozzle orifice will result in an increase of ion signal with an order of magnitude. Hence reexamination of this experiment might be very rewarding.

1.2 Experimental set-up

The experimental set-up to record the laser induced fluorescence spectra is schematically represented in figure 1.2. Two different parts can be distinguished: the laser system with its peripheral equipment and the molecular beam apparatus.

The laser system consists of a single frequency continuous wave ring dye laser (a modified Spectra Physics 380D) pumped by a Spectra Physics Argon-ion laser (model 2016-06) with an output power of 6 Watt all lines. The dye laser is usually operated with the dyes

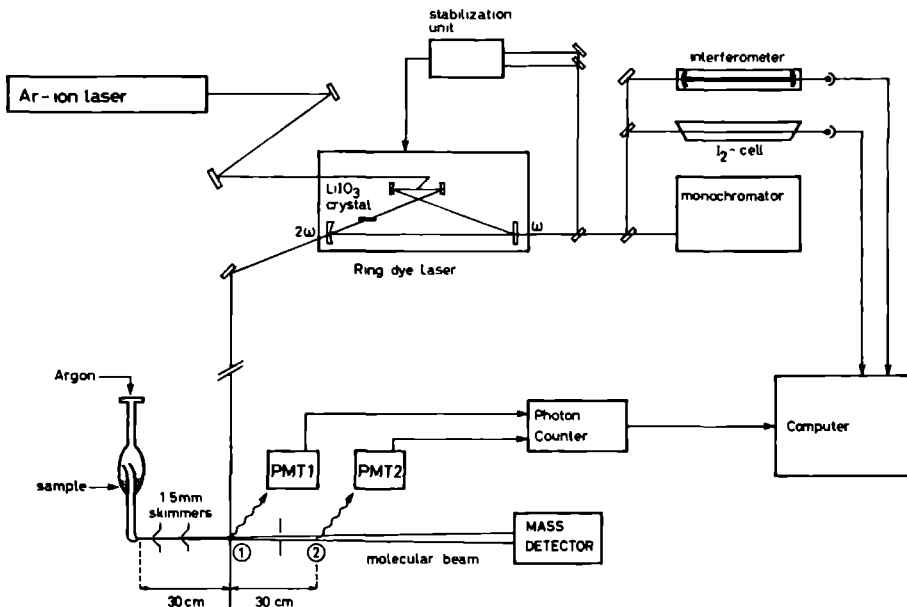


Figure 1.2: Outline of the experimental set-up

Rhodamine 6G and DCM in the red part of the electromagnetic spectrum. The fundamental frequency (ω) of the dye laser is controlled with a modified Coherent 599 stabilization system. Basically the frequency of the dye laser is locked to the transmission curve of a sealed off, temperature stabilized low finesse interferometer with a free spectral range of 1 GHz. Frequency scanning of the dye laser is performed by adjusting the optical length of the cavity of the interferometer with an inserted galvo driven plate. In this way stabilized scans of 60 GHz in the red could be made. The band width of the dye laser is 2 MHz and determined by the frequency jitter of the laser.

For a crude estimation of the absolute frequency of the laser a monochromator (Spex 1870) is used, whereas for precise absolute frequency measurements the absorption spectrum of the iodine molecule is recorded. Comparison of the measured iodine absorption spectrum with the well determined reference spectrum [22] allows the measurement of the absolute laser frequency with an accuracy better than 100 MHz.

For relative frequency measurements the transmission peaks of a high finesse temperature stabilized, sealed off Fabry-Perot interferometer (Burleigh CFT-500) with a free spectral range of 149.67 MHz is used. The free spectral range of the interferometer was calibrated by the measurement of the accurately known splittings in the $A^2\Sigma^+$ state of the OH radical [23]. The drift of the interferometer could be as large as 100 MHz per hour. Hence for accurate relative frequency measurements several scans have to be made with different scan directions.

The electronic transitions of the molecules considered here are in the ultraviolet part of the electromagnetic spectrum. Hence a LiIO_3 crystal is placed in the auxiliary waist in the cavity of the ring dye laser [24]. Due to the non-linear properties of the crystal laser radiation is efficiently generated at the second harmonic of the fundamental laser frequency. In order to minimize the losses in the laser cavity the LiIO_3 crystal is cut at Brewster angle. With three different crystals tunable continuous wave single frequency UV radiation is obtained in the range 294-330 nm with output powers up to 15 mW.

The UV radiation is used to excite the molecules in a molecular beam. The molecular beam is formed by an expansion of the molecules under investigation with a seeding gas through a quartz nozzle with a typical diameter of 100 μm . A sample of the molecules is stored in a quartz vessel. Both the quartz vessel and the quartz nozzle could be heated up to 500 $^\circ\text{C}$ in order to increase the vapour pressure of the sample.

A mixture of the vapour pressure of the sample and the seeding gas (usually argon or helium) is expanded into the vacuum chamber. In the expansion the internal degrees of freedom of the molecules are cooled down and only the lowest vibrational and rotational states are populated. In this way the spectra are simplified to a large extent. A typical rotational temperature in our molecular beam is 3 K in case of seeding with argon and a backing pressure of 400 Torr. The rotational temperature can be varied with the use of different pressures of the seeding gas and/or the use of different seeding gases. In this way the identification of the lines in the spectra is facilitated as shown for 1,4-dimethylnaphthalene (chapter 6).

A molecular beam is formed out of the expansion by two conical skimmers with diameters of 1.5 mm. The molecular beam can be monitored with a mass detector. In order to discriminate between stray laser light and an overall present fluorescence of the molecules the molecular beam could be chopped mechanically. With a differential pumping system the background pressure in the interaction region is well below 10^{-6} mbar. This assures we study isolated molecules under collision free circumstances.

At a distance of 30 cm from the nozzle orifice the molecular beam is crossed perpendicularly by the laser beam (position ① in figure 1.2). The laser beam is focused to a spot size of about 1 mm diameter at the position of the molecular beam. The total undispersed laser induced fluorescence is collected with two spherical mirrors and imaged on a photomultiplier tube [25]. The total line width of the molecular transitions is a result of several contributions. The homogeneous broadening of the lines due to the finite life time of the molecules in the excited state is small for the molecules considered here. Even for sym-triazine with an excited state life time of 100 nsec the broadening is less than 2 MHz. Contributions to the total line width of the time of flight broadening due to the finite interaction time of the molecules with the radiation field and the broadening due to the curvature of the wave front are determined to be less than 1 MHz [26]. The frequency jitter of the excitation laser is about 3 MHz in the ultraviolet. The line width of the transitions is however dominated under normal conditions by the Doppler width due to the residual divergence of the molecular beam. In our experimental set up the residual Doppler width amounts to 12 MHz with the use of argon as seeding gas and is determined by the spatial sensitivity of the collection optics.

At a distance of 60 cm from the nozzle orifice (position ② in figure 1.2) a second interaction zone is placed. At this position the phosphorescence of the molecules could be

detected (chapter 2) or the UV-UV pump-probe signal (chapter 4).

The laser induced fluorescence spectra were recorded with an Ortec 5C1 photon counting system connected to a PDP 11/23+ computer. During a scan of the laser simultaneously with the spectrum the markers of the interferometer and the iodine absorption spectrum are recorded. Also the power of the laser could be recorded simultaneously. Further data processing like the frequency linearisation of the spectra was performed with the computer [27].

References

- [1] H. Zuckermann, B. Schmitz and Y. Haas, *J. Phys. Chem.* 93 (1989) 4083
- [2] E. Abramson, C. Kittrell, J.L. Kinsey and R.W. Field, *J. Chem. Phys.* 76 (1982) 2293
J. Heintze, M. Drabbels and W.L. Meerts, to be published
- [3] E. Riedle, H.J. Neusser and E.W. Schlag, *J. Phys. Chem.* 86 (1982) 4847
- [4] D.J. Clouthier and D.A. Ramsay, *Ann. Rev. Phys. Chem.* 34 (1983) 31
- [5] J. Kommandeur, W.A. Majewski, W.L. Meerts and D.W. Pratt, *Ann. Rev. Phys. Chem.* 38 (1987) 433
- [6] B.J. van der Meer, H. Th Jonkman, J. Kommandeur, W.L. Meerts and W.A. Majewski, *Chem. Phys. Lett.* 92 (1982) 565
- [7] W.D. Lawrance and A.E.W. Knight, *J. Phys. Chem.* 89 (1985) 917
- [8] A. Amirav, *Chem. Phys.* 108 (1986) 403
- [9] W.M. van Herpen, W.L. Meerts, K.E. Drabe and J. Kommandeur, *J. Chem. Phys.* 86 (1987) 4396
- [10] A. Amirav and J. Jortner, *J. Chem. Phys.* 84 (1986) 1500
P.J. de Lange, B.J. van der Meer, K.E. Drabe, J. Kommandeur, W.L. Meerts and W.A. Majewski, *J. Chem. Phys.* 86 (1987) 4004
- [11] T. Suzuki, M. Sato, N. Mikami and M. Ito, *Chem. Phys. Lett.* 127 (1986) 292
- [12] T.E. Gough, R.E. Miller and G. Scoles, *Appl. Phys. Lett.* 30 (1977) 338
- [13] W.M. van Herpen, P.A.M. Uijt de Haag and W.L. Meerts, *J. Chem. Phys.* 89 (1988) 3939
- [14] A. Amirav, *Chem. Phys.* 126 (1988) 327
- [15] V.S. Letokhov, *Laser Photoionization Spectroscopy* (Academic Press) 1987
- [16] N. Mikami, Y. Sugahara and M. Ito, *J. Phys. Chem.* 90 (1986) 2080
- [17] Th. Weber, A. von Bargaen, E. Riedle and H.J. Neusser, *J. Chem. Phys.* 92 (1990) 90
- [18] J.B. Pallax and S.D. Colson, *Chem. Phys. Lett.* 119 (1985) 38

- [19] U. Boesl, H.J. Neusser and E.W. Schlag, *Chem. Phys.* 55 (1981) 193
- [20] A. Goto, M. Fujii and M. Ito, *J. Phys. Chem.* 91 (1987) 2268
- [21] E.W. Rothe, G.S. Ondrey and P. Andresen, *Optics Commun.* 58 (1986) 113
- [22] S. Gerstenkorn and P. Luc, *Atlas du spectroscopie d'absorption de la molecul e d'iode*
(Centre National de la Recherche Scientifique) 1978
S. Gerstenkorn and P. Luc, *Rev. Phys. Appl.* 14 (1979) 791
- [23] J.J. ter Meulen, W. Ubachs and A. Dymanus, *Chem. Phys. Lett.* 129 (1986) 533
- [24] W.A. Majewski, *Opt. Comm.* 45 (1983) 201
- [25] W.A. Majewski and W.L. Meerts, *J. Mol. Spectrosc.* 104 (1984) 271
- [26] J.P. Bekooij, thesis Katholieke Universiteit Nijmegen (1983)
- [27] W.M. van Herpen, thesis Katholieke Universiteit Nijmegen (1988)

Chapter 2

Study of dark states in naphthalene, pyrimidine and pyrazine by detection of phosphorescence after UV laser excitation

Paul Uijt de Haag and W. Leo Meerts
Fysisch Laboratorium, University of Nijmegen
Toernoorveld, 6525 ED Nijmegen, The Netherlands

abstract

The high resolution fluorescence and phosphorescence detected spectra after excitation of the $(3a_g)^1$ and $(4a_g)^1$ vibronic states of the $S_1(^1B_{3u})$ singlet state in naphthalene have been studied in a molecular beam. The residual Doppler line width of 20 MHz allowed rotational resolution. All lines were assigned and the rotational constants of the $(3a_g)^1$ and $(4a_g)^1$ states were determined. It has been shown that the intersystem crossing rates are independent of the rotational quantum numbers J and K up to $J = 10$ in both excited vibronic states. The strong ISC rate of the $(4a_g)^1$ state is confirmed. No evidence was found for a promoting second triplet T_2 state.

Detection of phosphorescence after excitation of the vibrationless $S_1(^1B_{3u})$ state in pyrazine and the $S_1(^1B_1)$ state in pyrimidine yielded no signal. This observation confirms the assumption that in pyrazine and in pyrimidine after excitation of the S_1 state the energy is transferred to high vibrational states of the S_0 state.

2.1 Introduction

In the theory of intramolecular radiationless transitions molecules are usually classified according to their behaviour under optical excitation as small, intermediate case or large molecules [1]. In a small molecule the excited state is coupled to only a few non-radiative, so called dark states. This results in an exponential decay with a quantum yield close to unity. In a large molecule on the other hand, the optical excited state is coupled to a dense manifold of dark background states, which acts as a quasi continuum. This opens an extra decay channel of the state, besides the radiative decay, to which the energy can flow. The decay will still be exponentially with a quantum yield less than unity. In the last years much attention has been paid to the intermediate case molecules. In such a molecule the optically excited state is coupled to a limited number of dark background states. The decay will in general be non-exponential, exhibiting quantum beats and/or biexponential decay, with quantum yields again smaller than unity.

This classification already indicates that most experiments in this field have been performed with pulsed laser systems, which allow a good resolution in the time domain, but a limited resolution in the frequency domain. This especially implies that for large molecules an ensemble of rovibronic states rather than a single well defined state is excited. Consequently little is known about the rotational effects on the intramolecular radiationless decay. The important role rotations play in such decays has clearly been demonstrated in benzene by Riedle et al [2]. High resolution Doppler-free two photon spectroscopy showed that in the "channel three" region only $K' = 0$ lines are present in the spectrum.

To elucidate the role of rotational effects on the intramolecular radiationless transitions we have studied in the present work the intersystem crossings with rotational resolution in pyrazine, pyrimidine and naphthalene by detecting the phosphorescence after excitation of the excited singlet S_1 state [3, 4]. The molecules collide shortly after their optical excitation with a cooled surface. The resulting phosphorescence from the molecules, which are stuck on the surface is measured and compared to the directly detected fluorescence spectrum. By this method we were able to determine the relative intersystem crossing rates for each single rovibronic state.

Pyrazine serves together with pyrimidine as prototypes for the intermediate case molecule, and many data are available at the moment. For a recent review we refer to [5]. It has been demonstrated for pyrazine that the temporal decay of the first excited $S_1(^1B_{3u})$ singlet state exhibits both quantum beats [6, 7] and biexponential decay, which has shown to be magnetic field dependent [8, 9]. These experimental findings have been interpreted in terms of a coupling between the first excited singlet state S_1 and nearly iso-energetic vibronically excited states of the lower lying triplet T_1 state. The vibrationless origin of the latter level is positioned 4056 cm^{-1} below the origin of the S_1 state. In a high resolution experiment with a cw single frequency laser we have demonstrated the existence of the molecular eigenstates (MEs) [10]. It was found that each single rotational transition appears as a large number of lines (approx. 40). This MEs spectrum can easily be deconvoluted into their zero order singlet and triplet states in the case only one optical doorway state is present [11], a situation encountered for the $P(1)$ and $R(0)$ transitions. Recently we have also succeeded in a deconvolution of all $J' K'$ states up to $J' = 3$ [12]. It was found for rotational states up to $J' = 3$ neither the singlet-triplet coupling matrix elements nor the number of coupled triplet

states systematically depend on the rotational quantum number J' . It appears however that the fluorescence intensities of the $K' = 0$ transitions is relatively weaker than the intensities of the $K' \neq 0$ transitions, which indicates a rotational effect on the intersystem crossing.

However, for a correct deconvolution procedure the absorption intensities should be used rather than the excitation intensities which are obtained in a laser induced fluorescence experiment. Therefore we have recently studied [13] the absorption intensities of the individual MEs. This is done by observing the amount of laser energy which is absorbed by the molecular beam with the help of a bolometer detector [14]. These experiments clearly indicated that the quantum yield is a smoothly varying function over the different MEs within a single rotational transition, but decreasing with increasing J' . This qualitative result is in agreement with low resolution measurements [15], which showed that the quantum yield (Y) can be written as $Y = 0.124/2J' + 1$ for J' values in the range between 5 and 22. The conclusions derived from the bolometric detected spectra were based on the assumption that non or very little phosphorescence emerges from the excited state molecules. It was shown, however, for other molecules that phosphorescence may occur. This has been demonstrated by Ito et al [3, 4] who detected the phosphorescence by the excited molecules after a collision with a surface. To clarify the situation for pyrazine we have applied the method of phosphorescence detection on this molecule.

Pyrimidine behaves very similar to pyrazine with as a main difference that the singlet-triplet gap in pyrimidine is of the order of 2000 cm^{-1} . As a consequence pyrimidine has a much less dense manifold of background states coupling to the S_1 state and therefore a smaller number of MEs, which simplifies the deconvolution procedure and analysis of the spectrum [16]. In pyrimidine it was also found that neither the singlet-triplet coupling matrix elements nor the number of coupled triplets show a systematical dependence on the rotational quantum numbers J' and K' [16]. The fluorescence lifetime on the other hand was found to be increasing with increasing K' , pointing to a rotational effect on the decay process. For this reason we have also studied the phosphorescence spectrum of pyrimidine.

The fluorescence decay of single low lying vibronic states of the first excited $S_1(^1B_{3u})$ singlet state of naphthalene have been studied in a cell [17, 18] and in a molecular jet [19]. All decays are single exponential with a quantum yield of approximately 0.3 for the low vibrational states of S_1 . This quantum yield generally decreases with increasing vibrational excess energy. This places naphthalene in the category of large molecules as might be expected from the large singlet-triplet gap of over $10,000 \text{ cm}^{-1}$ in this molecule [20].

Howard and Schlag [21] measured the rotational dependence of the quantum yield for some selected vibronic states in naphthalene under cell conditions. A clear variation of the quantum yield over the rotational contour has been found. This result has been interpreted in terms of a spin-orbit coupling between the excited singlet S_1 state and the dense manifold of dark background states which originate from vibrationally excited T_1 states. The rotational dependence of the ISC rate in such a case is determined by the Franck-Condon weighted density of states. Due to differences in rotational energies in both the S_1 and T_1 vibronic states the various rovibronic singlet states are coupled to different vibronic triplet states. Differences in the Franck-Condon factors then account for the variations in ISC rates. In the case of nearly constant Franck-Condon weighted density of states over the measured energy range the ISC rate will be independent of the rotational quantum numbers.

High resolution molecular beam spectra of the 0_0^0 and $(8b_{1g})_0^1$ vibronic bands of naph-

thalene have been measured previously with a resolution of 30 MHz [22]. This experiment clearly revealed the rotational substructure. All lines and intensities could be assigned in terms of an asymmetric rotor Hamiltonian with the appropriate intensities. Especially the well behaved intensity variations indicate that the ISC rate cannot be a strongly varying function of the rotational quantum numbers, at least in the 0^0 and $(8b_{1g})^1$ state of the S_1 electronic state. Furthermore the observation that all lines in the spectrum can be assigned, is in agreement with the large molecule limit.

The method of sensitized phosphorescence has been applied on the S_1 state of naphthalene with vibrational resolution by Ito et al [4]. Their experiments demonstrated a strong vibrational dependence of the ISC rate. In general the ratio of phosphorescence to fluorescence intensities increases with increasing vibrational excess energy. Some vibronic states (e.g. the $(4a_g)^1$) showed a strongly enhanced ISC rate. This was interpreted to result from an accidental resonance with a vibronic state of the second triplet T_2 which energy is expected to be close to that of the S_1 state. In the present work we have applied the phosphorescence method at rotational resolution to two vibronic states of naphthalene, the $(3a_g)^1$ and $(4a_g)^1$ vibrational states of S_1 , both with a vibrational excess energy of about 1400 cm^{-1} . The $S_1(3a_g)^1$ vibronic state was found to exhibit a normal ISC rate, while the $S_1(4a_g)^1$ vibronic state showed an enhanced ISC rate. In case such a strong ISC rate is due to an accidental resonance with a vibronic state of the second triplet state T_2 , it is expected to strongly affect the high resolution spectrum. For example molecular eigenstates can show up resulting from a coupling of the S_1 state and the sparse background of vibrational T_2 states. We have therefore focused our attention on this particular vibronic state.

2.2 Experimental

An extensive description of the molecular beam apparatus and the laser system is already given elsewhere [22]. Therefore only the relevant features are given here. The experimental setup is schematically depicted in figure 2.1. The molecular beam is formed by a continuous expansion of naphthalene (pyrimidine, pyrazine) seeded in argon through a nozzle with a diameter of $75\ \mu\text{m}$. The backing pressure of argon was varied in the range of 0.25-1.5 bar. The samples of pyrazine and pyrimidine (Janssen Chimica, purity better than 99 %) were kept at room temperature, while the sample of naphthalene (Riedel de Haen, purity 95 %, and Janssen Chimica, better than 99 %) was heated to $95\ ^\circ\text{C}$, in order to achieve enough vapour pressure. All samples were used without further purification. The molecular beam was strongly collimated by two conical skimmers (diameter 1.5 mm) and pumped differentially.

At a distance of 30 cm from the nozzle the molecules were excited to the singlet S_1 state by the continuous wave radiation field of an intracavity frequency doubled ring dye laser (a modified Spectra Physics 380D). About 2 mW of single frequency UV radiation with a bandwidth of 3 MHz was obtained by using an angle tuned LiIO_3 crystal. For relative frequency measurements a part of the fundamental laser beam was sent through a sealed off, temperature stabilized Fabry-Perot interferometer, while for absolute frequency calibration the absorption spectrum of iodine was recorded simultaneously. The total undispersed laser induced fluorescence was collected by two spherical mirrors and imaged at the photocathode of a photomultiplier (EMI 9789QA). Due to the low fluorescence quantum yield of the

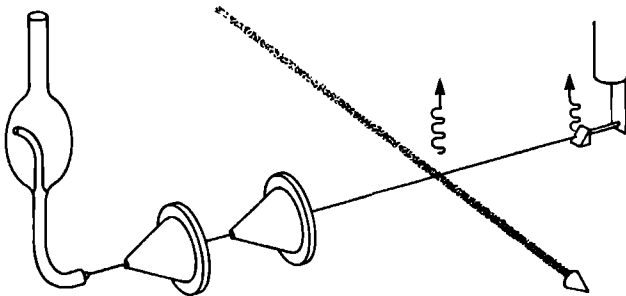


Figure 2.1: Outline of the experimental set-up. The molecular beam, formed from an expansion, is crossed by the laser. The beam collides with a cooled copper surface and the phosphorescence is detected.

molecules under consideration here, a large fraction of the absorbed energy will remain in the molecules in the beam. Depending on the nature of the coupling between the S_1 state and the background states the character of the state of the excited molecules in the beam will be either a high vibrationally excited state of the triplet T_1 or T_2 state or of the singlet ground state S_0 , or even a mixture of the two cases. In the present experiment the excited state molecules travel over a distance of 30 cm (which corresponds to a time of approximately 0.5 msec) from the excitation region downstream to the phosphorescence detector [3]. The detector exists of a copper surface cooled to liquid nitrogen temperature and a 1 cm diameter quartz light pipe placed 1 cm above the cooled surface. The photons emitted from the surface are guided by this light pipe to a photomultiplier (EMI 9635 QA). After a few minutes, the cooled surface is covered with molecules from the sample.

After the collision with the surface the molecules in the beam are frozen to the surface and may release their surplus energy either by emission of a photon, or by transferring heat to the surface. If the molecule is in the triplet state, the collision can induce phosphorescence. However, if the excited state consists of high vibrationally excited states of the electronic ground state the most probable process would be the transfer of heat, due to the low Franck-Condon factors for emission. It is clear that therefore different detection methods can be used for the measurement of the internal energy of the molecule: for measuring the excited vibrational states bolometer detection will be the most sensitive, while for the detection of molecules in the triplet state photon detection will give the best results. This indicates that these measurements give additional information: high phosphorescence signals indicates molecules in the triplet state. In the experiment performed here we have measured the total undispersed phosphorescence.

Because the laser excitation region and the phosphorescence detection region are separated with a diaphragm and since the large distance between these areas the amount of stray light from the laser as well as the light from the laser induced fluorescence at the place of the phosphorescence detector are down by a factor of 10^4 by that in the excitation

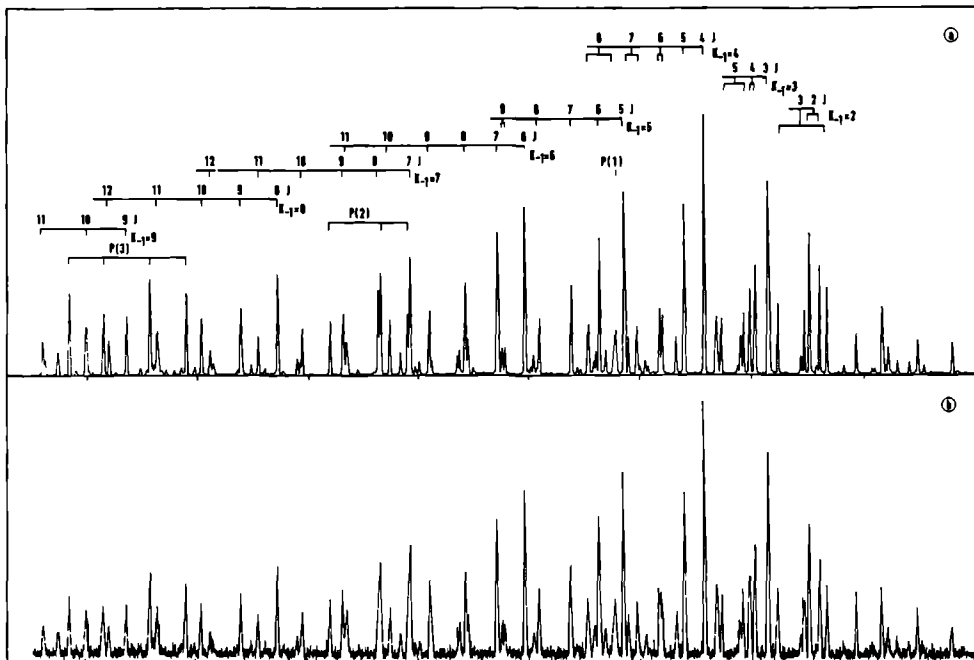


Figure 2.2: High resolution fluorescence (a) and phosphorescence detected (b) spectra of the Q-branch of the $(3a_g)_0^1$ vibronic transition in naphthalene. The intensity axis is in arbitrary units. The frequency increases from left to right and is marked every GHz.

region. For most transitions involved we therefore can neglect contributions from stray laser light and LIF on the phosphorescence detector. During the experiment the sensitivity of the phosphorescence detection varied slowly, probably due to the continuous deposition of molecules of the beam on the surface. Therefore all measurements have been performed several times. To eliminate the effects of changes in laser power and molecular beam, both the phosphorescence signal and the LIF signal were recorded simultaneously by a standard two channel photon counting system (Ortec Brookdeal 5C1), interfaced with a PDP 11/23+ computer.

2.3 Results

2.3.1 Naphthalene

With the experimental set-up described we have recorded simultaneously the laser induced fluorescence spectrum (LIF) and the phosphorescence spectrum (SP) for two vibronic bands,

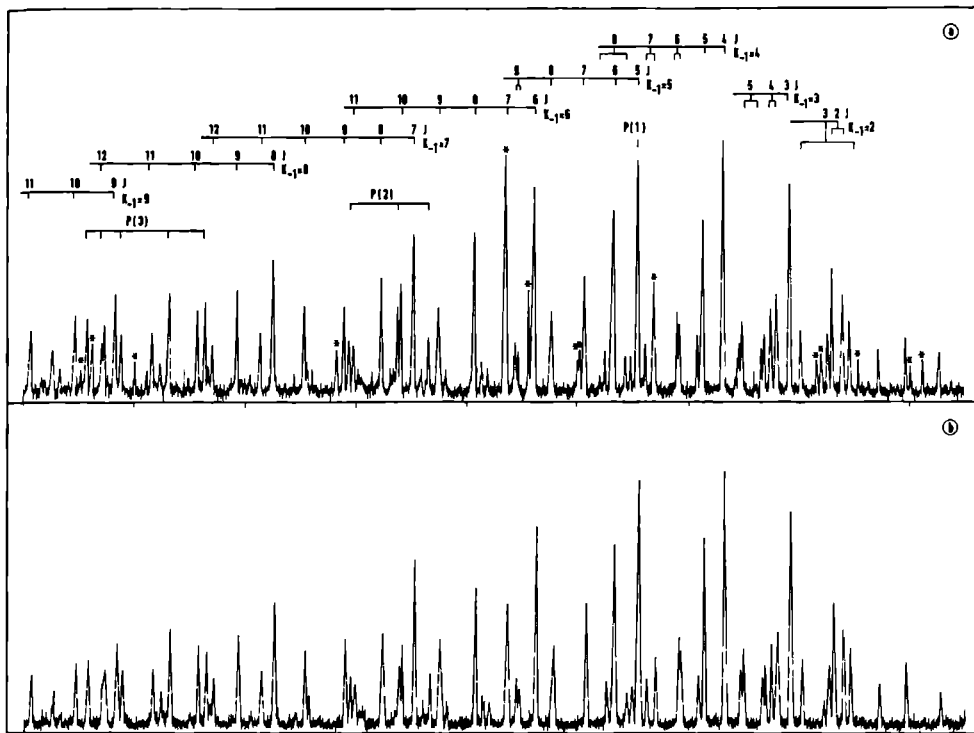


Figure 2.3: High resolution fluorescence (a) and phosphorescence detected (b) spectra of the Q-branch of the $(4a_g)_0$ vibronic transition in naphthalene. The intensity axis is in arbitrary units. The frequency increases from left to right and is marked every GHz. The lines marked with an asterisk only show up in the fluorescence spectrum.

the $(3a_g)_0$ and $(4a_g)_0$ of the $S_1(^1B_{3u}) \leftarrow S_0(^1A_g)$ electronic transition in naphthalene. Part of the naphthalene spectra are shown in figure 2.2 (the $(3a_g)_0$ band) and in figure 2.3 (the $(4a_g)_0$ band). The typical count rate of the spectrum of the $(3a_g)_0$ band is 50.000 counts/sec per mW laser power for the LIF spectrum and 4000 counts/sec per mW for the SP spectrum. For the $(4a_g)_0$ band these numbers are 3000 counts/sec per mW (LIF spectrum) and 2000 counts/sec per mW (SP spectrum), respectively. This clearly shows the vibrational dependence of the ratio $\frac{I_F}{I_P}$ of the intensities of the LIF spectrum (I_F) and SP spectrum (I_P), which is in agreement with the low resolution measurements [4]. The line widths of the transitions of the LIF spectrum and SP spectrum were 12 MHz and 20 MHz, respectively. In both cases the line width is dominated by the residual Doppler width due to the divergence of the molecular beam. Because of the spatial sensitivity of the collection

optics for the LIF spectra, only a part of the fluorescence of the molecular beam is detected. This slightly narrows the line width. In the SP spectra however the complete molecular beam is detected.

In comparing the LIF and SP spectra, we notice that in the $(3a_g)_0^1$ vibronic band all lines are present both in fluorescence as in phosphorescence. We furthermore see that the relative intensities of the rotational lines in each spectrum is approximately the same. In the $(4a_g)_0^1$ vibronic band all lines which appear in the SP spectrum can also be identified in the LIF spectrum. However, some additional lines appear throughout the whole investigated frequency range in the LIF spectrum of the $(4a_g)_0^1$ band. We attribute these extra lines to either an isotopic species or a contamination in our naphthalene sample. Several potential candidates such as thianaphthene (C_8H_6S) have been investigated as a pure sample. We failed however to find a molecule which reproduced the extra transitions in the spectrum of the $(4a_g)_0^1$ band.

In order to investigate the rotational dependence of the ratio of intensities between the corresponding transitions in the SP and LIF spectra we have made a rotational assignment of the lines in the $(3a_g)_0^1$ and $(4a_g)_0^1$ bands. Such an assignment is furthermore needed to allow a search for possible extra splittings in the spectra due to ISC. For the $(3a_g)_0^1$ vibronic band 200 lines in the central 30 GHz part of the LIF spectrum up to $J' = 12$ have been assigned. It turned out that it was possible to fit the observed transitions in the two bands with an asymmetric rotor Hamiltonian. The fit was made to a parallel a-type band, which confirms the symmetry of the vibration. All lines present in the spectrum could be identified. A least squares fit of the experimental spectrum to the asymmetric rotor Hamiltonian yielded the rotational constants in both the ground and excited electronic state. The standard deviation of this fit was 2.5 MHz, well within the experimental line width. Table 2.1 lists the obtained molecular constants. The errors given are the standard deviation from the fit. The dominating source of errors, however, is due to the drift of the interferometer. An estimate uncertainty can be found by comparing the ground state rotational constants as obtained from different vibronic bands. A comparison between the present results for the ground state constants and those from the 0_0^0 and $(8b_{1g})_0^1$ bands [22] shows that the uncertainties in the rotational constants are about five times the standard deviation.

The unperturbed relative intensities of the rotational lines in an a-type band are given by:

$$I = I_0 \cdot g_{J''K''_{-1}K''_{+1}} \cdot A_{J''K''_{-1}K''_{+1}} \cdot e^{-E(J'', K''_{-1}, K''_{+1})/kT_{rot}} \quad (2.1)$$

Where $A_{J''K''_{-1}K''_{+1}}$ are the Hönl-London factors, $g_{J''K''_{-1}K''_{+1}}$ are the statistical weights, T_{rot} the effective rotational temperature of the molecules in the beam and $E(J'', K''_{-1}, K''_{+1})$ the rotational energy of the electronic ground state; k is the Boltzmann constant and I_0 the normalized intensity. Since naphthalene is a near prolate symmetric rotor we employ for $A_{J''K''_{-1}K''_{+1}}$ the symmetric top expressions. The errors resulting from this approximation are negligible compared to the experimental inaccuracies in the intensity measurements. A fit of the experimental spectrum to equation 2.1 yielded a rotational temperature of 4 ± 0.5 K.

We have assigned 220 lines of the central 40 GHz part of the SP spectrum of the $(4a_g)_0^1$ vibronic band up to $J' = 12$. Despite the slightly larger line width we preferred to analyze the SP spectrum because of the additional lines in the LIF spectrum. This band again corresponds to a parallel a-type transition, in agreement with the previous assignments. We performed a least squares fit of the experimental spectrum to the asymmetric rotor

Table 2.1: Molecular constants of the naphthalene molecule in the electronic ground state S_0 and the $(3a_g)^1$ and $(4a_g)^1$ vibronic states of the singlet S_1 state ($\Delta A = A' - A''$ etc.).

		$(4a_g)_0^1$	$(3a_g)_0^1$
S_0	A'' (MHz)	3117.6(5.7)	3113.6(2.7)
	B'' (MHz)	1231.7(0.2)	1230.7(0.2)
	C'' (MHz)	883.1(0.2)	882.3(0.2)
S_1	ΔA (MHz)	-81.35(0.05)	-78.06(0.03)
	ΔB (MHz)	-18.89(0.07)	-19.60(0.04)
	ΔC (MHz)	-16.59(0.05)	-16.31(0.04)
	ν_0 (cm^{-1})	33408.229 (0.004)	33453.381(0.003)
	$\Delta\nu_0$ (cm^{-1})	1389.652 (0.007)	1434.804(0.005)

Indicated errors in the effective rotational constants are the standard deviation of the asymmetric rotor fit. Experimental errors in the rotational constants are about four times the indicated errors.

Hamiltonian. The resulting rotational constants are given in Table 2.1. The standard deviation of the fit was 7.5 MHz. The intensities were again fitted to equation 2.1 yielding a rotational temperature $T_{rot} = 4.5 \pm 0.5$ K. The slightly higher rotational temperature for the $(4a_g)_0^1$ band as compared to the $(3a_g)_0^1$ band is due to a somewhat different argon backing pressure in the source.

With the help of the rotational assignments for the $(3a_g)_0^1$ and $(4a_g)_0^1$ band as discussed above we are now in the position to determine the ratio $\frac{I_F}{I_P}$ for each individual rotational line in both bands. The most reliable result can be obtained using the Q-branch lines and P-branch lines with low J' value, because these lines are concentrated in a relative small frequency range. In this way the effect of changes in the sensitivity of the phosphorescence detector are minimized. Figure 2.4 displays the ratios for J' values up to $J' = 10$ for both vibronic bands. In this figure each point for a given J' value corresponds to a different rotational line. It is clear from figure 2.4 that the ratios are scattered randomly around an average value with J' and K' . We therefore conclude that the ratio $\frac{I_F}{I_P}$ is independent of the rotational quantum numbers J' and K'_{-1} up to $J' = 10$.

2.3.2 Pyrazine and pyrimidine

We have furthermore investigated the LIF and SP spectra of the $0_0^0 S_1(^1B_1) \leftarrow S_0(^1A_1)$ electronic transition in pyrazine and the $0_0^0 S_1(^1B_1) \leftarrow S_0(^1A_1)$ electronic transition in pyrimidine. In the case of pyrazine no SP signal was detectable, although the LIF signal on the

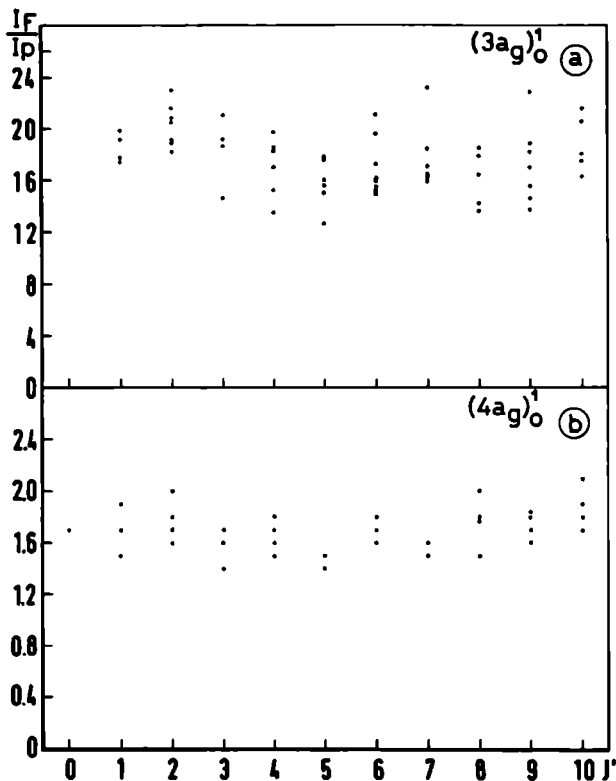


Figure 2.4: The ratio $\frac{I_F}{I_P}$ of the fluorescence intensity I_F and the phosphorescence intensity I_P as a function of the excited rotational state quantum number J' for the $(3a_g)^1$ state (a) and the $(4a_g)^1$ state (b). Different points correspond to different rotational lines.

strongest transitions amounts to 120,000 counts/sec per mW UV laser power. This result is in agreement with the nearly complete absence of a sensitized phosphorescence signal for pyrazine as found by Goto et al [23]. From the approximate average quantum yield of 0.01 of pyrazine for the low J' values [15], which is a factor 15 lower than that of the $(3a_g)^1$ vibronic state in naphthalene [19], we conclude that the energy contained in the beam of pyrazine molecules after laser excitation to the $S_1 0^0$ state is a factor of 40 higher than the energy contained in the beam of naphthalene molecules after excitation to the $S_1(3a_g)^1$ state. If we further assume that the conversion efficiency for photon emission from the triplet state is the same in both molecules, it follows that the branching ratio for a radiationless decay of the $S_1 0^0$ state of pyrazine to highly excited vibrational states of the singlet electronic

ground state is at least a factor of 200 higher than to the background triplet states. As a minimum detection limit a signal to noise ratio of three has been assumed.

For pyrimidine a weak signal with a countrate of 150 counts/sec per mW UV laser power (signal to noise ratio 1) has been obtained on the phosphorescence detector. This was for the strongest fluorescence lines, where the LIF intensity was 800,000 counts/sec per mW UV laser power. This signal on the photomultiplier of the SP detector is approximately the same as the estimated signal from the LIF, which mirrors by the copper surface of the SP detector onto the photomultiplier. It was therefore concluded that again for pyrimidine no SP signal is detectable. From an approximate quantum yield of 0.4 [24], and with the same assumptions made above for pyrazine we calculate that in the $S_1 0^0$ state of pyrimidine the branching ratio for radiationless decay of the $S_1 0^0$ to the S_0 state is at least a factor of 100 higher than to the T_1 state.

2.4 Discussion

The ratio of the phosphorescence signal I_P to the fluorescence signal I_F can be expressed as

$$\frac{I_P}{I_F} = A \cdot \frac{k_{nr}(S_1 \rightarrow T)}{k_r(S_1 \rightarrow S_0)} \cdot e^{-[k_r(T \rightarrow S_0) + k_{nr}(T \rightarrow S_0)]\tau} \cdot Q \quad (2.2)$$

In this equation A governs all experimental effects such as collection efficiency, photomultiplier sensitivity etc. Here $k_r(S_1 \rightarrow S_0)$ and $k_{nr}(S_1 \rightarrow T)$ represent the radiative decay rate and the non radiative ISC rate of the singlet S_1 state, respectively.

In the case that $k_r(S_1 \rightarrow S_0)$ is much smaller than $k_{nr}(S_1 \rightarrow T)$ and the internal conversion rate $k_{nr}(S_1 \rightarrow S_0)$ is negligible, the ratio $\frac{k_{nr}(S_1 \rightarrow T)}{k_r(S_1 \rightarrow S_0)}$ is equal to the inverse of the quantum yield. The exponential factor describes the decrease in the number of molecules in the excited triplet state during the travel time τ (in our case 0.5 msec) between laser excitation and the collision on the copper surface. This decrease takes place either through phosphorescence (the radiative decay rate $k_r(T \rightarrow S_0)$) or through ISC to high vibronic states of the singlet ground state $k_{nr}(T \rightarrow S_0)$. The factor Q gives the efficiency of emitting a photon by a molecule in the triplet state after it hits the copper surface. This factor is assumed to be independent of the rotational quantum numbers.

It is reasonable to assume that the factor Q in pyrazine and naphthalene will be of the same order of magnitude. Hence the absence of any phosphorescence signal detected in pyrazine is either due to a small value of $\frac{k_{nr}(S_1 \rightarrow T)}{k_r(S_1 \rightarrow S_0)}$ or to a large total triplet decay rate in this molecule. Since the fluorescence quantum yield of pyrazine is 0.01 it follows that a large triplet decay is responsible for the lack of phosphorescence signal. The oscillator strength of the $T_1 \leftarrow S_0$ transition is known to be very small. Therefore the radiative decay of the molecules in the excited triplet state in the travel time τ will be negligible. The combination of a strong signal with a bolometer detector [13] and an absence of signal with a phosphorescence detector leads to the conclusion that the electronic excitation energy of the S_1 state in pyrazine is converted to highly excited vibrational states of the singlet ground state.

This conclusion is in agreement with previous studies on pyrazine, where the decay rates of triplet states near the S_1 origin were found to be $3 \cdot 10^6 \text{ s}^{-1}$ [25]. This fast decay rate can be ascribed to a strong T- S_0 ISC. It was found furthermore from a deconvolution procedure

of the MEs of pyrazine that the zero order triplet states have decay rates on the average of $2 \cdot 10^6 \text{ s}^{-1}$ [26]. The present results confirm that the T_1 triplet background states are strongly coupled to the highly vibrational excited states S_0^* of the singlet ground state. The first excited singlet state transfers its energy on a time scale which is short compared to 1 msec to vibrational energy of the singlet groundstate either directly ($S_1 \rightarrow S_0^*$) or via the triplet channel ($S_1 \rightarrow T_1 \rightarrow S_0^*$). The model proposed by Amirav in which the S_1 state couples to a small number of T_1 states which in turn are coupled by internal conversion to a high background of triplet states is in contradiction with the combined results of the present phosphorescence and bolometer experiments.

In pyrimidine the situation is very similar to that in pyrazine. There too it is found that the triplet decay rates are in the order of $2 \cdot 10^6 \text{ s}^{-1}$ [25]. We conclude that the electronic excitation energy of the S_1 state in pyrimidine is also converted into vibrational energy of the singlet ground state.

For naphthalene it was shown that the ratio of the phosphorescence signal to the fluorescence signal is constant for each rotational J' , K' state up to $J' = 10$. Because the singlet radiative decay rate is independent of the rotational quantum numbers, this means that the ratio $\frac{I_P}{I_F}$ directly reflects the ISC rate $k_{nr}(S_1 \rightarrow T)$. This is under the reasonable assumption that the dependence of the triplet decay rate on J' is negligible. We therefore conclude that the ISC in naphthalene for the vibronic states investigated in the present work is independent of the rotational quantum numbers. This is consistent with the case of a spin-orbit coupling of the excited singlet state to a very dense manifold of triplet states. With the formula of Haarhoff [27] and a S_1 - T_1 energy gap of 12000 cm^{-1} a triplet background density of $10^{10}/\text{cm}^{-1}$ is calculated. It is therefore reasonable to assume that the density of background states is uniform over the energy range we are probing, which indeed results in a rotational independent decay rate in accord with the observation. A rotational independent ISC rate was found in benzene too by Schubert et al [28]. The temporal decay of some selected rotational states was shown to be independent of the rotational quantum numbers. The constant ISC rate appears to be typical for a large molecule as benzene and naphthalene.

Special attention should be paid to the $(4a_g)^1$ vibronic state of naphthalene. All lines in our high resolution spectrum could be assigned with the appropriate relative intensities. Furthermore an ISC rate independent of J' has been found. These observations make an enhanced ISC with the sparse manifold of the nearly degenerate second triplet state T_2 highly improbable. In the case of a strong S_1 - T_2 ISC extra splittings of the rotational lines are expected while due to the difference in rotational energy in the S_1 and the T_2 state a strong rotational dependence of the ISC rate is to be expected. Neither of the two effects have been observed in the present work. This indicates the absence of a strong ISC between the S_1 and T_2 state.

Acknowledgments

We would like to thank Professor J. Kommandeur for bringing the method of phosphorescence under our attention and dr. W.M. van Herpen for helpful discussions. Furthermore we thank the referees for their valuable comments. This work is part of the research program of the Stichting voor Fundamenteel Onderzoek der Materie (FOM) and has been made possible by financial support from the Nederlandse Organisatie voor Wetenschappelijk Onderzoek (NWO).

References

- [1] F. Lahmani, A. Tramer and C. Tric, *J. Chem. Phys.* 60 (1974) 4431
- [2] E.Riedle, H.J. Neusser and E.W. Schlag, *J. Phys. Chem.* 86 (1982) 4847
- [3] H. Abe, S. Kamei, N. Mikami and M. Ito, *Chem. Phys. Lett.* 109 (1984) 217
- [4] T. Suzuki, M. Sato, N. Mikami and M. Ito, *Chem. Phys. Lett.* 127 (1986) 292
- [5] J. Kommandeur, W.A. Majewski, W.L. Meerts and D.W. Pratt, *Ann. Rev. Phys. Chem.* 38 (1987) 433
- [6] B.J. van der Meer, H.T. Jonkman, G. ter Horst and J. Kommandeur, *J. Chem. Phys.* 76 (1982) 2099
- [7] S. Okajima, H. Saigusa and E.C. Lim, *J. Chem. Phys.* 76 (1982) 2096
- [8] P.M. Felker, W.R. Lambert and A.H. Zewail, *Chem Phys. Lett.* 89 (1982) 309
- [9] Y. Matsumoto, L.H. Sprangler and D.W. Pratt, *Laser Chem.* 2 (1983) 91
- [10] B.J. van der Meer, H.T. Jonkman, J. Kommandeur, W.L. Meerts and W.A. Majewski, *Chem. Phys. Lett.* 92 (1982) 565
- [11] W.D. Lawrance and A.E.W. Knight, *J. Phys. Chem.* 89 (1985) 917
- [12] W. Siebrand, W.L. Meerts and D.W. Pratt, *J. Chem. Phys.* 90 (1989) 1313
- [13] W.M. van Herpen, P.A.M. Uijt de Haag and W.L. Meerts, *J. Chem. Phys.* 89 (1988) 3939
- [14] T.E. Gough, R.E. Miller and G. Scoles, *Appl. Phys. Lett.* 30 (1977) 338
- [15] A. Amirav and J. Jortner, *J. Chem. Phys.* 84 (1986) 1500
- [16] J.A. Konings, W.A. Majewski, Y. Matsumoto, D.W. Pratt and W.L. Meerts, *J. Chem. Phys.* 89 (1988) 1813
- [17] A.E.W. Knight, B.K. Selinger and I.G. Ross, *Australian J. Chem.* 26 (1973) 1159
- [18] U. Boesl, H.J. Neusser and E.W. Schlag, *Chem. Phys. Lett.* 31 (1975) 1
- [19] F.M. Behlen and S.A. Rice, *J. Chem. Phys.* 75 (1981) 5672
- [20] D.M. Hanson and G.W. Robinson, *J. Chem. Phys.* 43 (1965) 4174
- [21] W.E. Howard and E.W. Schlag, *Chem. Phys.* 17 (1976) 123
- [22] W.A. Majewski and W.L. Meerts, *J. Mol. Spectrosc.* 104 (1984) 271
- [23] A. Goto, M. Fujii, N. Mikami and M. Ito, *J. Phys. Chem.* 90 (1986) 2370

- [24] A.E.W. Knight, J.T. Jones and C.S. Parmenter, *J. Phys. Chem.* 87 (1983) 973
- [25] T.G. Dietz, M.A. Duncan, A.C. Pulu and R.E. Smalley, *J. Phys. Chem.* 86 (1982) 4026
- [26] W.M. van Herpen, W.L. Meerts, K.E. Drabe and J. Kommandeur, *J. Chem. Phys.* 86 (1987) 4396
- [27] P.C. Haarhoff, *Mol. Phys.* 7 (1963) 101
- [28] U. Schubert, E. Riedle and H.J. Neusser, *J. Chem. Phys.* 84 (1986) 5326

Chapter 3

Vibrational and rotational effects on the intersystem crossing in pyrazine and pyrimidine

Paul Uijt de Haag and W. Leo Meerts
Fysisch Laboratorium, University of Nijmegen
Toernoouweld, 6525 ED Nijmegen, The Netherlands

Abstract

We have measured the laser induced fluorescence spectra of the $6a_0^1$ and the $6b_0^2$ vibronic bands of the $S_1 \leftarrow S_0$ electronic transition in pyrimidine as well as the $6a_0^1$ vibronic band of the $S_1 \leftarrow S_0$ electronic transition in pyrazine. The instrumental line width of 12 MHz allowed the recording of rotationally resolved spectra. Each rotational transition consists of a group of lines due to the coupling of the excited singlet state to background triplet states.

The rotational constants of the S_1 $6a^1$ and the S_1 $6b^2$ states in pyrimidine were determined. Using the standard deconvolution method the singlet-triplet coupling constants and the density of coupled states are derived for several excited rotational states in both bands. The result shows that the intersystem crossing in pyrimidine is independent of the rotational quantum numbers up to $J' = 4$. Comparison with the 0_0^0 vibronic band shows an absence of a strong vibrational effect on the intersystem crossing.

We have also applied the deconvolution method on the P(1)-branch of the $6a_0^1$ vibronic band of pyrazine. The density of background triplet states is increased with a factor of 2.4, in good agreement with the calculated increase in the density of states. Except for a minor diminution of the average coupling matrix element no vibrational effect on the intersystem crossing was found.

3.1 Introduction

In the last years considerable attention has been paid to the problem of a bright state coupled to a manifold of dark background states. Dependent on the density of the coupled states the molecules are historically classified in terms of a small molecule or a large molecule [1]. In the small molecule limit the number of coupled dark states is very low. After excitation the molecule exhibits a single exponential decay with or without quantum beats and the quantum yield equals one. In the large molecule limit on the other hand, an excited molecule still decays exponentially. The quantum yield is however less than one as the high density of dark background states acts as a reservoir to which the energy flows irreversibly.

A molecule can exhibit characteristics of both limiting cases if several different types of background states are available. An example is pyrazine [2]. In this molecule the first excited singlet state is coupled to a sparse manifold of iso-energetic vibronically excited triplet states. This coupling results in the molecular eigenstates. These mixed singlet-triplet states are in turn coupled to a dense manifold of high vibrationally excited states of the electronic ground state. This results in a low quantum yield.

It is interesting to investigate a continuous transition from the small molecule limit to the large molecule limit. An extensive mixing in the manifold of background states results in an averaging of the coupling matrix elements between the bright state and the dark states. A decrease in coupling matrix elements is also expected due to lower Franck-Condon factors. Level repulsion in the manifold of background states in combination with an averaging of the coupling matrix elements leads to an equally spaced molecular eigenstate spectrum with a Lorentzian intensity distribution. In this way information about chaotic behaviour could be derived [3].

A transition from the small molecule limit to the large molecule limit can be achieved by addition of one or more methyl groups [4] or by forming complexes [5]. In both ways the density of background states is increased. The density of background states can also be varied by a change in the excess energy over the vibrationless origin of the dark states. The density of vibronic states depends exponentially on the vibrational excess energy. We have therefore decided to study some vibronically excited states in pyrazine and pyrimidine with high resolution laser spectroscopy. In this way we can also investigate a possible vibrational effect on the intersystem crossing. It has been shown for naphthalene that some vibrational modes exhibit a strongly enhanced intersystem crossing [6]. Also effects of Inter Vibrational Randomization (IVR) may show up in the spectrum [7]. This would result in a scrambling of the rotational quantum number K' [8].

Pyrazine is a prototype for the coupling of a bright state to a set of dark states. Much information has been acquired over the years and a review is given in reference [2]. The experimental data are interpreted in terms of a bright singlet state coupled to a set of nearly iso-energetic triplet states. The high resolution spectrum of the P(1)-branch of the $0_0^0 S_1 \leftarrow S_0$ transition shows about 40 lines [9, 10]. This number of lines in the P(1)-branch is an order of magnitude larger than an estimation based on the formula of Haarhoff [11]. The vibronically excited S_1 $6a^1$ state is located about 583 cm^{-1} above the vibrationless origin [12, 13]. The state exhibits a relatively low quantum yield and the analysis of the biexponential decay suggests an increase in the number of coupled states by an order of magnitude [12]. We report here the high resolution spectrum of the $6a_0^1$ vibronic band

of the $S_1 \leftarrow S_0$ electronic transition in pyrazine. A preliminary experimental spectrum is presented in reference [13]. However, improvements in the experimental set up allowed the recording of more detailed spectra.

Pyrimidine is quite similar to pyrazine. However, the high resolution spectrum of the $0_0^0 S_1 \leftarrow S_0$ transition in pyrimidine appears less distorted [14]. This is due to both the lower density of dark states and the lower magnitude of the coupling matrix elements [14]. The vibrational dependence of the intersystem crossing up to 1300 cm^{-1} was investigated by Saigusa et al [15]. They measured a smooth increase in the number of coupled states. Dispersed fluorescence spectra revealed no evidence for IVR up to a vibrational excess energy of 1000 cm^{-1} [16]. We have therefore measured the high resolution spectra of the $6a_0^1$ and the $6b_0^2$ vibronic bands of the $S_1 \leftarrow S_0$ electronic transition in pyrimidine. The $6a^1$ and $6b^2$ vibronically excited states are the two components of a Fermi resonance with excess energies of 613 cm^{-1} and 670 cm^{-1} [16].

3.2 Experimental

An extensive description of the molecular beam apparatus and the laser system has been given elsewhere [17]. Narrow band UV radiation is generated by intracavity frequency doubling in a single mode ring dye laser (a modified Spectra Physics 380D). Up to 15 mW of UV radiation with a band width of 3 MHz is obtained by using a 2 mm thick, Brewster cut LiIO_3 crystal. For relative frequency measurements a temperature stabilized sealed off Fabry-Perot interferometer is used, while for absolute frequency measurements the iodine absorption spectrum was recorded simultaneously [18].

The molecular beam is formed by a continuous expansion of a mixture of pyrazine (pyrimidine) and argon through a nozzle with a diameter of $100 \mu\text{m}$. Both the pyrimidine sample (Janssen Chimica, purity 99 %) and the pyrazine sample (Janssen Chimica, purity 99+ %) were used at room temperature. The molecular beam is skimmed twice in a differential pumping system. In order to distinguish between stray laser light and the possibility of an overall present background fluorescence the molecular beam is chopped with 10 Hz. The rotational temperature in our molecular beam is typically 3 K.

Excitation of the molecules took place 30 cm from the nozzle orifice. The residual Doppler width in the beam is about 12 MHz and determined by the spatial filtering in the collection optics. The total undispersed fluorescence is imaged on a photomultiplier (EMI 9789QA). Data processing took further place with a standard photon counting system interfaced with a PDP11/23+ computer. In this way the full dynamical range of the spectrum could be used.

3.3 Results and Analysis

3.3.1 Pyrimidine

With the experimental set-up described we have measured the laser induced fluorescence spectrum of two different vibronic bands of the $S_1 \leftarrow S_0$ electronic transition in pyrimidine, the $6a_0^1$ band at 315.6 nm and the $6b_0^2$ band at 315.0 nm. Both spectra consist of a Q-branch and P- and R-branches, clusters of lines separated by about 13 GHz. The observation of

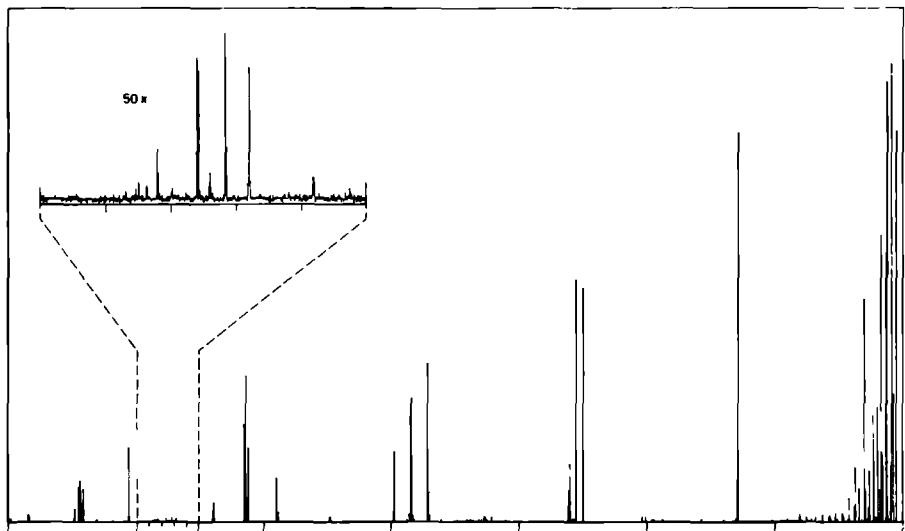


Figure 3.1: Part of the laser induced fluorescence spectrum of the $6a_0^1$ vibronic band of the $S_1 \leftarrow S_0$ electronic transition in pyrimidine showing the P(5)- to Q-branch. The frequency is marked every 10 GHz and increases from left to right. The insert gives an exploded view of the spectrum showing the unidentified lines. Here the frequency is marked every GHz.

a parallel transition is in accord with the symmetry assignments. In figure 3.1 part of the $6a_0^1$ band is given. In figure 3.2 the transitions to the excited state with rotational quantum number $J' = 3$, i.e. the P(4)- and R(2)-branch, are shown for the $6b_0^2$ vibronic band. It is clearly visible that the rotational transitions to the same excited state consist of the same groups of lines. Comparison of these spectra of the two vibronic bands with the high resolution spectrum of the vibrationless $S_1 \leftarrow S_0$ electronic transition [14] clearly reveals that both the $6a_0^1$ band as well as the $6b_0^2$ band appear to be more distorted than the 0_0^0 band. Comparison of the transitions to the same excited state with rotational quantum numbers (J', K'_{-1}, K'_{+1}) is used to identify the lines in the spectrum. The resemblance between the transitions to the same excited upper state proves that the perturbation occurs in the excited vibronic state.

Except for the lines in the spectrum that could be identified with the vibronic transition in pyrimidine, both in the spectrum of the $6a_0^1$ band and in the spectrum of the $6b_0^2$ band unidentified lines appear throughout the whole investigated frequency range. The intensity of the strongest unidentified lines is about 4% of the strongest identified lines. A clear piling up of these unknown lines is visible in between the P- and R-branches. This is shown in the insert in figure 3.1. There is no correspondence between the extra lines in the neighbourhood

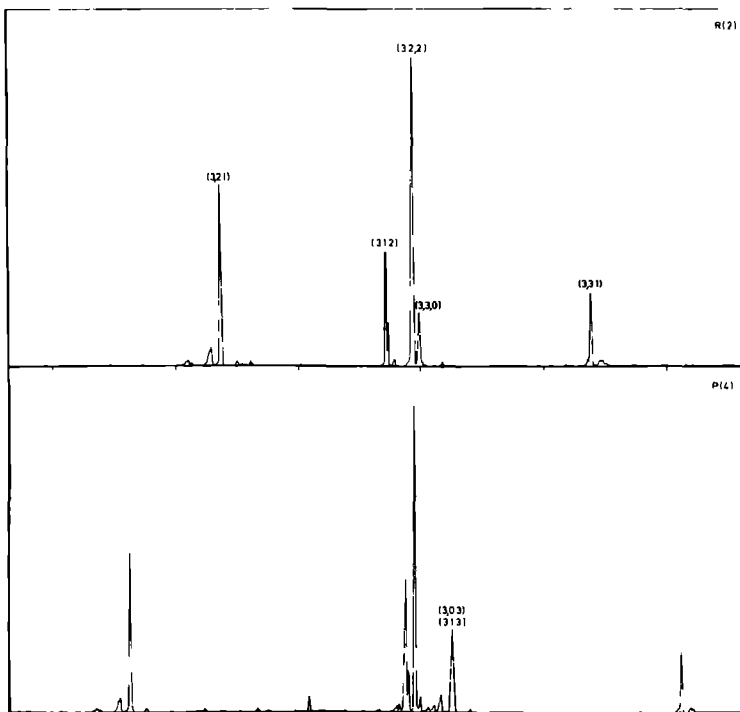


Figure 3.2: The P(4) and R(2) transition of the $6b_0^2$ vibronic band of the $S_1 \leftarrow S_0$ electronic transition in pyrimidine. The frequency is marked every GHz and increases from left to right. The strongest lines are identified by the upper state rotational quantum numbers (J', K'_{-1}, K'_{+1}) .

of a P-branch and the extra lines in the neighbourhood of the R-branch to the same excited state. Hence we conclude that these unidentified lines are not due to a perturbation in the excited vibronic state. Several alternative explanations are also rejected:

- A vibronically induced dipole moment might result in a hybrid band with some perpendicular band intensity. We have therefore simulated both an a-type transition as a b-type transition for these vibronic bands in pyrimidine. In the simulation we have used the rotational constants derived in the fit of the parallel c-type band. No resemblance between the simulated spectrum and the unidentified lines was found however.
- Transitions starting in highly excited rotational states results in extra lines in between the branches. Therefore we have measured the part of the spectrum including

the P(2)- and P(3)-branch with different backing pressures of the seeding gas argon. This results in spectra with different rotational temperatures. The unidentified lines however exhibit the same pressure dependence as the identified lines in the P(2)- and P(3)-branch. Hence we conclude that these lines are not due to transitions from highly excited rotational states. This observation also excludes complexes of pyrimidine.

The unidentified lines appear in both the $6a_0^1$ band and the $6b_0^2$ band and a clear piling up between the branches of pyrimidine is measured. Hence it is unlikely that the unidentified lines are due to a contamination of our pyrimidine sample. The origin of these lines remains therefore an enigma. The existence of these lines does however not interfere with our analysis.

In order to detect a possible rotational dependence of the singlet-triplet coupling we have made a rotational assignment for the lines in the P(5)-branch to the R(3)-branch. We have fitted the spectrum to an asymmetric rotor Hamiltonian [19]. The center of gravity of the excitation intensity of the group of lines belonging to the same rotational transition is used. About 40 transitions were fitted to a parallel c-type band with axis-switching. The selection rules are in this case given by $(K''_{-1}, K''_{+1}) \rightarrow (K'_{-1}, K'_{+1}) = (ee) \rightarrow (oe), (eo) \rightarrow (eo), (oe) \rightarrow (ee), (oo) \rightarrow (oo)$ [20]. In the fit the rotational constants of the ground state were fixed to the values derived by microwave absorption spectroscopy [21] and only the rotational constants of the excited state and the center frequency of the rotationless vibronic transition were used as variables. Table 3.1 lists the obtained molecular constants. The standard deviation of the fit is about 30 MHz. In view of the interval of 300 MHz over which a group of lines belonging to the same rotational transition extends the fit is quite satisfactory. The rotational constants derived here are similar to the results for the 0_0^0 vibronic band [14].

We are now able to determine for some selected rotational states the number of coupled triplet states N , the density of the background triplet states ρ_T and the singlet-triplet coupling matrix elements V_{st} . However, some difficulties arise in this analysis. Since pyrimidine is an oblate near-symmetric rotor ($\kappa = 0.87$ in the electronic ground state and $\kappa = 0.74$ and 0.72 in the S_1 $6a^1$ and the S_1 $6b^2$ excited states respectively) several lines are overlapping. Furthermore, the extra unidentified lines in the spectra are disturbing. We have therefore restricted our analysis to the rotational transitions which were clearly separated in the spectra. Only those lines were taken into account which were present in both the P-branch and the R-branch to the same excited state. Exceptions to this rule are the lines in the P(2)-branch to the excited state with rotational quantum number $K'_{+1} = 1$. Although these lines have no counterpart in the R(0)-branch we have used them in our analysis, as these lines were clearly separated from all other lines.

In the calculation of the singlet-triplet coupling matrix elements V_{st} and the density of coupled triplet states ρ_T we use the procedure developed by Lawrance and Knight [22] to deconvolute the spectrum into the zero order singlet and triplet states. However, this method is in principle only applicable to a spectrum with known absorption intensities, whereas we have measured the laser induced fluorescence spectrum, i.e. a spectrum with excitation intensities. In case of a molecular eigenstate $|z\rangle$ with decay rate γ_i the relation

Table 3.1: Rotational constants of the pyrimidine molecule in the electronic ground state S_0 and the $6a^1$ and $6b^2$ vibronic states of the singlet S_1 state. Also given are the center frequency ν_0 of the vibronic transition and the vibrational excess energy $\Delta\nu_0$ in the singlet S_1 state.

		$6a^1$	$6b^2$
S_0	A'' (MHz)		6276.86 ^a
	B'' (MHz)		6067.18 ^a
	C'' (MHz)		3084.49 ^a
S_1	A' (MHz)	6321.6(0.5)	6294.7(0.5)
	B' (MHz)	5863.2(0.5)	5877.7(0.5)
	C' (MHz)	3029.4(0.5)	3040.5(0.5)
ν_0 (cm ⁻¹)		31686.029(0.004)	31741.934(0.004)
$\Delta\nu_0$ (cm ⁻¹)		613.371(0.008)	669.276(0.008)

^a Ground state rotational constants were fixed to the values derived by microwave absorption spectroscopy [21]. The given errors in the rotational constants are the standard deviations of the fit.

between the excitation intensity E_i and the absorption intensity A_i is given by:

$$E_i = \beta \cdot \frac{A_i^2}{\gamma_i}$$

In this equation β is a proportionality constant. Therefore we can derive the absorption spectrum from the laser induced fluorescence spectrum if the decay rates of the molecular eigenstates are known [10]. However, as the decay rates are not known for the molecular eigenstates in the $6a^1$ and $6b^2$ vibronic states in pyrimidine, two mutually exclusive approximations can be used:

- In case the decay rates of the zero order triplet states are negligible with respect to the decay rate of the zero order singlet state it is easy to show that the decay rate of the molecular eigenstate is proportional to the intensity of the molecular eigenstate [10]. Therefore the excitation intensity is proportional to the absorption intensity.
- In case the decay rates of the zero order triplet states are comparable to the decay rate of the zero order singlet state we can make the approximation that the lifetimes of all molecular eigenstates are equal. In this case the absorption intensity is proportional to the square root of the excitation intensity.

The measured life time of the strongest lines in the P(1)-branch of the $0_0^0 S_1 \leftarrow S_0$ electronic transition in pyrazine showed that there is no clear correspondence between the intensity

Table 3.2: The number of coupled states N , the density of coupled states ρ_T and the average coupling matrix element $\langle V_{st} \rangle$ for some selected rotational states (J', K'_{-1}, K'_{+1}) of the S_1 $6a^1$ and the S_1 $6b^2$ vibronic states in pyrimidine.

	J'	K'_{-1}	K'_{+1}	N	ρ_T (/cm ⁻¹)	$\langle V_{st} \rangle$ (MHz)
$6a^1$	1	0	1	5	41	17
	1	1	1	0		
	1	1	0	2	19	67
	2	1	1	2	3	30
	2	2	1	5	24	13
	2	2	0	6	8	42
	3	2	1	7	25	15
	3	3	1	6	11	37
	4	2	2	3	12	40
	4	3	1	7	22	25
	4	4	1	2	40	19
$6b^2$	1	0	1	5	16	22
	1	1	1	5	8	62
	1	1	0	5	4	54
	2	1	1	7	14	38
	2	2	1	10	16	46
	2	2	0	3	7	33
	3	2	1	11	19	36
	3	3	1	12	16	35
	4	2	2	5	26	19
	4	3	1	5	29	18
	4	4	1	12	16	30

of the transition to the molecular eigenstate and the decay rate of the molecular eigenstate. Also the deconvolution procedure applied to the eigenstates revealed that the decay rates of the zero order triplet states are comparable to the decay rate of the zero order singlet state [10]. Hence we have set in our analysis the decay rates of the measured molecular eigenstates in the $6a_0^1$ and the $6b_0^2$ vibronic transitions in pyrimidine all equal. We have however applied both the deconvolution procedure with an assumed constant life time and the deconvolution procedure with an assumed life time proportional to the intensity for some excited rotational states. The differences between the results of the two deconvolution procedures were minor. Hence the conclusions derived from the deconvolution of the spectra are not influenced by the assumption of the equal life times for the different molecular eigenstates.

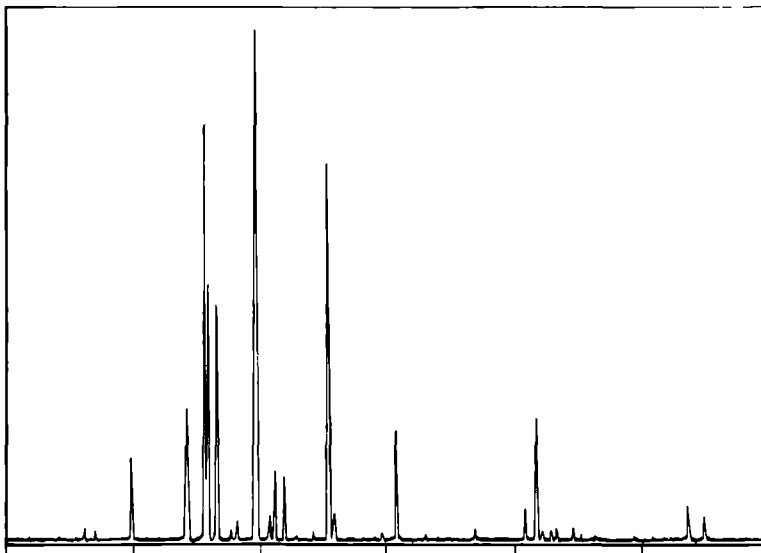


Figure 3.3. The P(1)-branch of the $6a_0^1$ vibronic band of the $S_1 \leftarrow S_0$ electronic transition in pyrazine. The frequency is marked every GHz and increases from left to right.

With the assumed constant life time and the measured fluorescence intensities we are now able to deconvolute the spectrum for some selected rotational states into the zero order singlet and triplet states. The result of the deconvolution procedure is given in table 3.2. The density of coupled triplet states ρ_T is here defined for a set of triplet states $\{|T_1\rangle \dots |T_N\rangle\}$ with energies $\{E_1 \dots E_N\}$ by:

$$\rho_T = \frac{N - 1}{E_N - E_1}$$

3.3.2 Pyrazine

With the experimental set-up described we have also measured the $6a_0^1$ vibronic band of the $S_1 \leftarrow S_0$ vibronic transition in pyrazine at 317.9 nm. The vibrational excess energy in the excited singlet state is 583 cm^{-1} . The spectrum consists of a Q-branch with clearly separated P- and R-branches. The spectrum corresponds to a c-type transition in an oblate near-symmetric rotor, in accord with the symmetry assignments. In figure 3.3 the P(1)-branch is depicted. In between the branches no broad background fluorescence is observed. This means with the present signal to noise ratio that a possible overall present broad band fluorescence [12, 23] is at least a factor 1000 weaker compared to the strong lines in the P(1)-branch.

In order to determine whether there are any lines present which do not belong to the $6a_0^1$ vibronic band of pyrazine we have compared the R(0)-branch with the P(2)-branch. All lines present in the R(0)-branch have their counterpart in the P(2)-branch. Hence we conclude that all lines measured in our laser induced fluorescence spectrum belong to the $6a_0^1$ vibronic band in pyrazine.

Even in the R(0)-branch many lines are overlapping. Therefore we have restricted our analysis to the P(1)-branch. A list of the measured frequencies and intensities is given in table 3.3. We have applied the procedure of Lawrance and Knight [22] to deconvolute

Table 3.3: Observed frequencies and intensities of the transitions in the P(1)-branch of the $S_1(6a^1) \leftarrow S_0$ vibronic transition in pyrazine. Frequencies are given relative to the center of gravity of the excitation intensity.

frequency (MHz)	intensity	frequency (MHz)	intensity
2087	52	149	142
1848	57	268	5829
1654	127	317	435
1566	134	695	113
-1280	1277	811	1689
-877	66	1036	68
-855	2076	1416	158
-837	184	1809	500
-711	6440	1898	1893
-689	3979	1944	137
-620	3618	2017	155
-499	163	2059	177
456	301	2183	183
-308	7883	2245	62
198	383	2369	61
-158	1078	3085	515
-83	1000	3099	240
15	54	3215	372

the spectrum into the zero order singlet and triplet states. In this procedure we have assumed that the decay rates of all the molecular eigenstates are equal. The result of this deconvolution procedure is given in table 3.4. The singlet position is calculated at +194 MHz. This value corresponds to the center of gravity of the absorption intensities.

Table 3.4: Calculated triplet state positions and singlet-triplet coupling matrix elements V_{st} for the $J' = 0$ state of the $S_1(6a^1)$ vibronic state of pyrazine. The singlet position is calculated at 194 MHz. The positions are given relative to the center of gravity of the excitation intensity. Also given are the density of triplet states ρ_T and the average coupling matrix element $\langle V_{st} \rangle$.

frequency (MHz)	V_{st} (MHz)	frequency (MHz)	V_{st} (MHz)
-2074	145	182	194
-1836	129	308	53
-1640	126	660	277
1548	161	750	244
1237	209	1020	162
875	20	1364	404
843	36	1626	651
-817	106	1840	155
-700	28	1935	71
-647	80	1999	132
-523	150	2046	95
-477	110	2161	166
-409	200	2235	102
-226	136	2356	136
-179	81	2962	570
-106	109	3093	33
6	97	3188	172
109	251		

$\rho_T = 194$ states per cm^{-1}
 $\langle V_{st} \rangle = 178$ MHz

3.4 Discussion

It has been shown for the $6a_0^1$ and the $6b_0^2$ vibronic bands in pyrimidine that each rotational transition corresponds to a well-defined group of lines. As these groups of lines are entirely different for the transitions to the states with different K'_{-1}, K'_{+1} quantum numbers, it is concluded that the rotational quantum numbers K'_{-1}, K'_{+1} are still valid in the $6a^1$ and $6b^2$ vibronic states in pyrimidine. In case of an extensive K' -scrambling in the excited state the transitions to states with the same rotational quantum number J' but different rotational quantum number K' would consist of identical groups of lines but with different relative intensities. This result shows that there is neither a direct coupling within the excited singlet state nor an indirect coupling via an intermediate triplet state in pyrimidine up to

670 cm^{-1} of vibrational excess energy. This result is not surprising as two nearby excited rotational states cannot interact due to different symmetry species (the rotational symmetry in the excited S_1 state is A_1 in case $(K_{-1}, K_{+1}) = (e, e)$, A_2 in case $(K_{-1}, K_{+1}) = (e, o)$, B_1 in case $(K_{-1}, K_{+1}) = (o, o)$ and B_2 in case $(K_{-1}, K_{+1}) = (o, e)$). Rotational states with the same symmetry have large energy separations with respect to the typical singlet-triplet coupling matrix elements of 50 MHz. The fact that there is no coupling within the singlet state justifies the use of the deconvolution procedure as this procedure is only applicable to a single bright state coupled to a set of dark states.

The results of the deconvolution procedure for the two vibronic bands in pyrimidine as listed in table 3.2 indicates that neither the number of coupled states N nor the average coupling matrix elements $\langle V_{st} \rangle$ systematically depend on the rotational quantum numbers (J', K'_{-1}, K'_{+1}) . In case of an extensive K -scrambling in the set of background states the number of coupled states would increase linearly with the rotational quantum number J' . Hence we conclude that there is no extensive K -scrambling in the triplet state of pyrimidine at 3200 cm^{-1} excess energy. The absence of a rotational effect on the coupling matrix elements V_{st} indicates an absence of a Coriolis induced intersystem crossing in pyrimidine. It should be noted however that this result is not in contradiction with the rotational dependence of the decay process of the mixed singlet-triplet eigenstates in the vibrationless excited singlet state [14].

We can compare the measured density of coupled states ρ_T with the density of vibronic states calculated with the formula of Haarhoff [11]. In the calculation the ground state vibrational frequencies are used [16]. This probably results in an underestimation of the calculated density of states since ground state frequencies tend to be higher. A singlet-triplet gap of 2543 cm^{-1} is assumed [24]. The calculation results in a density of vibronic states $\rho_T^v = 6$ states per cm^{-1} at a triplet excess energy of 3200 cm^{-1} .

To calculate the density of coupled triplet states the selection rules for spin-orbit coupling have to be considered. Since direct spin-orbit coupling is forbidden between singlet and triplet states of the same electronic configuration we have to consider second order spin-orbit coupling. The matrix elements and selection rules for vibronically induced spin-orbit coupling and rotationally induced spin-orbit coupling are derived by Stevens and Brand [25].

In case of vibronically induced spin-orbit coupling vibrations of the symmetry species a_2 , b_1 and b_2 in the T_1 state can couple to the excited singlet state. The rotational selection rules (symmetric top limit) are $\Delta J = 0$, $\Delta N = 0, \pm 1$ and $\Delta K = 0$ (if the symmetry species of the vibration is b_2) and $\Delta J = 0$, $\Delta N = 0, \pm 1$ and $\Delta K = \pm 1$ (if the symmetry species of the vibration is a_2 or b_1). Hence an estimation of the calculated density of triplet states coupled via vibrationally induced spin-orbit coupling amounts to $\rho_T = 20$ states per cm^{-1} .

In case of rotationally induced spin-orbit coupling vibrations of the symmetry species a_1 can couple to the excited singlet state with the rotational selection rules $\Delta J = 0$, $\Delta N = 0, \pm 1$ and $\Delta K = 0, \pm 2$ (symmetric top limit). Hence the calculated density of triplet states coupled via rotationally induced spin-orbit coupling amounts to $\rho_T = 14$ states per cm^{-1} .

The measured total density of states is on the order of 20 states per cm^{-1} , in good agreement with the calculation.

The results for the $6a_0^1$ and the $6b_0^2$ vibronic bands in pyrimidine show no marked difference. As the vibrational wave functions are extensively mixed due to the Fermi-resonance [16], this result is not surprising. A comparison of the results for the 0_0^0 band and

the results for the $6a_0^1$ and $6b_0^2$ vibronic bands is hampered by the low dynamical range of the spectra of the 0_0^0 band [14]. However, the coupling matrix elements are the same order of magnitude in these three states. Hence we conclude that there is no strong vibrational effect on the intersystem crossing in pyrimidine for the lower vibronic states considered here.

The spectrum of the $6a_0^1$ vibronic band in pyrazine clearly reveals that (K'_{-1}, K'_{+1}) are still valid quantum numbers in the excited state at a vibrational excess energy of 583 cm^{-1} . Therefore the use of the deconvolution procedure is justified. We are now able to compare the results for the $(J', K'_{-1}, K'_{+1}) = (0, 0, 0)$ rotational state in the S_1 $6a^1$ state, as listed in table 3.4, with the results for the $(J', K'_{-1}, K'_{+1}) = (0, 0, 0)$ rotational state in the vibrationless S_1 state, as given in reference [10]. However, the signal to noise ratio for the P(1)-branch was better in the 0_0^0 vibronic band than in the $6a_0^1$ vibronic band. This means that more weak lines are visible in the 0_0^0 vibronic band. Furthermore, the deconvolution procedure for the vibrationless S_1 state was performed with the known decay rates of the molecular eigenstates. In order to compare the results for the different vibronic states we have repeated the deconvolution procedure for the P(1) branch of the 0_0^0 band. In this new deconvolution of the spectrum only the 14 strongest lines with an intensity of more than 0.6% of the strongest line were taken into account, in accord with the signal to noise ratio of the $6a_0^1$ band. A constant life time was used for the excited molecular eigenstates.

The result for the measured density of triplet states is $\rho_T = 82$ states per cm^{-1} in the vibrationless excited state and $\rho_T = 194$ states per cm^{-1} in the $6a^1$ excited state. This corresponds with an increase in the density of triplet states with a factor 2.4. A calculation using the ground state frequencies [26] results in an increase in the density of background states with a factor of 2.7, in good agreement with the experimental value.

The calculation resulted in a density of vibronic triplet states $\rho_T^v = 35$ states per cm^{-1} at a triplet vibrational excess energy of 4056 cm^{-1} and $\rho_T^v = 93$ states per cm^{-1} at a triplet vibrational excess energy of $4056 + 582 \text{ cm}^{-1}$. These calculated densities are somewhat less than results reported elsewhere [2, 27]. With the selection rules for indirect spin-orbit coupling [25] we deduce a calculated density of coupled triplet states to the $(J', K'_{-1}, K'_{+1}) = (0, 0, 0)$ rotational singlet state as $\rho_T = 4$ states per cm^{-1} at a vibrational excess energy of 4056 cm^{-1} and $\rho_T = 12$ states per cm^{-1} at a vibrational excess energy of $4056 + 582 \text{ cm}^{-1}$.

This result is two orders of magnitude less than the measured density of states. Since the density of triplet states is measured for the $J' = 0$ state we can not explain this large discrepancy by the assumption of a resolved hyperfine structure [27]. The large discrepancy between the calculated density of states and the measured density of states suggests therefore a coupling within the triplet manifold. Such an interstate coupling is also assumed in the explanation of the high resolution magnetic field spectra of the pyrimidine molecule [14].

The average coupling strength is given by $\langle V_{st} \rangle = 214 \text{ MHz}$ in the vibrationless excited state and $\langle V_{st} \rangle = 178 \text{ MHz}$ in the $6a^1$ excited state. This small decrease in coupling constant can be attributed to a diminishing Franck-Condon overlap between the bright singlet state and the vibronically excited triplet states.

It is interesting to determine whether the vibrational states in the triplet state are completely mixed. In case of an extensive mixing we expect an averaging of the coupling

matrix elements. As a measure of the degree of mixing we have calculated the number:

$$\frac{1}{N} \sum \frac{(V_{st} - \langle V_{st} \rangle)^2}{\langle V_{st} \rangle^2}$$

This number amounts to 0.54 in the vibrationless excited state and 0.65 in the $6a^1$ excited state. We conclude that the increase in vibrational excess energy with 583 cm^{-1} does not result in an additional mixing of the vibrational wave functions of the vibronic background states. Hence the variation in the singlet-triplet coupling matrix elements is determined by the Franck-Condon overlap between the bright singlet state and the dark background states.

Acknowledgment

This work was financially supported by the Dutch Organisation for Scientific Research (FOM/NWO). We thank dr. W.M. van Herpen for experimental assistance.

References

- [1] F. Lahmani, A. Tramer and C. Tric, *J. Chem. Phys.* 60 (1974) 4431
- [2] J. Kommandeur, W.A. Majewski, W.L. Meerts and D.W. Pratt, *Ann. Rev. Phys. Chem.* 38 (1987) 433
- [3] S.L. Coy and K.K. Lehmann, *Phys. Rev. A* 36 (1987) 404
- [4] K. Uchida, I. Yamazaki and H. Baba, *Chem. Phys.* 35 (1978) 91
- [5] H. Abe, Y. Ohyanagi, M. Ichijo, N. Mikami and M. Ito, *J. Phys. Chem.* 89 (1985) 3512
- [6] T. Suzuki, M. Sato, N. Mikami and M. Ito, *Chem. Phys. Lett.* 127 (1986) 292
P. Uijt de Haag and Leo Meerts, *Chem. Phys.* 135 (1989) 139
- [7] G.M. Nathanson and G.M. McClelland, *J. Chem. Phys.* 84 (1986) 3170
- [8] P.J. de Lange, B.J. van der Meer, K.E. Drabe, J. Kommandeur, W. L. Meerts and W.A. Majewski, *J. Chem. Phys.* 86 (1987) 4004
- [9] B.J. van der Meer, H.T. Jonkman, J. Kommandeur, W.L. Meerts and W.A. Majewski, *Chem. Phys. Lett.* 92 (1982) 565
- [10] W.M. van Herpen, W.L. Meerts, K.E. Drabe and J. Kommandeur, *J. Chem. Phys.* 86 (1987) 4396
- [11] P.C. Haarhoff, *Mol. Phys.* 7 (1963) 101
- [12] A. Amirav, *Chem. Phys.* 126 (1988) 365
- [13] B.J. van der Meer thesis (1985)
- [14] W.L. Meerts and W.A. Majewski, *Laser. Chem.* 5 (1986) 339
J.A. Konings, W.A. Majewski, Y. Matsumoto, D.W. Pratt and W.L. Meerts, *J. Chem. Phys.* 89 (1988) 1813
- [15] H. Saigusa, A.K. Jameson and E.C. Lim, *J. Chem. Phys.* 79 (1983) 5228
- [16] A.E.W. Knight, C.M. Lawburgh and C.S. Parmenter, *J. Chem. Phys.* 63 (1975) 4336
- [17] W.A. Majewski and W.L. Meerts, *J. Mol. Spectrosc.* 104 (1984) 271
W.M. van Herpen, thesis 1988
- [18] S. Gerstenkorn and P. Luc, *Atlas du spectroscopie d'absorption de la molecule d'iode* (Centre National de la Recherche Scientifique) 1978
S. Gerstenkorn and P. Luc, *Rev. Phys. Appl.* 14 (1979) 791
- [19] J.K.G. Watson, *J. Chem. Phys.* 46 (1967) 1935
J.K.G. Watson, *J. Chem. Phys.* 48 (1968) 4517

- [20] R.E. Smalley, L.H. Wharton, D.H. Levy and D.W. Chandler, *J. Mol. Spec.* 66 (1977) 375
- [21] G.L. Blackman, R.D. Brown and F R. Burden *J. Mol. Spec.* 35 (1970) 444
- [22] W.D. Lawrance and A.E.W. Knight, *J. Phys. Chem.* 89 (1985) 917
- [23] A. Amirav, *Chem. Phys.* 108 (1986) 403
- [24] T. Takemura, K. Uchida, M. Fujita, Y. Shindo, N. Suzuki and H. Baba, *Chem. Phys. Lett* 73 (1980) 12
- [25] C.G. Stevens and J.C.D. Brand, *J. Chem. Phys.* 58 (1973) 3324
- [26] G. Herzberg, *Molecular spectra and molecular structure*, Vol 3, (Van Nostrand Company Inc.) 1966
- [27] W. Siebrand, W.L. Meerts and D.W. Pratt, *J. Chem. Phys.* 90 (1989) 1313

Chapter 4

Rotational assignments in the S_1 ($^1B_{3u}$) state of pyrazine by UV-UV pump-probe laser spectroscopy

Paul Uijt de Haag, Johannes Heinze and W. Leo Meerts

*Fysisch Laboratorium, University of Nijmegen
Toernooeweld, 6525 ED Nijmegen, The Netherlands*

abstract

We have applied an UV-UV pump-probe experiment on the $0_0^0 S_1(^1B_{3u}) \leftarrow S_0(^1A_g)$ vibronic transition in pyrazine. The use of two single frequency lasers and a molecular beam apparatus made it possible to verify experimentally the rotational assignments for the strongest lines in the high resolution spectrum of the S_1 state in pyrazine. The experimental results confirm the previously made identifications [1].

4.1 Introduction

It is nowadays well established that the first excited singlet state in pyrazine ($p\text{-C}_4\text{H}_4\text{N}_2$) is subjected to an intersystem crossing with nearly iso-energetic vibrationally excited triplet states [2]. Due to this coupling mixed singlet-triplet states result, the molecular eigenstates. As a result each single rovibronic transition of the $S_1(^1B_{3u}) \leftarrow S_0(^1A_g)$ electronic transition in pyrazine consists of a cluster of lines: the molecular eigenstate spectrum. The analysis of such a molecular eigenstate spectrum is usually performed with the deconvolution procedure developed by Lawrance and Knight [3]. In this procedure the zero order singlet state and the zero order triplet states are reconstructed with the use of the line positions and the absorption intensities of the molecular eigenstate spectrum. However, this deconvolution procedure is only valid in the case of a single bright state coupled to a set of dark states. Therefore the procedure was in first instance only applied to the P(1)-branch of the $0_0^0 S_1 \leftarrow S_0$ transition in pyrazine [4].

Recently the analysis of the molecular eigenstate spectrum of the $0_0^0 S_1 \leftarrow S_0$ electronic transition in pyrazine (a parallel c-type band) was extended to excited states with rotational quantum number $J' \leq 3$ [1]. This was accomplished by a careful comparison of the transitions in the P-branch and the R-branch to the same excited rovibronic state. In this way the complex spectrum could be disentangled into clusters of lines belonging to the same rovibronic transition. However, transitions to the excited rovibronic state with rotational quantum number $K'_{+1} = J'$ are not present in the R-branch. In principle a comparison of the Q-branch and the P-branch can be used for the assignment of the lines to the excited states with $K'_{+1} = J'$. However, due to the strong accumulation of the lines in the Q-branch this method is not practically applicable. Therefore the positions in the P-branch of the transitions to the excited states with $K'_{+1} = J'$ were calculated with the deduced rotational constants. The extra lines in the P-branch with respect to the corresponding R-branch were then attributed to the transitions to the $K'_{+1} = J'$ states in such a manner that the centers of gravity of the assigned lines correspond to the calculated positions. However, as the frequency spread of the lines in the spectrum is comparable to the rotational splittings, part of the identifications are somewhat arbitrary.

We have therefore decided to verify experimentally some of the assignments of the lines in the $0_0^0 S_1 \leftarrow S_0$ vibronic transition in pyrazine. The method used is a pump-probe experiment. The pyrazine molecule has no permanent electric dipole moment as it belongs to the molecular symmetry group D_{2h} . Hence it is not possible to use microwave radiation as the pumping source. Therefore an UV-UV pump-probe experiment is chosen.

4.2 Experimental

The experimental set-up is shown in figure 4.1. A molecular beam is formed by a continuous expansion of pyrazine vapor seeded in argon through a nozzle with a diameter of $100 \mu\text{m}$. The pyrazine sample (Janssen Chimica, purity 99+ %) was kept at room temperature. The molecular beam is skimmed twice in a differentially pumped system.

At a distance of 30 cm from the nozzle orifice the molecules are excited by the continuous wave radiation field of a single frequency ring dye laser (a modified Spectra Physics 380D). By intracavity frequency doubling with a Brewster cut LiIO_3 crystal about 8 mW UV

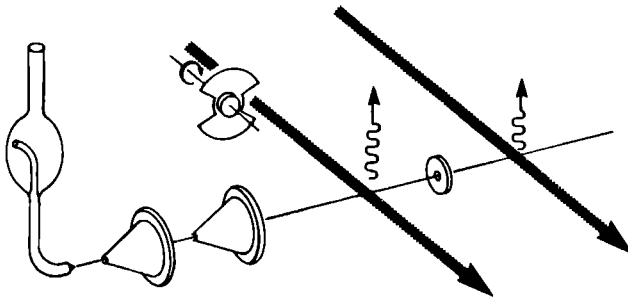


Figure 4.1: Outline of the experimental set-up. The molecular beam is crossed with an UV pump laser at a distance of 30 cm from the nozzle. The pump laser is modulated by a chopper. The hole in the population distribution of the molecules in the beam produced by the pump laser is probed with a second UV laser 60 cm away from the nozzle.

radiation was obtained. The band width of the laser is 3 MHz as a result of the frequency jitter of the laser. This pump laser is tuned to a strong line belonging to the rovibronic $(J', K'_{-1}, K'_{+1}) \leftarrow (J'', K''_{-1}, K''_{+1})$ cluster of lines of the $0_0^0 S_1 \leftarrow S_0$ transition in pyrazine. In this way a hole is pumped in the population distribution in the electronic ground state at the state with rotational quantum numbers $(J'', K''_{-1}, K''_{+1})$. In order to keep the pump laser tuned on the molecular transition the laser induced fluorescence signal is monitored continuously. The line width of the molecular transition is Doppler limited and amounts to 12 MHz. The pump laser is modulated with a mechanical chopper. This allows the use of standard lock-in techniques and the possibility to measure against zero background.

After excitation of the molecules with rotational quantum numbers $(J'', K''_{-1}, K''_{+1})$ by the pump laser the molecules travel for another 30 cm. The life time of the molecules in the excited state is about 200-600 nsec [4]. This is much shorter than the estimated travel time of 0.5 msec. However, the hole burnt in the population distribution remains almost completely due to the low quantum yield of pyrazine [5, 6] and due to the distribution over the different rovibronic states in the electronic ground state after fluorescence relaxation. This hole in the population distribution at the rotational ground state $(J'', K''_{-1}, K''_{+1})$ is probed with a second cw single frequency ring dye laser (also a modified Spectra Physics 380D). The UV output power of the probe laser was 3 mW and the band width of the laser was 0.5 MHz due to frequency jitter. In the experiment the probe laser is scanned across the P-branch containing the pumped line and the laser induced fluorescence is detected. As the pump laser is modulated the intensities of the lines with the same rotational ground state as the pumped line are also modulated. In this way a rotational identification can be made for the lines in the molecular eigenstate spectrum of the $0_0^0 S_1 \leftarrow S_0$ transition in pyrazine.

4.3 Results and Discussion

Some severe experimental difficulties are encountered in such a molecular beam UV-UV pump-probe experiment. The life time of the excited molecular eigenstates are known to be in the 200-600 nsec range [4]. Hence the homogeneous line width $\Delta\nu_L$ of the transitions due to the life time broadening is 0.8 - 0.3 MHz. This is small compared to the inhomogeneous Doppler line width in our molecular beam of 12 MHz. The frequency jitter of the pump laser amounts to 3 MHz, i.e. about five times the homogeneous line width $\Delta\nu_L$ whereas the frequency jitter of the probe laser is comparable to the homogeneous line width $\Delta\nu_L$. As a consequence the pump laser and the probe laser interact to a large extend with different velocity groups of molecules in our molecular beam, even if the center frequencies of the lasers are equal.

We have therefore focused the lasers to an estimated spot size of 70 μm in the molecular beam. In this way the lines are homogeneously broadened due to the small interaction time of the molecules with the laser beams. In the case of a Gaussian laser beam shape the time of flight broadened line width $\Delta\nu_T$ (FWHM) is given by [7]:

$$\Delta\nu_T = \frac{2}{\pi} \sqrt{2 \ln 2} \frac{v_B}{d}$$

In this equation v_B represents the beam velocity and d equals the laser beam diameter between the points where the intensity drops to e^{-2} . With the values appropriate to our experimental conditions a homogeneous time of flight line width $\Delta\nu_T = 3$ MHz is obtained.

In this way the pump laser and the probe laser interact with the same group of molecules despite the frequency jitter of the lasers. However, the disadvantage of the strong focusing of the two lasers is obvious. In order to interact with the same molecules the interaction point of the probe laser and the molecular beam has to be on the line connecting the nozzle and the interaction point of the pump laser and the molecular beam. Therefore the probe laser and the pump laser have to be aligned within a few tens micrometers. As a result small vibrations of the building and/or the beam machine affect the pump-probe signal strongly.

Despite the experimental difficulties we were able to obtain an UV-UV pump-probe signal on the strongest lines of the $0_0^0 S_1 \leftarrow S_0$ transition in pyrazine. In figure 4.2 the laser induced fluorescence spectrum of the P(2) branch of the $0_0^0 S_1 \leftarrow S_0$ transition in pyrazine is shown. The insert shows the pump-probe spectrum recorded with the pump laser tuned to the line marked with an asterisk. Although the signal to noise ratio in the pump-probe spectrum is low it is clearly established that the two strong lines lying closely together are members of the same rotational transition, whereas the strong line on the low frequency side of the P(2)-branch is part of a different rotational transition. In the rotational assignments based on a comparison of the P(2)-branch and the R(0)-branch the strong line on the lower frequency side of the P(2)-branch is identified as a $(J', K'_{-1}, K'_{+1}) \leftarrow (J'', K''_{-1}, K''_{+1}) = (1, 1, 0) \leftarrow (2, 2, 0)$ transition, whereas the two strong lines lying closely together were identified as $(J', K'_{-1}, K'_{+1}) \leftarrow (J'', K''_{-1}, K''_{+1}) = (1, 1, 1) \leftarrow (2, 2, 1)$ transitions [1]. The result of the pump-probe experiment therefore affirms conclusively these assignments based on the comparison of the different branches and based on the calculation of the center of gravity of the rotational transition. It is clear however that we can hardly comment on the small lines in the laser induced fluorescence spectrum of the P(2)-branch due to the low signal to noise ratio in the pump-probe experiment.

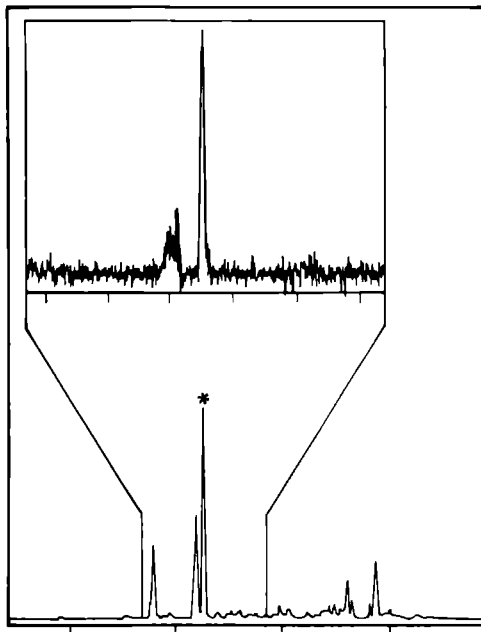


Figure 4.2: The laser induced fluorescence spectrum of the P(2)-branch of the $0_0^0 S_1 \leftarrow S_0$ transition in pyrazine. The frequency is marked every GHz and increases from left to right. The insert shows the pump-probe spectrum with the pump laser tuned to the line marked with a *. Here the frequency is marked every 200 MHz.

In the P(3)-branch there is only one relatively strong line. In order to determine the rotational quantum numbers of this line, we have also measured the pump-probe signal in the Q-branch, with the pump laser tuned to the same strong line in the P(2)-branch (marked with a * in figure 4.2). In this way we probe the lines of the rovibronic transition $(J', K'_{-1}, K'_{+1}) \leftarrow (J'', K''_{-1}, K''_{+1}) = (2, 1, 1) \leftarrow (2, 2, 1)$. It appeared that there is a strong line in the Q-branch exhibiting a detectable pump-probe signal. This result proves that the transition to the $(J', K'_{-1}, K'_{+1}) = (2, 1, 1)$ rovibronic state is a relatively strong line in the P(3)-branch and the R(1)-branch. This result justifies the assignment made previously [1], where the strongest line in the P(3)-branch is assigned as the transition to the $(J', K'_{-1}, K'_{+1}) = (2, 1, 1)$ rovibronic state.

We conclude that it is possible to obtain the rotational assignments for the strongest lines in the high resolution spectrum of the $0_0^0 S_1 \leftarrow S_0$ transition in pyrazine despite the experimental problems. The assignments made previously [1] were confirmed for some lines with this experimental method.

Acknowledgment

This work was financially supported by the Dutch Organisation for Scientific Research (FOM/NWO).

References

- [1] W. Siebrand, W.L. Meerts and D.W. Pratt, *J. Chem. Phys.* 90 (1989) 1313
- [2] for a review see: J. Kommandeur, W.A. Majewski, W.L. Meerts and D.W. Pratt, *Ann. Rev. Phys. Chem.* 38 (1987) 433
- [3] W.D. Lawrance and A.E.W. Knight, *J. Phys. Chem.* 89 (1985) 917
- [4] W.M. van Herpen, W.L. Meerts, K.E. Drabe and J. Kommandeur, *J. Chem. Phys.* 86 (1987) 4396
- [5] A. Amirav and J. Jortner, *J. Chem. Phys.* 84 (1986) 1500
- [6] P.J. de Lange, B.J. van der Meer, K.E. Drabe, J. Kommandeur, W.L. Meerts and W.A. Majewski, *J. Chem. Phys.* 86 (1987) 4004
- [7] W. Demtröder, *Laser Spectroscopy* (Springer-Verlag) 1982

Chapter 5

A study of the $S_1 6^1(1A_2'')$ vibronically excited state of sym-triazine by high resolution UV laser spectroscopy

Paul Uijt de Haag and W. Leo Meerts
Fysisch Laboratorium, University of Nijmegen
Toernoouweld, 6525 ED Nijmegen, The Netherlands

Jon T. Hougen¹
Molecular Spectroscopy Division
National Institute of Standards and Technology
Gaithersburg, MD 20899, USA

Abstract

We have measured the laser induced fluorescence spectrum of the $S_1 6^1(1A_2'') \leftarrow S_0(1A_1')$ vibronic transition in sym-triazine at 317 nm. An instrumental line width of 12 MHz was achieved by the use of a molecular beam in combination with a cw single frequency laser. In this way rotationally resolved spectra were obtained. Furthermore we have measured the life time of some selected ensembles of rovibronic states with a narrow band pulsed laser system.

It is shown that the excited $S_1 6^1(A_2'')$ vibronic state is strongly perturbed by a singlet-triplet interaction. This interaction results in additional lines in the high resolution spectrum. A nearly complete rotational assignment is given for the transitions to the upper state with rotational quantum number J up to $J = 4$ and the rotational constants are derived. No evidence is found for a Jahn-Teller distortion of the rotational states in the $S_1 6^1(A_2'')$ vibronic state.

With some assumptions the singlet-triplet coupling matrix elements were deduced as well as the energy separation between the singlet state and the perturbing triplet state. A singlet-triplet gap of $4800 \pm 600 \text{ cm}^{-1}$ is estimated.

¹Nederlandse organisatie voor Wetenschappelijk Onderzoek, visiting scientist University of Nijmegen, spring 1989

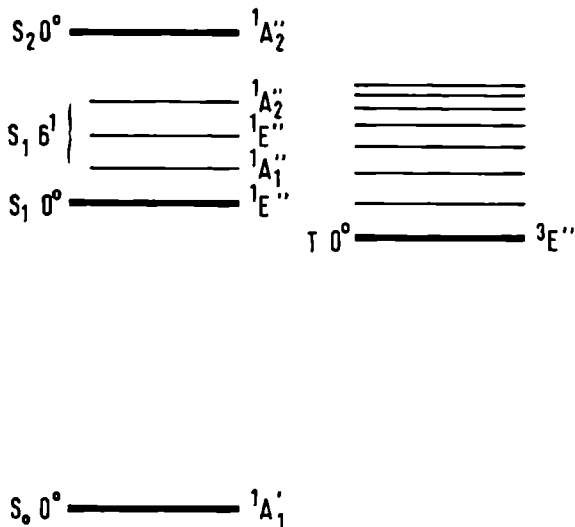


Figure 5.1: Energy level diagram of the different vibronic states in sym-triazine. The exact location of the $S_1 6^1$ states with symmetry E'' and A_1'' is not known.

5.1 Introduction

The molecule sym-triazine (sym- $C_3H_3N_3$) is the most symmetric azabenzene. In the electronic ground state the molecule belongs to the molecular point group D_{3h} . The vibronic structure of sym-triazine has received a lot of attention over the years and appears to be rather complex [1]. The first excited singlet state is double degenerate and of symmetry E'' . It arises from a $n(e') \rightarrow \pi^*(e'')$ electron promotion. This electron promotion also gives rise to singlet states of symmetry A_1'' and A_2'' . These states are expected in the vicinity of the E'' state. The electronic transition from the ground state $1A_1'$ to the first excited singlet state $1E''$ is one photon electronically forbidden, but two photon allowed. However, excitation of vibrations of symmetry e' in the electronic state of symmetry E'' results in vibronic states of symmetry A_2'' ($E'' \otimes e' = A_1'', A_2''$ and E''). These states may be subject to a Jahn-Teller distortion [2]. The transition to these vibronically excited states are one photon allowed whereas coupling of these vibronically excited states to the nearby electronic state with symmetry $1A_2''$ may enhance the transition probability. An energy level diagram is given in figure 5.1.

Several spectroscopic studies on the vibronic structure of the first excited singlet state have been performed with such distinct techniques as one photon absorption spectroscopy [3], two photon absorption spectroscopy via photo acoustic detection [4], one photon laser induced fluorescence spectroscopy [5, 6, 7, 8] and two photon resonant multi photon ionization

spectroscopy [9]. The analysis of the spectra indicates that the vibrationless electronic transition to the E'' electronic state is situated at 30869 cm^{-1} [4]. The coupling between the ${}^1E''$ and ${}^1A_2''$ electronic states is induced by vibrations of mode ν_6 . The first strong line in the one photon laser induced fluorescence spectrum is situated 677 cm^{-1} above the electronic origin and is assigned as the transition to the $S_1\ 6^1$ state with vibronic symmetry A_2'' [5]. The rotational structure of this line showed nicely resolved P-, Q- and R-branches and indicates a parallel transition, in agreement with the symmetry assignment. However, the spectral resolution was too low to reveal the K -substructure. Furthermore no evidence was found for a Jahn-Teller perturbation in this excited state. This resulted in an upper limit for the Coriolis coupling constant between the different vibronic states. It was our aim to examine the Jahn-Teller perturbation in this excited state by measuring a high resolution spectrum with resolved K -substructure.

Besides the coupling to the different nearby singlet states, it is likely that excited vibronic singlet states are also coupled via intersystem crossing to iso-energetic rovibronic states of the lower lying triplet states. However, the available data at the moment are not very conclusive. First of all, neither the origin of the ${}^3E''$ state is known nor the position of the other low lying triplet states. An absorption band located at 28935 cm^{-1} is attributed to an excited ${}^3E'' \otimes e'$ vibronic state [10]. This indicates that at least one triplet state is located more than 2600 cm^{-1} below the $S_1\ 6^1(A_2'')$ state. Photoelectron spectra after excitation of the $S_1\ 6^1(A_2'')$ state were interpreted in terms of a strong intersystem crossing to a triplet state lying at about 5000 cm^{-1} below the $S_1\ 6^1(A_2'')$ state [9].

Time resolved fluorescence spectra of the $S_1\ 6^1(A_2'')$ state showed either a biexponential decay [7] or a single exponential decay [8, 11] depending on the experimental conditions. These experimental results were interpreted in the classical terms of a small molecule or an intermediate case molecule with respect to the singlet-triplet coupling [12]. Intriguing was the measured life time dependence on the rotational quantum number of the upper state J' in one of the experiments [8]. The life time varied from 85 nsec for $J' = 1$ to 120 nsec for $J' = 6$. However, other experiments showed a more random variation in the measured life time with respect to the excited rotational state [11]. The low quantum yield of sym-triazine indicates that internal conversion to the dense manifold of the singlet ground state and/or intersystem crossing to a dense set of triplet states is the predominant decay channel of the excited state. The dependence of the life time shows that rotation might be important in this process.

We felt that a high resolution spectrum could reveal the molecular eigenstates, and thus conclusively determine the density of coupled states as well as the rotational effects on the decay process. The high resolution spectrum of the $S_1\ 6^1(A_2'')$ state of sym-triazine has been reported previously [11]. However, improvements on the experimental apparatus made it possible to remeasure the spectrum with an improved signal to noise ratio. Furthermore, a home-built pulsed dye amplifier allowed us to measure life times of clearly distinct ensembles of excited rovibronic states. The results of these measurements are also reported here.

5.2 Experimental

The experimental set-up for the measurement of the high resolution spectra has been described elsewhere [13]. Only the relevant features are given here. A continuous expansion of

sym-triazine (Janssen Chimica, purity 98 % and used without further purification) seeded in argon is formed through a nozzle with a diameter of 100 μm . The sym-triazine sample was kept at room temperature (the vapour pressure is 9.6 Torr at 298 K). The backing pressure of the seeding gas was varied between 0.2 and 1 bar. This allowed the recording of the fluorescence spectra at different rotational temperatures. In this way the rotational assignments of the lines in the spectra were verified. In order to reduce the Doppler line width, the molecular beam is skimmed twice (diameter of the skimmers is 1.5 mm) in a differential pumping system.

At a distance of 30 cm from the nozzle orifice the molecular beam is crossed at right angles by the laser beam. Narrow band UV radiation is generated by intracavity frequency doubling in a single frequency ring dye laser (a modified Spectra Physics 380D). About 10-15 mW UV radiation with a band width of 3 MHz was obtained by using a Brewster cut LiIO_3 crystal. For relative frequency measurements two temperature stabilized, sealed off Fabry-Perot interferometers were used, with free spectral ranges of 150 MHz and 75 MHz, respectively. All frequency scans were performed twice with different scan directions. In this way the frequency measurements were corrected for the residual drift in the interferometers. For the absolute frequency calibration the iodine absorption spectrum was recorded simultaneously [14].

The total undispersed fluorescence was collected by two spherical mirrors and imaged on the photocathode of a photomultiplier (EMI 9789QA). Data processing took place with a standard photon counting system (Ortec Brookdeal 5C1) interfaced with a PDP 11/23+ computer [15]. The instrumental line width in the recorded laser induced fluorescence spectra amounts to 12 MHz. This line width is mainly determined by the residual Doppler width of the molecular beam in combination with the spatial sensitivity of the collection optics.

For the magnetic field measurements a pair of coils was mounted. The magnetic field was directed parallel to the laser beam. In this way magnetic fields up to 6 mT could be applied.

For the measurement of the time resolved laser induced fluorescence spectra a mixture of sym-triazine (room temperature) and argon (or helium) was expanded through a pulsed nozzle. The pulsed valve was a modified Bosch fuel injector with a nozzle diameter of 1 mm. At a distance of 30 mm from the nozzle orifice the molecules were excited by the radiation field of a home built Pulsed Dye Amplifier (PDA) [16]. The single frequency output of the continuous wave ring dye laser was amplified in three dye cells, pumped by the frequency doubled output of a Nd:Yag laser (Quantel 681C-10). The output pulses of the PDA were frequency doubled in an angle tuned KDP crystal. In this way tunable radiation around 317 nm with a band width of 250 MHz and a pulse energy of 10 mJ was obtained. This means that the spectral brightness of the pulsed dye laser system is about 10^5 times the spectral brightness of the cw ring dye laser system. Therefore care must be taken to avoid saturation effects. The fluorescence was collected and imaged on the entrance slit of a monochromator (Oriel 77250) to suppress the stray light of the laser. The transmitted light was detected with a photomultiplier (EMI 9863). Further data processing took place by a LeCroy 9400 digital oscilloscope and a SRS 250 boxcar averager.

5.3 Results and Analysis

5.3.1 High resolution experiment

With the high resolution experimental set-up as described, we have measured the laser induced fluorescence spectrum of the S_1 $6^1(^1A_2') \leftarrow S_0(^1A_1')$ vibronic transition in sym-triazine at 317 nm. Parts of the spectrum are shown in figure 5.2 and figure 5.3.

Despite the forbidden nature of the electronic transition and the low quantum yield of the excited vibronic state it was possible to record spectra of good quality. The signal to noise ratio in the spectrum amounts to 500 on the strongest lines. The spectrum shows clearly distinct P-, Q- and R-branches, clusters of lines separated by approximately 13 GHz. This is as expected for a parallel transition with the selection rules $\Delta K = K' - K'' = 0$ and $\Delta J = J' - J'' = 0, \pm 1$ [17] (J', K' are the rotational quantum numbers of the excited state and J'', K'' are the rotational quantum numbers of the ground state). In general each branch up to $J' = 4$ consists of a small number of relatively strong lines. This number corresponds roughly to the number of states with different quantum number K . Besides these strong lines in every branch there are several weak features present. In some branches also some extra relatively strong lines appear (e.g. in the P(4)-branch). Comparison of different transitions to the same upper state clearly reveals that the extra features are due to a perturbation in the excited vibronic state. Starting from the R(4)-branch the spectrum is more and more distorted. We have therefore limited our rotational analysis to the branches P(5)-R(3).

The measured line width of the lines in the spectrum is not constant, but varies between the instrumental line width of 12 MHz up to about 50 MHz. A general tendency is that the strong lines have an instrumental line width of 12 MHz and the weak lines have larger line widths.

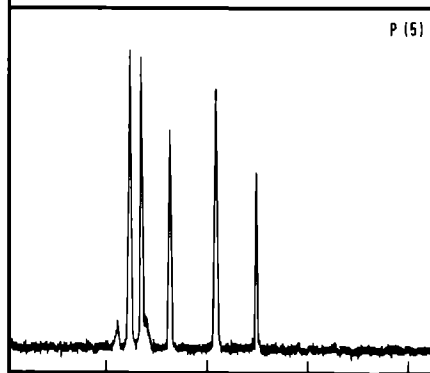
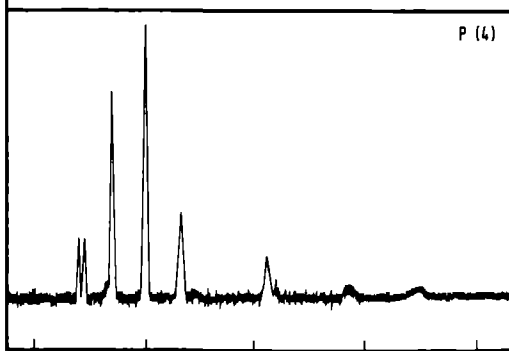
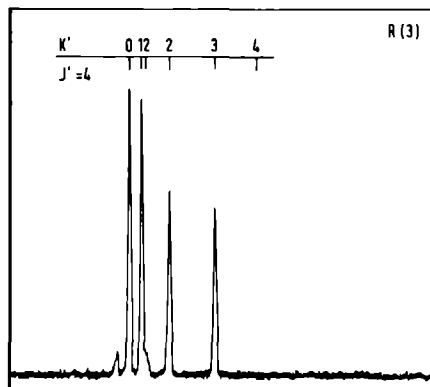
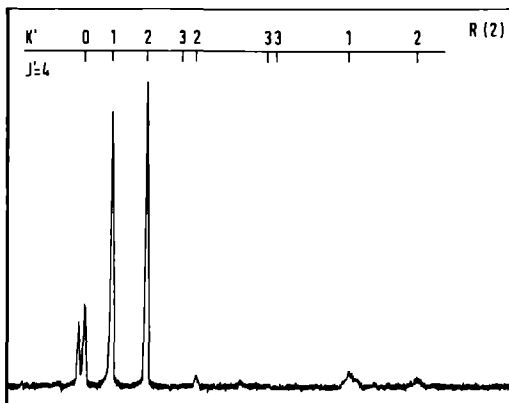
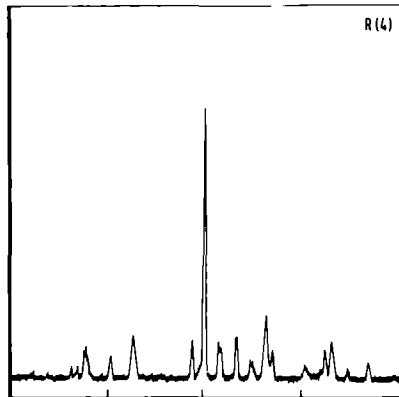
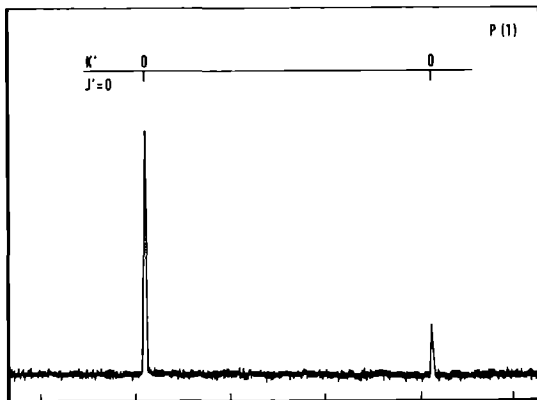
Rotational analysis

It turned out that it was possible to identify most of the lines in the high resolution spectrum. The assignments of the rotational quantum numbers were based on the following principles:

- Identification of transitions to states with $K = J'$

An upper state with the rotational quantum numbers J', K can be accessed via a P-branch transition ($\Delta J = -1$) or via a R-branch transition ($\Delta J = +1$) in case $K < J'$. However, an upper state with $K = J'$ can not be accessed via a R-branch transition. In this case the selection rule $\Delta K = 0$ and $\Delta J = +1$ would require a ground state with $K > J''$. Hence the P-branch contains more lines than the R-branch to the upper state with the same J' and the additional lines in the P-branch are unambiguously assigned as transitions to $K = J'$ states. This method is applied on the combinations R(1)-P(3), R(2)-P(4) and R(3)-P(5).

As the R(0)-branch consists of only one line, it is not possible to apply this method to the R(0)-P(2) combination. However, by means of combination differences between transitions to the same upper state we are able to determine the ground state rotational constant B'' . With the known ground state rotational constant B'' the frequency difference between the



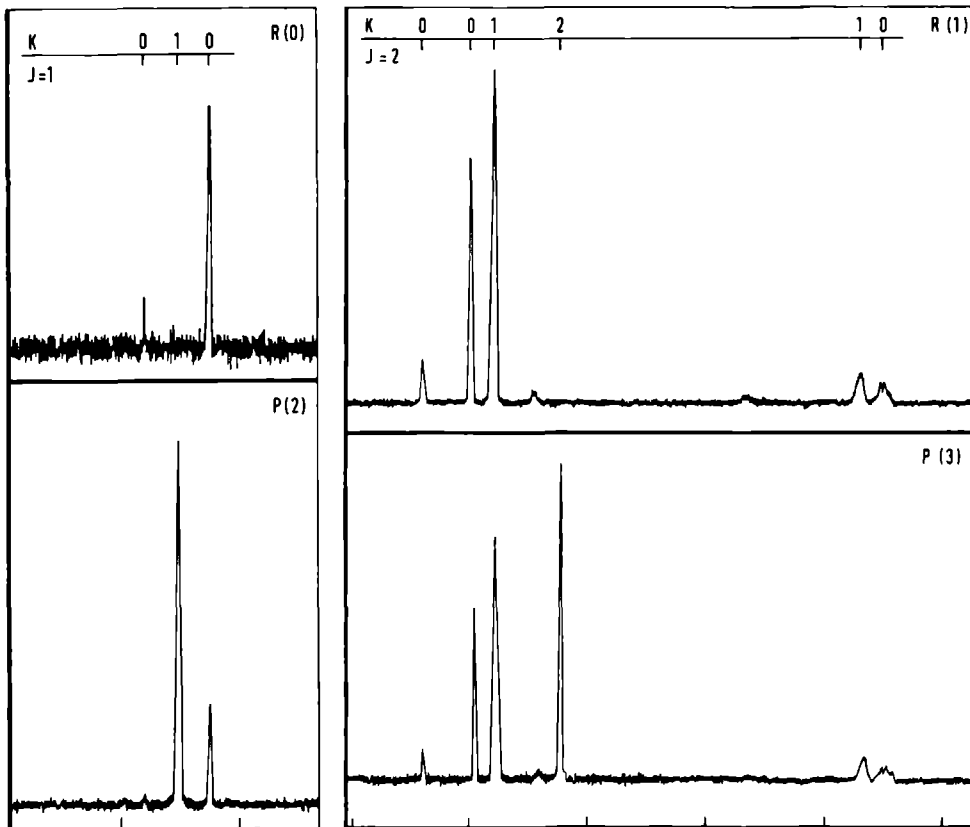


Figure 5 2 The P(5)-P(1) and R(0) R(4) branches of the $S_1 6^1(1A_2'') \leftarrow S_0(1A_1')$ vibronic transition in sym triazine The rotational identification J' , K' of the upper state is given for all assigned lines All spectra were recorded with 10 mW UV radiation The backing pressure of the seeding gas Argon is 160 Torr for the branches P(5) P(3) and R(3)-R(4) and 400 Torr for the branches P(2)-P(1) and R(0) R(2) The frequency is marked every 500 MHz and increases from left to right

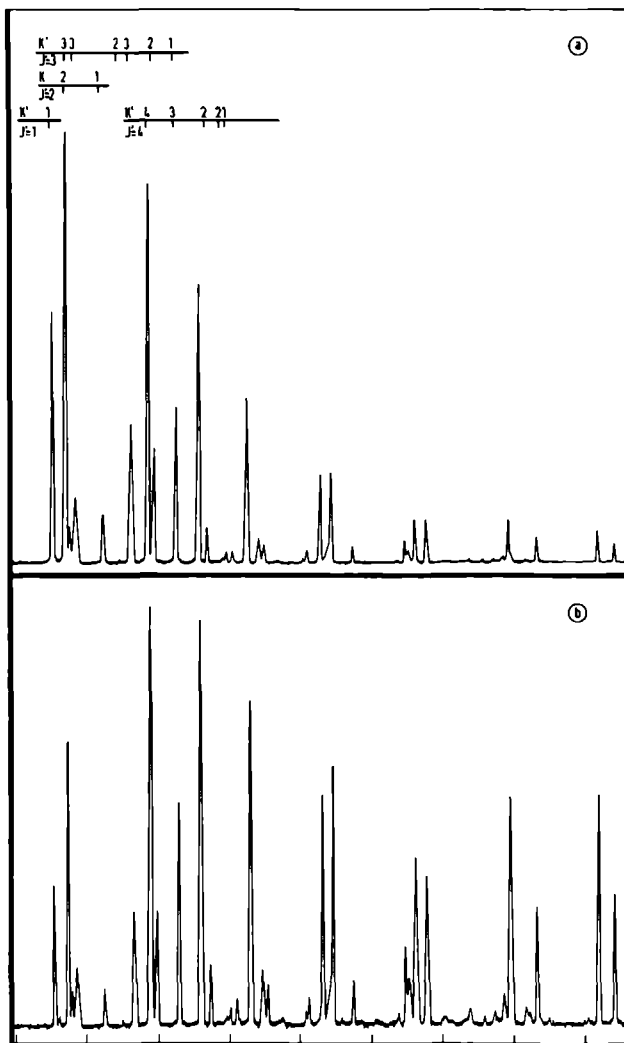


Figure 5.3: The Q-branch of the $S_1 6^1(A_2'') \leftarrow S_0(1A_1')$ vibronic transition in sym-triazine recorded at two different backing pressures of the seeding gas Argon, 400 Torr (a) and 150 Torr (b). The frequency is marked every 500 MHz and increases from left to right. The rotational identification of the lines is given for all assigned lines. The difference in rotational temperature is clearly visible.

R(0) line and the line with $K = 0$ in the P(2)-branch can be calculated. In this way the identification of transitions to states with $K = J'$ is completed.

- Identification of transitions to states with $K \neq J'$

For an asymmetric top molecule it is possible to identify transitions with different quantum number K (where $K = K_{+1}$ (K_{-1}) in the oblate (prolate) symmetric top limit) by a careful comparison of transitions to the same upper state [18]. This method is based on the fact that the asymmetry splitting is dependent on the rotational quantum number J . However, in an oblate symmetric top molecule (like sym-triazine) the rotational energy E_{rot} is given by:

$$E_{rot} = BJ(J+1) + (C-B)K^2 \quad (5.1)$$

In this equation J and K are the rotational quantum numbers and B and C are the rotational constants. In case of a planar symmetric rotor (sym-triazine is planar at least in the vibronic ground state) the relation $B = 2C$ holds. It is therefore clear that in a parallel transition the frequency separation between the lines with different K quantum number is the same in the P-branch, Q-branch and R-branch.

The identification of the lines with different K quantum number is for that reason based on the relative intensities of the lines in the spectrum. The relative intensities of single rotational lines in the spectrum, assuming a Boltzmann distribution in the molecular beam, is given by

$$I = I_0 \cdot (2J'' + 1) \cdot g_n \cdot A_{J''K''} \cdot e^{-E_{rot}/kT_{rot}} \cdot \Phi \quad (5.2)$$

In this equation J'' , K'' are the rotational quantum numbers of the lower state and E_{rot} is the rotational energy of the lower state as given in equation 5.1. The rotational temperature of the molecules in the molecular beam is given by T_{rot} . Under the conditions used in this experiment a rotational temperature of 3 K is expected. The nuclear spin statistical weight factor is denoted by g_n and adopts the values [19]:

$$\begin{array}{lll} K = 0 & \text{and } J \text{ odd} & g_n = 56 \\ K = 0 & \text{and } J \text{ even} & g_n = 20 \\ K = 3p & (p \text{ integer} \neq 0) & g_n = 76 \\ K = 3p \pm 1 & (p \text{ integer} \neq 0) & g_n = 70 \end{array} \quad (5.3)$$

$A_{J''K''}$ are the Hönl-London factors. In case of a parallel band these are given by [17]:

$$\begin{array}{ll} A_{J''K''} = \frac{J''^2 - K''^2}{J''(2J''+1)} & \Delta J = -1 \\ A_{J''K''} = \frac{K''^2}{J''(J''+1)} & \Delta J = 0 \\ A_{J''K''} = \frac{(J''+1)^2 - K''^2}{(J''+1)(2J''+1)} & \Delta J = +1 \end{array} \quad (5.4)$$

I_0 is the normalized intensity and k is the Boltzmann constant. The factor Φ finally takes the perturbations in the upper state into account and denotes the relative excitation and fluorescence efficiency of a certain upper rovibronic state. The presence of this factor makes it impossible to fit the relative intensities in the spectrum to a normal Boltzmann distribution.

Equation 5.2 is correct as long as all nuclear spin functions are allowed to relax to the same rotational ground state. It is well known that nuclear spin is conserved in the cooling process. This means that equation 5.2 holds only within one nuclear spin symmetry group. However, calculations only show a noticeable deviation from equation 5.2 at temperatures below 1 K. With the typical rotational temperature of 3 K in our molecular beam equation 5.2 is assumed to be valid.

For the identification of the rotational quantum numbers in the spectrum of sym-triazine in two manners use has been made of equation 5.2. Although the relative intensities contain an unknown factor Φ it is still possible to compare the intensities of transitions to the same upper state. Especially corresponding lines in the Q-branch and P-branch have completely different Hönl-London factors. Most identifications are based on this principle. Furthermore, all spectra were measured with two different backing pressures (0.2 bar and 0.5 bar) of the seeding gas argon, corresponding to two different rotational temperatures in the molecular beam. This is clearly visible in figure 5.3. In this way the relative intensities of the transitions with different quantum number K are varied within one branch. This method is however less suited for low K values due to the small difference in rotational energy.

With these two methods a nearly complete assignment of the rovibronic transitions in the S_1 $6^1(A_2'') \leftarrow S_0(1A_1')$ band system of sym-triazine was achieved for the P(5)-R(3) branches. The identifications are given in figure 5.2 and figure 5.3. With this identification the rotational constants of sym-triazine in the ground and excited vibronic state could be deduced.

The ground state rotational constant B'' is found by means of combination differences between the P- and R- branches and is given in table 5.1. The error in this rotational constant is determined by the uncertainty in the free spectral range of the used Fabry-Perot interferometers and residual drift effects. The value of the rotational ground state constant derived from our high resolution spectrum is in reasonable agreement with the value $B'' = 6434$ MHz derived from rotational Raman spectroscopy [20].

The rotational constant B' of the vibronic excited state S_1 $6^1(A_2'')$ is more difficult to obtain due to the perturbations in the vibronic excited state. It is immediately clear from the reversed K structure in the P(2)-branch with respect to the other branches (see figure 5.2) that it is not possible to fit the normal symmetric top energy formulas. However, if we assume that the strong lines are more or less randomly shifted from their symmetric top positions by the perturbation, we can try to fit these lines to the normal symmetric top energy formulas. The results are given in table 5.1 and in table 5.2. The observed line frequencies listed in table 5.1 correspond to the strongest lines of the transitions. Exceptions are the line position for the P(1)-branch and the $K' = 3$ line position for the P(3)-branch. In these cases the intensity weighted center of gravity of the lines is used.

The observed frequencies were fitted to the energy expressions of equation 5.1 for both the ground and upper vibronic state. The relation $B = 2C$ was used in both states and the ground state rotational constant B'' was kept fixed. Therefore only the center frequency of the transition ν_0 and the rotational B' constant of the upper state were fitted. The result of the fit is given in table 5.2. The error in the excited state constant is determined by the accuracy of the fit. The error in the center frequency ν_0 of the transition is determined by

Table 5.1: Observed and calculated rovibronic frequencies of the S_1 $6^1(1A_2'')$ \leftarrow $S_0(1A_1')$ vibronic transition in sym-triazine relative to the center frequency $\nu_0 = 31546.70 \text{ cm}^{-1}$.

Observed frequency (MHz)	Calculated frequency (MHz)	obs-calc (MHz)	J''	K''	J'	K'
-65742	-65758	16	5	0	4	0
-65687	-65724	37	5	1	4	1
-65554	-65624	70	5	2	4	2
-65329	-65456	127	5	3	4	3
-65136	-65221	85	5	4	4	4
-52587	-52338	-249	4	0	3	0
-52470	-52304	-166	4	1	3	1
-52313	-52204	-109	4	2	3	2
-52087*	-52036	-51	4	3	3	3
-39179	-39052	-127	3	0	2	0
-39086	-39019	-67	3	1	2	1
-38823	-38919	96	3	2	2	2
-25722	-25900	178	2	0	1	0
-25856	-25867	11	2	1	1	1
-12817*	-12883	66	1	0	0	0
-1288	-1307	19	4	1	4	1
-1152	-1202	55	4	2	4	2
-930	-1039	109	4	3	4	3
-779	-903	124	3	2	3	2
740	-805	65	4	4	4	4
-553	-503	-50	3	3	3	3
-427	-369	-58	2	1	2	1
166	-268	102	2	2	2	2
77	-101	24	1	1	1	1
12938	12749	189	0	0	1	0
25250	25365	-115	1	0	2	0
25343	25398	-55	1	1	2	1
37599	37945	-246	2	0	3	0
37717	37879	-162	2	1	3	1
37874	37979	-105	2	2	3	2
50193	50193	0	3	0	4	0
50247	50226	21	3	1	4	1
50381	50327	54	3	2	4	2
50606	50495	111	3	3	4	3

Lines marked with an asterisk are combinations of different lines in the spectrum. See text.

Table 5.2: Molecular constants of the sym-triazine molecule in the electronic ground state S_0 and the vibronically excited state $S_1 6^1(A_2'')$.

B''	6442 ± 4	MHz
B'	6375 ± 10	MHz
ν_0	31546.70 ± 0.01	cm^{-1}

the combination of the accuracy of the fit and the accuracy in the determination of the peak positions of the iodine absorption lines. It is clear from table 5.1 that the deviations between the observed frequencies and the calculated frequencies are on the order of 100 MHz. This is well above the experimental accuracy. However, if we would take the intensity weighted center of gravity of the lines with the same rotational quantum numbers, the line positions would shift over 200 MHz. Hence we can not expect a more accurate fit.

It is well known that a degenerate vibration in a degenerate electronic state (like the excited vibronic state in sym-triazine) is subjected to a Jahn-Teller distortion. In this case the rotational energy is not longer given by equation 5.1, but [2, 21]:

$$E_{rot} = BJ(J+1) + (C-B)K^2 \pm \sqrt{\frac{1}{4}(\Delta\nu)^2 + 4C^2K^2\zeta_{eff}^2} \quad (5.5)$$

In this equation $\Delta\nu$ is the energy splitting between the A_1'' and A_2'' vibronic states and ζ_{eff} is the effective vibronic angular momentum. This energy expression reduces for very large $\Delta\nu$ to the normal symmetric top energy expression (equation 5.1)). For very small energy splittings $\Delta\nu$ equation 5.5 reduces to:

$$E_{rot} = BJ(J+1) + (C-B)K^2 \pm 2CK\zeta_{eff}^2 \quad (5.6)$$

In case of intermediate energy splittings expansion of equation 5.5 leads again to equation 5.1, but with slightly different rotational constants.

In order to determine any effects of a Jahn-Teller distortion in the excited vibronic state $S_1 6^1(A_2'')$ in sym-triazine, we have fitted the frequencies listed in table 5.1 both to equation 5.1 and to equation 5.6 as the energy expressions for the excited state. However, no significant improvement of the fit is achieved. We conclude therefore that there is no evidence for a Jahn-Teller effect in the high resolution spectrum of the $S_1 6^1(A_2'')$ vibronic state.

Magnetic field measurement

As already stated the high resolution spectrum of the $S_1 6^1(A_2'') \leftarrow S_0(1A_1')$ vibronic transition in sym-triazine appears perturbed. This is evidently shown by the extra lines in the spectrum and the deviations of the observed frequencies with respect to the calculated symmetric rotor line positions. The similarity of the view of the P- and the R-branch to the same upper state clearly reveals that the perturbations occur in the $S_1 6^1(A_2'')$ excited

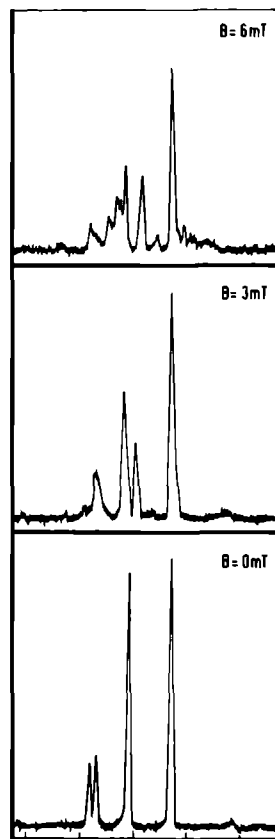


Figure 5.4: Part of the R(2)-branch of the $S_1\ 6^1(1A_2'') \leftarrow S_0(1A_1')$ vibronic transition in sym-triazine recorded with different magnetic fields.

vibronic state. However, the nature of the perturbing state is not known since many singlet and triplet vibronic states are expected in the vicinity of the excited state. We have therefore measured a part of the high resolution spectrum in a magnetic field. In figure 5.4 a part of the R(2)-branch is shown with magnetic field strengths up to 6 mT. It is clearly seen that the view of the spectrum is completely altered at even moderate magnetic fields. This establishes that the perturbing state is a triplet state, similar to the situation in other azabenzene-like pyrimidine and pyrazine. The magnetic field spectra are too complex for a profound analysis.

5.3.2 Life time measurements

It was shown in the high resolution experiments that the line widths varied between 12 MHz (the instrumental line width) up to 50 MHz. The strong lines tend to have the instrumental limited line width, where the weak lines tend to have a broader line width. However, due to the low signal to noise ratio it was not possible to determine conclusively whether the lines were broadened homogeneously or inhomogeneously. Comparison of several scans indicates that the lines are presumably inhomogeneously broadened, i.e. consist of a number of lines overlapping within the instrumental line width.

If the weak lines are broadened homogeneously, a measured line width of 50 MHz would correspond to a life time of 3 nsec for the excited state. As the known life time is about 100 nsec for an excited ensemble of rovibronic states [7, 8, 11] this would indicate that the weak lines exhibit a strong non radiative decay. Hence the quantum yield of the broadened lines is at least a factor 30 less than the quantum yield of the strong lines. This would change the interpretation of the spectrum tremendously. Furthermore, the strong lines are transitions to molecular eigenstates with mainly singlet character where the weak lines are expected to be transitions to molecular eigenstates with mainly triplet character (see Appendix). Hence a homogeneous broadening of the weak lines would indicate a strong non radiative decay of the triplet states. There are models for the intersystem crossing in pyrazine proposed based on such a strong triplet decay rate [22].

To determine conclusively whether the lines are broadened homogeneously or inhomogeneously, we have measured the life times of some selected ensembles of rovibronic states with the pulsed experimental set up as described. The life time measurements were made in the R(1)-branch (see figure 5.2). The R(1)-branch consists of two clusters of lines separated by about 1600 MHz, i.e. five times the instrumental resolution in the pulsed experiment. On the low frequency side three lines are found with a line width between 12-15 MHz. On the high frequency side two relatively weak lines are found with line widths of 40 and 50 MHz.

Figure 5.5 shows the spectrum of the R(1)-branch measured with the pulsed experimental set-up. The spectrum is obtained with a backing pressure of 0.9 bar of the seeding gas argon. In order to avoid saturation effects the output of the pulsed dye amplifier was attenuated and a pulse energy of only 30 μ J was used. The spectrum clearly shows two lines, about 1560 MHz apart and with line widths of 350 MHz. The experimental width of the lines is determined by the combination of the Doppler line width in the molecular beam and the laser band width of the pulsed dye amplifier system. The separation of 1560 MHz of the two lines is in good agreement with the separation of the two groups of lines in the high resolution spectrum. Furthermore, the intensity ratios of the lines measured with the pulsed laser system is within the experimental accuracy in accord with the intensity ratio of the two groups of lines in the high resolution spectrum, taking the line widths into account. As the spectrum of figure 5.5 is measured in a time interval between 40 and 180 nsec after the laser pulse, this clearly proves that the life times of the two lines are comparable. Hence the lines in the high resolution spectrum are broadened inhomogeneously.

We have measured the decay curves after excitation of line ① and after excitation of line ②. The results are given in figure 5.6. The life times τ measured from these decay curves are $\tau = 100 \pm 10$ nsec after excitation of line ① and $\tau = 140 \pm 20$ nsec after excitation of line

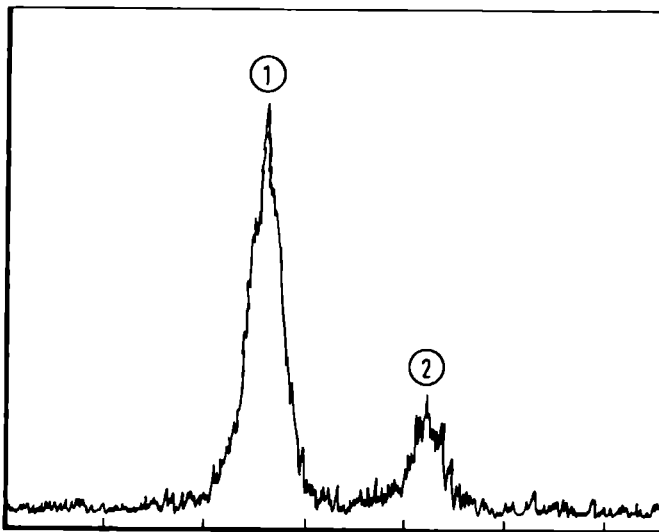


Figure 5.5: The R(1)-branch of the $S_1 6^1(1A_2'') \leftarrow S_0(1A_1')$ vibronic transition in sym-triazine recorded with the narrow band pulsed laser system. The backing pressure of the seeding gas argon was 0.9 bar, and the pulse energy of the laser was $30 \mu\text{J}$. The frequency is marked every 500 MHz and increases from left to right. The fluorescence is collected with a gate between 40 and 180 nsec after the stray light pulse of the laser.

②. These life times are in good agreement with the life times measured previously [7, 8, 11].

These measured life times clearly reveal that the broadening of weak lines in our high resolution spectrum is due to several overlapping transitions. It is also shown that the life times of the two lines are comparable and do not scale with the intensity. This indicates (see the Appendix) that the triplet states coupled to the singlet state have a (non radiative) decay rate comparable to the singlet state decay rate. This result is also found in pyrazine [23] and pyrimidine [24].

5.4 Discussion

It has been shown that the high resolution spectrum of sym-triazine is strongly perturbed. We have identified the perturbing state as a triplet state. The basic principles of a singlet state interacting with a set of triplet states are well known and they are summarized in the Appendix.

We can use the rotational assignment of the high resolution spectrum to calculate the coupling matrix elements V_{st} between the singlet state and the triplet states for every set of

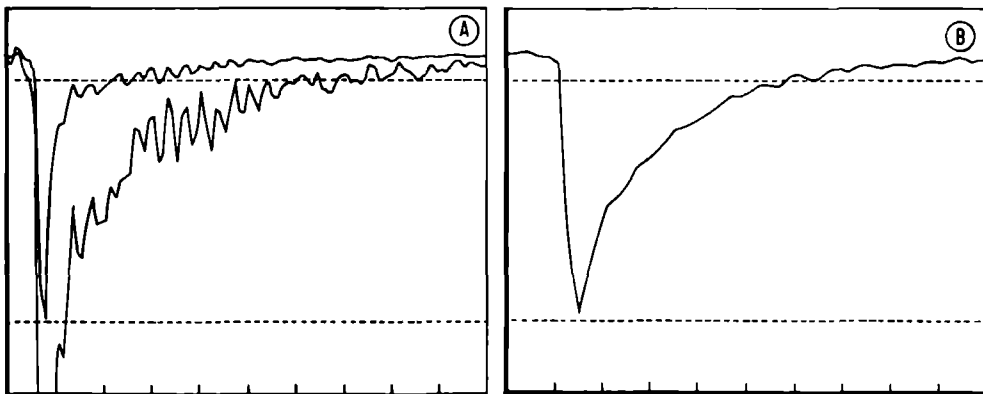


Figure 5.6: Fluorescence decay curves after excitation of the lines in the R(1)-branch. The measured life times are $\tau = 140 \pm 20$ nsec ((A) excitation of the weak line) and $\tau = 100 \pm 10$ nsec ((B) excitation of the strong line). Markers are indicated every 100 nsec in figure (A) and every 50 nsec in figure (B).

lines with the same quantum numbers J', K' . In this the unassigned lines in the spectrum are omitted. The coupling matrix elements are given in table 5.3. It is assumed in the calculation of these matrix elements that the laser induced fluorescence intensities directly reflect the absorption intensities. Furthermore, in the deconvolution procedure the different line widths in the spectrum were not taken into account and the peak heights were used as a measure of the intensities. We can compare the singlet-triplet coupling matrix elements

Table 5.3: Singlet-triplet coupling matrix elements V_{st} in the vibronic excited state $S_1 6^1(A_2'')$ of sym-triazine.

J'	K'	V_{st} (MHz)
0	0	590
1	0	64
2	0	75, 430
2	1	415
3	1	232
3	2	38, 174
3	3	25, 198
4	2	35

deduced for sym-triazine (table 5.3) with the singlet-triplet coupling matrix elements of pyrazine [18, 23] and pyrimidine [24]. We conclude that the average singlet-triplet coupling strength V_{st} in sym-triazine is comparable to the average coupling strength in pyrazine and much larger than the average coupling strength in pyrimidine. However it must be noticed that the much weaker signal to noise ratio in the spectrum of sym-triazine relative to the spectrum of pyrimidine has the tendency to suppress the small coupling matrix elements.

As the coupling strengths in sym-triazine and pyrazine are comparable, we can use the density of lines in the spectrum to estimate the singlet-triplet gap. The density of lines in the spectrum of sym-triazine is about one-third of the density of lines in the spectrum of pyrazine. In this we take the lower signal to noise ratio into account. We can calculate with the formula of Haarhoff [25] the magnitude of the singlet-triplet gap in sym-triazine at which the calculated density of triplet states is one-third of the calculated density of triplet states in pyrazine. Using the ground state vibrational frequencies for both molecules the energy separation between the excited $S_1 6^1(A_2'')$ state in sym-triazine and the interacting triplet state is calculated to be 4800 cm^{-1} . If we assume a factor three as the uncertainty in the estimated density of lines (i.e. the density of lines in the spectrum of sym-triazine is between one and one-tenth of the density of lines in the spectrum of pyrazine) the error in the calculated singlet-triplet gap is 600 cm^{-1} . Hence we conclude that the energy separation between the $S_1 6^1(A_2'')$ state and the triplet state is $4800 \pm 600 \text{ cm}^{-1}$. This result is in excellent agreement with the singlet-triplet gap deduced from the electron spectroscopy [9].

We have shown that most weak lines in the high resolution spectrum are in fact clusters of several overlapping transitions. A same clustering of lines has been observed in pyrazine [18]. The question arises why the triplet states appear in clusters. A possible mechanism assumes that the hyperfine splittings in the triplet state of sym-triazine are on the order of 10 MHz, i.e. observable in our high resolution spectrum. This mechanism is proposed to explain the experimental determined density of states in pyrazine [18]. This would suggest that different hyperfine components of the triplet state interact with different hyperfine components in the singlet state. In this way a broadening of a few MHz of the almost pure singlet molecular eigenstate is expected. Such a broadening is in fact observed in our high resolution spectrum of sym-triazine (e.g. the transition to the $(J', K') = (2, 1)$ excited state). However, it was not possible to measure such an effect for every state as the additional broadening is small compared to the instrumental line width. The nature of the clustering of lines in sym-triazine remains therefore still uncertain.

Acknowledgments

We would like to thank M. Drabbels, M. Ebben and J. Heinze for experimental assistance. This work was financially supported by the Dutch Organisation for Scientific Research (FOM/NWO).

Appendix: A simple theory of molecular eigenstates

The case of a singlet state coupled to a set of triplet states can be described in a simple model with the effective Hamiltonian H :

$$H = H_0 + \sum_t V_{st} \quad (\text{A} - 1)$$

Here the zero order Hamiltonian H_0 is diagonal on the basis formed by the zero order singlet state $|s\rangle$ and the zero order triplet states $\{|t\rangle\}$. The singlet state $|s\rangle$ is coupled to the set of triplet states $\{|t\rangle\}$ by the matrix elements V_{st} .

The effective Hamiltonian H is diagonal on the basis of the molecular eigenstates $|n\rangle$. These molecular eigenstates can be expanded in the zero order states

$$|n\rangle = c_{ns}|s\rangle + c_{nt}|t\rangle \quad (\text{A} - 2)$$

In this way the decay rate γ_n of the molecular eigenstate $|n\rangle$ is given in terms of the zero order singlet decay rate γ_s and the zero order triplet decay rates γ_t by:

$$\gamma_n = |c_{ns}|^2 \cdot \gamma_s + \sum_t |c_{nt}|^2 \cdot \gamma_t \quad (\text{A} - 3)$$

The decay rate γ can have both radiative and non radiative contributions, denoted by γ^r and γ^{nr} respectively.

The zero order singlet state $|s\rangle$ is assumed to carry the oscillator strength from the ground state. Hence the absorption intensity A_n of the molecular eigenstate $|n\rangle$ is proportional to the amount of singlet character in the molecular eigenstate:

$$A_n \propto |c_{ns}|^2 \quad (\text{A} - 4)$$

In a laser induced fluorescence experiment however the intensity I_n of a molecular eigenstate $|n\rangle$ is proportional to the absorption intensity times the quantum yield of the excited state:

$$I_n \propto |c_{ns}|^2 \cdot \frac{\gamma_n^r}{\gamma_n} \quad (\text{A} - 5)$$

It is easy to see that in case the singlet decay rate is much larger than the triplet decay rate ($\gamma_s \gg \gamma_t$) the laser induced fluorescence intensity I_n is proportional to the absorption intensity A_n and also proportional to the decay rate γ_n of the excited state.

In the case that one singlet state is coupled to a set of triplet states it is possible to deduce the positions of the zero order states $|s\rangle$, $\{|t\rangle\}$ and the coupling matrix elements V_{st} via a deconvolution procedure [26]. In this procedure the line positions and the absorption intensities of the molecular eigenstates are required. The situation where one singlet state is present in the spectrum is encountered only in the P(1)- and R(0)-branch in case of a parallel transition. Hence the deconvolution procedure can be applied directly to the lines in the P(1)- and R(0)-branch. In the other branches a rotational assignment is needed and the deconvolution procedure is made for every set of J', K' lines independently. However, in the case that the zero order triplet states are split by hyperfine interactions or magnetic field effects the deconvolution procedure is not valid when applied to the whole set of J', K'

lines. This is caused by the fact that the different components of the triplet states interact with the corresponding (overlapping) components of the singlet state. Therefore effectively more than one singlet state is present. Application of the deconvolution procedure to the whole set of lines in the spectrum leads in this case to an underestimation of the coupling matrix elements V_{st} .

References

- [1] For a review see K.K. Innes, I.G. Ross and W.R. Moomaw, *J. Mol. Spec.* 132 (1988) 492
- [2] G. Herzberg, *Molecular spectra and molecular structure*, Vol 3, (Van Nostrand Company Inc.) 1966
- [3] Y. Udagawa, M. Ito and S. Nagakura, *J. Mol Spec.* 39 (1971) 400
- [4] J.D. Webb, K.M. Swift and E.R. Bernstein, *J. Chem. Phys.* 73 (1980) 4891
- [5] M. Heaven, T. Sears, V.E. Bondybey and T.A. Miller, *J. Chem. Phys.* 75 (1981) 5271
- [6] A.E.W. Knight and C.S. Parmenter, *Chem. Phys.* 43 (1979) 257
- [7] N. Ohta and H. Baba *Chem. Phys. Lett.* 84 (1981) 308 ; N. Ohta and H. Baba *Chem. Phys.* 82 (1983) 41 ; N. Ohta and H. Baba *Chem. Phys. Lett* 106 (1984) 382
- [8] H. Saigusa and E.C. Lim, *J. Chem. Phys.* 78 (1983) 91
- [9] J.B. Pallix and S.D. Colson, *Chem. Phys. Lett.* 119 (1985) 38
- [10] D.A. Wiersma, *Chem. Phys. Lett.* 16 (1972) 517
- [11] B.J. van der Meer, thesis (1985)
- [12] G.W. Robinson *J. Chem. Phys.* 47 (1967) 1967
- [13] W.A. Majewski and W.L. Meerts, *J. Mol. Spectroc.* 104 (1984) 271
- [14] S. Gerstenkorn and P. Luc, *Atlas du spectroscopie d'absorption de la molecul e d'iode* (Centre National de la Recherche Scientifique) 1978 ; S. Gerstenkorn and P. Luc, *Rev. Phys. Appl.* 14 (1979) 791
- [15] W.M. van Herpen, W.L. Meerts and A. Dymanus *J. Chem. Phys.* 87 (1987) 182
- [16] E. Cromwell, T. Trickl, Y.T. Lee and A.H. Kung *Rev. Sci. Instrum.* 60 (1989) 2888
- [17] G. Herzberg, *Molecular spectra and molecular structure*, Vol 2 (Van Nostrand Company Inc.) 1966
- [18] W. Siebrand, W.L. Meerts and D.W. Pratt, *J. Chem. Phys.* 90 (1989) 1313
- [19] A. Weber, *J. Chem. Phys.* 73 (1980) 3952
- [20] J.E. Lancaster and B.P. Stoicheff, *Can. J. Phys.* 34 (1956) 1016
- [21] J.T. Hougen, *J. Chem. Phys.* 38 (1963) 1167
- [22] A. Amirav, *Chem. Phys.* 108 (1986) 403

- [23] W.M. van Herpen, W.L. Meerts, K.E. Drabe and J. Kommandeur, *J. Chem. Phys.* 86 (1987) 4396
- [24] J.A. Konings, W.A. Majewski, Y. Matsumoto, D.W. Pratt and W.L. Meerts, *J. Chem. Phys.* 89 (1988) 1813
- [25] P.C. Haarhoff, *Mol. Phys.* 7 (1963) 101
- [26] W.D. Lawrance and A.E.W. Knight, *J. Phys. Chem.* 89 (1985) 917

Chapter 6

Internal rotation in 1,4-dimethylnaphthalene studied by high resolution laser spectroscopy

Paul Uijt de Haag, Rudie Spooren, Maarten Ebben and W. Leo Meerts

*Fysisch Laboratorium, University of Nijmegen
Toernooiveld, 6525 ED Nijmegen, The Netherlands*

Jon T. Hougen ¹

*Molecular Spectroscopy Division
National Institute of Standards and Technology
Gaithersburg, MD 20899, USA*

Abstract

The high resolution laser induced fluorescence spectrum of the $0_0^0 S_1(^1A_1) \leftarrow S_0(^1A_1)$ in 1,4-dimethylnaphthalene has been studied in a molecular beam. The residual Doppler width of 12 MHz allowed rotational resolution and the study of the effects of the internal rotation of the two methyl groups. All strong lines were assigned and the rotational constants in both the ground and excited electronic states were determined. The internal rotation of the two methyl groups manifests itself in the spectrum by a splitting of each rotational transition into three lines. The splitting of the lines is 40 ± 1 MHz and constant up to $J = 11$ and $K_{+1} = 11$. The intensity ratio of the lines is 1 : 2 : 1 within 10 %. No further splittings were observed in the investigated frequency range.

It is shown that the spectrum is totally explained by the simple model of two independent internal rotors attached to an asymmetric rotor frame. The effect of the interaction of the two rotors is negligible with the present resolution as well as the effect of the interaction between internal rotation and overall rotation. The measured splitting of 40 MHz yields information about the barriers to internal rotation in the two electronic states. With some assumptions a barrier height of $570 \pm 10 \text{ cm}^{-1}$ in the excited S_1 state is deduced.

¹Nederlandse organisatie voor Wetenschappelijk Onderzoek. visiting scientist University of Nijmegen, spring 1988

6.1 Introduction

Hindered internal rotation of a methyl group attached to an asymmetric rotor frame has been a subject of research for some time, and many different techniques have been used [1]. The most well known determinations of barrier shapes and barrier heights stem from microwave spectroscopy. With this method one directly probes the splittings in the energy states due to the hindered rotation. There are however some severe limitations to this method. The molecules must possess a permanent electric dipole moment to exhibit a microwave spectrum, while for symmetric top molecules the selection rule $\Delta K = 0$ hampers the direct observation of the torsional splittings. Therefore symmetric top molecules are studied by other methods like the avoided crossing molecular beam technique [2]. However, for a large molecule the microwave spectrum is rather complex. This makes it difficult to unravel the effect of the internal rotation.

A different approach is the direct observation of the torsional vibrations either by infrared absorption spectroscopy or by Raman spectroscopy. Especially the overtones of the torsional vibration give information about the barrier heights and barrier shapes. These torsional vibrations can also be seen in the fluorescence excitation spectrum of an excited electronic state [3]. By measuring in the dispersed fluorescence spectrum progressions in the ground state torsional vibration information is obtained about the barrier to internal rotation in the electronic ground state. In the same way information about the barrier in the excited electronic state can be deduced from progressions of the torsional vibration in the fluorescence excitation spectrum. It is clear however that high barriers in a large molecule will produce torsional vibrations hardly distinguishable from the normal vibrations. On the other hand, a low barrier will produce spectral features undetectable at medium resolution.

These limitations can be overcome by the measurement of the fluorescence excitation spectrum of an excited electronic state with high resolution in a cold molecular beam. Like in microwave spectroscopy information on the barrier height to internal rotation is deduced from the splittings in the energy states. The strong rotational cooling in the molecular beam reduces the complexity of the electronic spectrum considerably. However, in this method two electronic states are involved and we probe the difference in splittings in the electronic states. As we will show, it is in principle still possible to determine from the high resolution spectrum the barrier heights to internal rotation in both electronic states independently.

We report here the high resolution fluorescence excitation spectrum of the $0_0^0 S_1 \leftarrow S_0$ electronic transition in 1,4-dimethylnaphthalene (1,4-DMN) in a cold molecular beam. In these large molecules the interaction between the two methyl groups takes place via the conjugated electron system of the frame. Up to now little is known about the internal rotation and couplings in such molecules. The fluorescence excitation spectrum at medium resolution performed in a molecular jet is published elsewhere [4]. Previous data on the internal rotation in 1,4-DMN stem from nuclear spin relaxation measurements in the solid state phase [5]. The resulting barrier to internal rotation in the electronic ground state was found to be about 2.2 kcal/mole (770 cm^{-1}). This relatively high barrier allows us to use the high barrier approximation in the analysis of our results.

6.2 Experimental

The experimental set-up is already described elsewhere [6]. Briefly, a molecular beam was formed by a continuous expansion of 1,4-DMN seeded in argon through a nozzle with a diameter of 75 μm . The sample of 1,4-DMN was heated to a temperature of 80 $^{\circ}\text{C}$ in order to achieve enough vapour pressure. The backing pressure of argon was varied between 0.25 - 1.5 bar. In this way the rotational temperature of the ensemble of molecules in the molecular beam was varied. This facilitated the analysis of the spectrum considerably. To reduce the Doppler width, the molecular beam was strongly collimated by two conical skimmers with a diameter of 1.5 mm in a differential pumping system. The molecular beam was chopped at a rate of 16 Hz, allowing phase sensitive detection.

Excitation of the molecules took place 30 cm downstream from the nozzle by the continuous wave radiation field of an intracavity frequency doubled ring dye laser (a modified Spectra Physics 380D). By using an angle tuned LiIO_3 crystal, about 2 mW of single frequency UV radiation was obtained. The laser line width was about 3 MHz and stabilized scans of 120 GHz could be made. The total line width of a single line in the spectrum was 12 MHz and was dominated by the residual Doppler width in the molecular beam. For relative frequency measurements a part of the fundamental laser beam was sent to a sealed off, temperature stabilized Fabry-Perot interferometer. The line width of 12 MHz in the spectrum allowed relative frequency measurements with an accuracy of 3 MHz. However, frequency drift in the interferometer was the dominating source of errors when relative frequencies over 1 GHz were measured. For absolute frequency measurements the absorption spectrum of iodine was recorded simultaneously [7]. The accuracy in the absolute frequency measurement was determined by the line width in the recorded iodine absorption spectrum. This line width was about 850 MHz.

The total undispersed laser induced fluorescence was collected by two spherical mirrors and imaged on the photocathode of a photomultiplier (EMI 9789QA). The signals were processed by a standard photon counting system (Ortec Brookdeal 5C1) interfaced with a PDP 11/23+ computer. Further reduction of the spectra was also done on the computer.

6.3 Results and asymmetric rotor analysis

With the experimental set-up described we have measured the $0_0^0 S_1 \leftarrow S_0$ transition in 1,4-DMN. A part of the spectrum is shown in figure 6.1. The spectrum is obtained with 1 mW of UV radiation and with 0.5 bar backing pressure of the seeding gas argon. The line width in the spectrum is 12 MHz. Due to the high density of spectral lines more than half of the lines in the spectrum were overlapping. The intensities were typical in the order of 5000 counts per second per mW UV radiation.

In a low density region of the spectrum it is easy to see that every rotational transition consists of a group of three lines. This is visible in the insert in figure 6.1. The splitting of these lines is 40 ± 1 MHz and constant at the precision of measurement throughout the whole investigated frequency range. Furthermore no additional splittings were observed in the investigated frequency range. The intensity ratio of the three lines is 1 : 2 : 1 within the accuracy in the measured intensities of 10 %. It seems clear that this splitting is due to the internal rotation of the two methyl groups. Because the splitting of 40 MHz

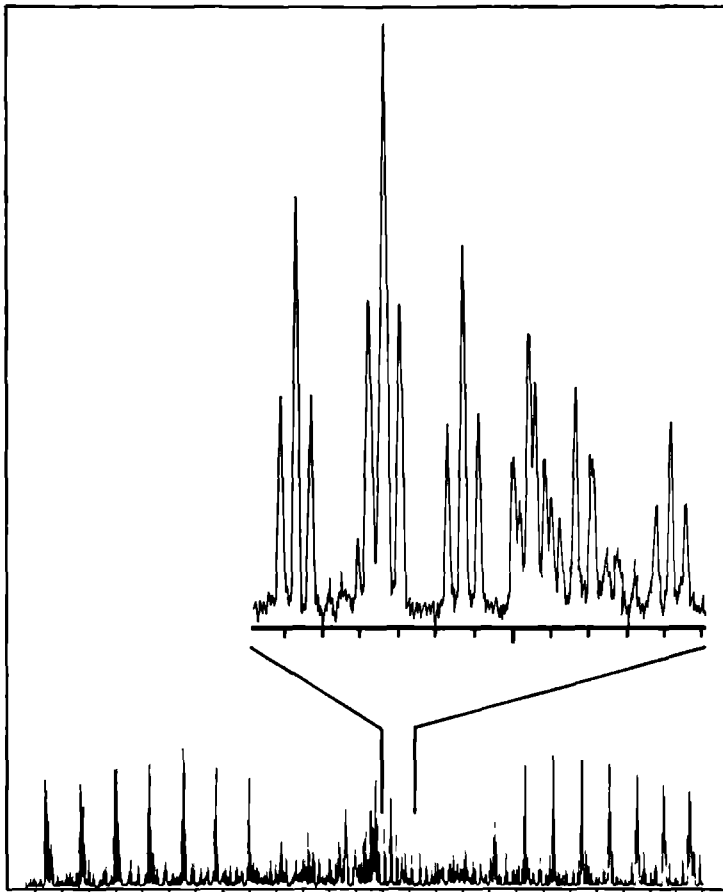


Figure 6.1: Part of the laser induced fluorescence spectrum of the $0_0^0 S_1 \leftarrow S_0$ electronic transition in 1,4-DMN. The frequency is marked every GHz and increases from left to right. The insert gives an exploded view of the spectrum, showing clearly the groups of three lines. Here the frequency is marked every 100 MHz.

is constant over the whole investigated frequency range we chose the central line of each group of three lines for a rotational analysis of the spectrum. The analysis of the rotational spectrum was facilitated by an estimated structure of the 1,4-DMN molecule and the results of earlier performed laser induced fluorescence measurements on the electronic transition in naphthalene [6]. The 1,4-DMN molecule is a near oblate symmetric top with the a-, b- and

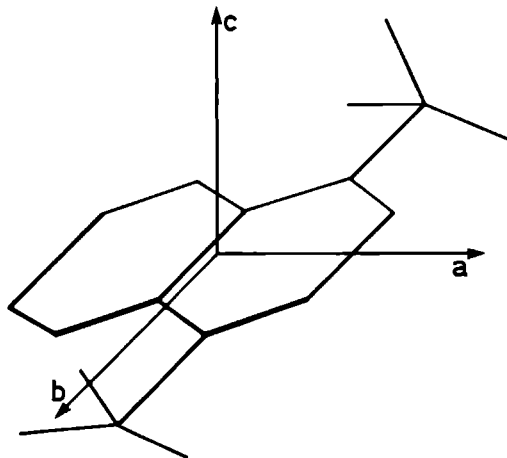


Figure 6.2: The 1,4-dimethylnaphthalene molecule with the principal axis of inertia a , b and c . The measured electronic transition is polarised along the a -axis.

c -axis as indicated in figure 6.2. The results for naphthalene showed that the vibrationless electronic transition is polarised along the a -axis [6]. This axis corresponds to the a -axis in the 1,4-DMN molecule. We started with the assumption that the direction of the transition dipole moment is not changed by the addition of the two methyl groups.

About 200 lines in the central 30 GHz of the spectrum up to $J = 13$ were assigned. In the congested central region of the spectrum use was made of the recordings with different backing pressures. In figure 6.3 a part of these spectra is shown. In this way it was possible to identify unambiguously the transitions where states with low quantum number J were involved. It turned out that it was possible to fit the observed transitions to an asymmetric rotor Hamiltonian. The fit was made to a perpendicular a -type transition, in accordance with the results for naphthalene. This established the symmetry of the excited S_1 state to be 1A_1 in the molecular point group C_{2v} . A least squares fit of the observed transitions to the asymmetric rotor Hamiltonian yielded the effective rotational constants in both ground and excited electronic state. The standard deviation of the fit was 4.6 MHz, well within the experimental line width. The obtained molecular constants are given in table 6.1. The indicated errors are determined by the fit. The dominant source of errors is however the drift of the interferometer. The magnitude of this error can be estimated by comparison of different scans and is about four times the error determined by the fit. The absolute frequency of the transition ν_0 was determined with the use of the iodine absorption spectrum. Here the indicated error is due to the accuracy in the measurement of the iodine absorption line positions.

The relative intensities of single rotational lines, assuming a Boltzmann distribution in

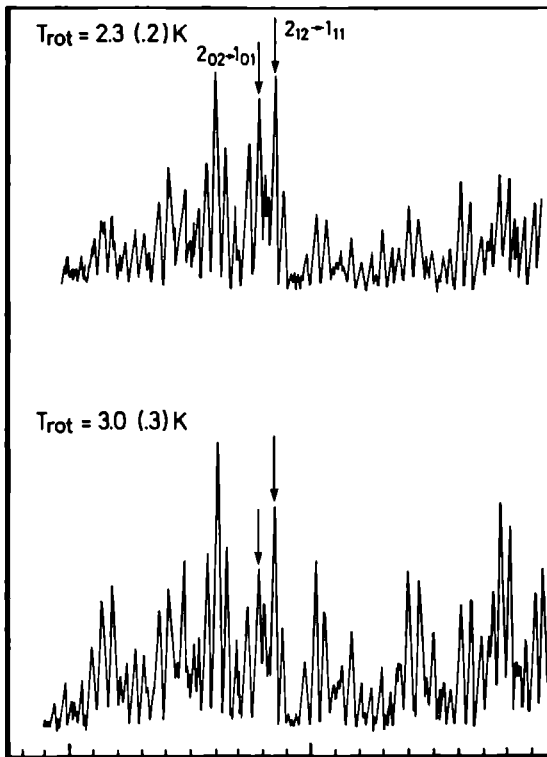


Figure 6.3: Part of the laser induced fluorescence spectra of the $0_0^0 S_1 \leftarrow S_0$ electronic transition at two different rotational temperatures. The frequency is marked every 100 MHz and increases from left to right. Rotational transitions are indicated by $J''_{K''_{-1}K''_{+1}} \rightarrow J'_{K'_{-1}K'_{+1}}$.

the molecular beam, is given by

$$I = I_0 \cdot (2J'' + 1) \cdot g_n \cdot A_{J''K''_{-1}K''_{+1}} \cdot e^{-E(J'', K''_{-1}, K''_{+1})/kT_{rot}} \quad (6.1)$$

In this equation J'', K''_{-1}, K''_{+1} are the rotational quantum numbers of the electronic ground state. g_n are the statistical weights due to the nuclear spin, $A_{J''K''_{-1}K''_{+1}}$ are the Hönl-London factors and $E(J'', K''_{-1}, K''_{+1})$ is the energy of the electronic ground state. T_{rot} is the effective rotational temperature of the molecules in the molecular beam, k is the Boltzmann constant and I_0 is the normalized intensity. Since 1,4-DMN is a near oblate symmetric rotor ($\kappa = 0.78$) we can approximate $A_{J''K''_{-1}K''_{+1}}$ with the corresponding symmetric top expressions [8]. The spin statistical weight g_n for the electronic ground state is derived in the next section. A

Table 6.1: Molecular constants of the 1,4DMN molecule in the electronic ground state S_0 and the excited electronic state S_1 . ($\Delta A = A' - A''$ etc.).

$S_0(^1A_1)$		$S_1(^1A_1)$	
A'' (MHz)	1178.17(14)	ΔA (MHz)	-14.420(64)
B'' (MHz)	1111.92(12)	ΔB (MHz)	-17.046(67)
C'' (MHz)	576.54(10)	ΔC (MHz)	-7.993(27)
ν_0 (cm^{-1})	31491.553(0.004)		

Indicated errors in the effective rotational constants are the standard deviation of the asymmetric rotor fit. Experimental errors in the rotational constants are about four times the indicated errors.

fit of the experimental spectrum to equation 6.1 yielded a rotational temperature of $T_{rot} = 3.0 \pm 0.3$ K. This value is in agreement with previously determined rotational temperatures for similar molecules under comparable conditions.

6.4 Internal rotation analysis

It is well known for a single methyl group connected to an asymmetric rotor frame that every rotational state with quantum numbers J, K_{-1}, K_{+1} in the torsional vibration state characterized by the quantum number v gives rise to three torsion-rotation states. These states are indicated by the quantum number σ . There is one non degenerate A state ($\sigma = 0$) and one degenerate E state ($\sigma = \pm 1$). For $K \geq 1$ (with K the limiting near oblate or near prolate value), this degenerate E state splits up due to the interaction between the overall rotation and the internal rotation [1]. In 1,4-DMN there are two methyl groups attached to an asymmetric rotor frame. Hence there are nine torsion-rotation states associated with every rotational state in the torsional vibration state characterized by v_1, v_2 .

In order to determine the energies of these torsion-rotation states we calculate the different energy terms in the Hamiltonian. In this we use the PAM expressions. The direction of the symmetry axes of the two methyl groups is almost parallel to the b-axis of the molecule (figure 6.2). In the approximate case that the direction of the symmetry axes of the methyl groups is perpendicular to the a-axis of the molecule, the Hamiltonian for the internal rotation in 1,4-DMN can directly be obtained from the internal rotation problem in acetone, and is given to lowest order by [9] :

$$H = H_{rot} + H_{tor} + H_{tt} + H_{rt} \quad (6.2)$$

$$H_{rot} = AP_a^2 + BP_b^2 + CP_c^2 \quad (6.3)$$

$$H_{tor} = Fp_1^2 + \frac{1}{2}V_1(1 - \cos 3\alpha_1) + Fp_2^2 + \frac{1}{2}V_2(1 - \cos 3\alpha_2) \quad (6.4)$$

$$H_{tt} = F'(p_1p_2 + p_2p_1) + V_{12} \cos 3\alpha_1 \cos 3\alpha_2 \quad (6.5)$$

$$H_{rt} = -2\lambda_c CP_c(p_1 + p_2) - 2\lambda_b BP_b(p_1 - p_2) \quad (6.6)$$

In these equations P_i ($i = a, b, c$) is the total angular momentum operator around the corresponding axis of inertia i and p_i ($i = 1, 2$) is the internal angular momentum operator of methyl group i around its symmetry axis. The angle α_i ($i = 1, 2$) is the internal angle of methyl group i . A , B and C are the effective rotational constants. These are in this Hamiltonian connected to the moments of inertia I by

$$A = \frac{\hbar^2}{8\pi^2} \left(\frac{1}{r_a I_a} \right) \quad (6.7)$$

With

$$r_a = 1 - 2 \frac{\lambda_a^2 I_a}{I_a} \quad (6.8)$$

Similar equations hold for B and C , involving r_b , I_b , and λ_b , r_c , I_c , and λ_c . Here I_a is the moment of inertia of a single methyl group and λ_x is the direction cosine of the symmetry axis of a methyl group to the principal axis of inertia x . By symmetry the direction cosines have the same magnitude for the two methyl groups. The approximation that the symmetry axes of the two methyl groups are perpendicular to the a -axis implies that λ_a is equal to zero. Furthermore we have

$$F = \frac{\hbar^2}{16\pi^2 I_a} \left(\frac{1}{r_b} + \frac{1}{r_c} \right) \quad (6.9)$$

$$F' = \frac{\hbar^2}{16\pi^2 I_a} \left(\frac{1}{r_b} - \frac{1}{r_c} \right) \quad (6.10)$$

The barriers for internal rotation for the methyl groups are given by V_1 and V_2 . These are by symmetry equal in 1,4-DMN. The two methyl groups experience a threefold barrier because the naphthalene frame is asymmetric with respect to the position of the two methyl groups. The higher order terms in the barriers are neglected. The coupling between the two methyl groups is given by V_{12} . In our analysis we take $V_{12} = 0$.

The interaction between internal rotation and overall rotation is given by H_{rt} . In 1,4-DMN the two methyl groups are directed almost parallel to the principal b -axis of inertia (figure 6.2). An estimated value for the direction cosines can be obtained from structure calculations on 1-methylnaphthalene [10]. The values derived in this way are $\lambda_a = 0.0026$, $\lambda_b = 1 - 1.6 \cdot 10^{-5}$ and $\lambda_c = 0.0051$. This implies that λ_c , the direction cosine of the methyl groups to the unique c -axis in this near oblate symmetric top is almost equal to zero. However, the term $-2\lambda_c CP_c(p_1 + p_2)$ couples states which are nearly degenerate for high J , K_{+1} values and has therefore a first order effect. Despite the fact that λ_c is very small, we will take this term into account. It has been assumed that λ_c has the same sign for both methyl groups. In the analysis this has no further consequences. The term with λ_b interacts between states with different K_{+1} with the selection rules $\Delta J = 0$ and $\Delta K_{+1} = \pm 1$. The contribution of this term is therefore a second order effect. As mentioned before we have made the approximation $\lambda_a = 0$. In this we neglect terms which are also

second order effects. The magnitudes of these terms are a factor of λ_a/λ_b less than terms with λ_b and hence negligible. This justifies the approximation $\lambda_a = 0$.

We start the analysis by ignoring the interaction term H_{tt} between the two methyl groups and the interaction term H_{rt} between the internal rotation and the overall rotation. In this case the Hamiltonian consists of an asymmetric rotor part H_{rot} and two uncoupled internal rotors. The wave functions and energies are well known in this case [11] :

$$E_{tot} = E(J, K_{-1}, K_{+1}) + E(v_1, \sigma_1) + E(v_2, \sigma_2) \quad (6.11)$$

with the corresponding product wave functions $|JK_{-1}K_{+1}\rangle |v_1\sigma_1\rangle |v_2\sigma_2\rangle$. In this formula $E(J, K_{-1}, K_{+1})$ is the normal asymmetric rotor energy and $E(v_i, \sigma_i)$ is the energy of a single internal rotor. The asymmetric rotor wave functions are denoted by $|JK_{-1}K_{+1}\rangle$ and $|v_i\sigma_i\rangle$ are the single internal rotor wave functions [1].

To determine the electronic spectrum emerging from these energy states, we have to classify these torsion-rotation wave functions according to the symmetry species of the molecular symmetry group. The rigid 1,4-DMN molecule belongs to the C_{2v} molecular point group. In this all carbon atoms are taken in one plane. The torsional tunneling of the two methyl groups contains nine feasible operations. Hence the molecular symmetry group of 1,4-DMN with torsional tunneling contains 36 elements, G_{36} [12]. This is e.g. the molecular symmetry group for acetone with torsional tunneling. With the ground state barrier of 770 cm^{-1} [5], only the ground torsional vibration state is populated in our molecular beam, and we set $v_1 = v_2 = 0$. The wave functions are classified according to the symmetry species of G_{36} , and the nuclear spin statistical weight is calculated. There are 12 hydrogen atoms in the molecule. They give rise to 4096 nuclear spin functions, divided among the symmetry species as

$${}^n\Gamma = 528A_1 + 496A_4 + 136E_1 + 120E_2 + 136E_3 + 120E_4 + 512G$$

In table 6.2 the wave functions are given together with the statistical weights. Every rotational state J, K_{-1}, K_{+1} gives rise to nine rotation-torsion states characterized by the quantum numbers $J, K_{-1}, K_{+1}, \sigma_1, \sigma_2$ ($\sigma_i = 0, \pm 1$). The non degenerate A_i ($i = 1..4$) states have both $\sigma_1 = \sigma_2 = 0$. The fourfold degenerate G states have either σ_1 or σ_2 equal to zero, while the two twofold degenerate E_i ($i = 1..4$) states have both σ_1 and σ_2 unequal to zero.

With equation 6.11 we see that the two E_i states are also degenerate for each rotational state as long as the interaction terms H_{rt} and H_{tt} in the Hamiltonian are neglected. The energy splitting between the A_i and G states equals the energy splitting between the G and the two E_i states. The magnitude is equal to the energy splitting for one internal rotor between the A ($\sigma = 0$) and E ($\sigma = \pm 1$) states. This is exactly as expected from the simple addition of the energy levels of two independent rotors. An energy scheme is depicted in figure 6.4.

The rotation of the methyl groups does not affect the electronic transition dipole moment and the selection rule $\Delta\sigma_1 = \Delta\sigma_2 = 0$ holds for an electronic transition. In the corresponding electronic spectrum we thus expect three lines for each rotational transition. This is indicated in figure 6.4. The splitting of the lines in the spectrum $\Delta E = \Delta E' - \Delta E''$ is thus determined by the difference in splittings in the upper and lower electronic states.

Table 6.2: Symmetry species and statistical weights of the basis wave functions in G_{36} .

K_{-1}	K_{+1}	σ_1	σ_2	symmetry	statistical weight
e	e	0	0	A_1	528
		0	± 1	G	1024
		± 1	0		
		+1	-1	E_1	256
-1	+1				
e	o	0	0	A_3	528
		0	± 1	G	1024
		± 1	0		
		+1	-1	E_2	256
-1	+1				
o	e	0	0	A_4	496
		0	± 1	G	1024
		± 1	0		
		+1	-1	E_2	256
-1	+1				
o	o	0	0	A_2	496
		0	± 1	G	1024
		± 1	0		
		+1	-1	E_1	256
-1	+1				
o	o	0	0	A_2	496
		0	± 1	G	1024
		± 1	0		
		+1	-1	E_1	256
-1	+1				
o	o	0	0	A_2	496
		0	± 1	G	1024
		± 1	0		
		+1	-1	E_1	256
-1	+1				
o	o	0	0	A_2	496
		0	± 1	G	1024
		± 1	0		
		+1	-1	E_1	256
-1	+1				

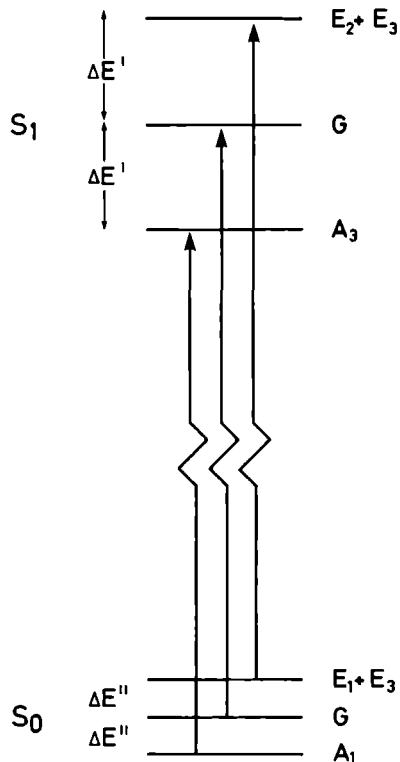


Figure 6.4: Energy level scheme in 1,4-DMN for a transition $(K'_{-1}, K'_{+1}) = (e, o) \leftarrow (K''_{-1}, K''_{+1}) = (e, e)$. The splitting of the lines in the spectrum amounts to $\Delta E' - \Delta E''$.

The intensities of these three lines are given by the nuclear spin statistical weight and are

$$A_1 : G : E_1, E_3 = A_3 : G : E_2, E_3 = 528 : 1024 : 528 \quad \text{for } (K_{-1}, K_{+1}) = (e, e) \text{ or } (e, o)$$

$$A_2 : G : E_1, E_4 = A_4 : G : E_2, E_4 = 496 : 1024 : 496 \quad \text{for } (K_{-1}, K_{+1}) = (o, e) \text{ or } (o, o)$$

Here the degeneracy of the E states is taken into account.

From the splitting of 40 ± 1 MHz between the three lines in the spectrum we can calculate the barrier height V_1 to internal rotation. This results in a barrier height of 570 cm^{-1} in the excited electronic state S_1 . In this we have taken a barrier height to internal rotation of 770 cm^{-1} [5] in the electronic ground state S_0 . However, the splitting of the lines in the electronic spectrum is dominated by the splitting $\Delta E'$ in the excited electronic state : a 10 % error in the ground state barrier height results in only a 1 % error in the excited state barrier height. The uncertainty of 1 MHz in the measured splitting gives an 0.5 %

uncertainty in the calculated barrier height. We conclude therefore that the barrier height to internal rotation for the methyl groups in the excited S_1 electronic state is $570 \pm 10 \text{ cm}^{-1}$.

With these results the contributions of the various neglected interaction terms in the Hamiltonian to the energy can be estimated. Useful basis wave functions for the calculations of the matrix elements are the Wang functions [13] $|S_{JKM\gamma}\rangle$ for the asymmetric rotor part and the product of the single internal rotor wave functions $|v_1\sigma_1\rangle|v_2\sigma_2\rangle$ for the internal rotor part. As mentioned before we take $v_1 = v_2 = 0$. Due to the large energy difference between states with different torsional quantum number v we neglect all matrix elements off diagonal in v . Only states with the same symmetry interact. Therefore we calculate the energy contributions from the interaction terms in the Hamiltonian for each symmetry species apart.

A state with A_i ($i = 1, 4$) symmetry has both $\sigma_1 = \sigma_2 = 0$ (table 6.2). For a single internal rotor the matrix elements are well known [12]:

$$\langle v = 0 \sigma = 0 | p | v = 0 \sigma = 0 \rangle = 0 \quad (6.12)$$

$$\langle v = 0 \sigma = 1 | p | v = 0 \sigma = 1 \rangle = w_{01}^1 \quad (6.13)$$

The matrix elements w_{01}^1 are given for the different barrier heights [12]. With these matrix elements it is clear from equation 6.2- 6.6 that the interaction terms H_{tt} and H_{rt} do not contribute to the energy of a state with $\sigma_1 = \sigma_2 = 0$. Therefore it is possible to fit the A_i states to an asymmetric rotor Hamiltonian. This yields the effective rotational constants in the electronic ground state and the first excited electronic state. In the present asymmetric rotor fit we have used the central line of each group of three, i.e. transitions connecting states with G symmetry. However, the constant splitting in the spectrum between the lines connecting states with G symmetry and the lines connecting states with A_i symmetry guarantees the correctness of our fit.

A state with G symmetry has either $\sigma_1 = 0$ or $\sigma_2 = 0$. Therefore the contribution of H_{tt} equals zero. The interaction term H_{rt} has non zero matrix elements. The contribution of this term to the energy consists of two parts, $-2\lambda_c C P_c(p_1 + p_2)$ and $-2\lambda_b B P_b(p_1 - p_2)$. It is clear that only states with the same σ_1 and σ_2 interact.

The first term, $-2\lambda_c C P_c(p_1 + p_2)$ interacts between the symmetric and antisymmetric Wang functions with the same J and K_{+1} . These two states of G symmetry are for high J and K_{+1} values nearly degenerate. The effect of the Hamiltonian interaction term on the energy states is an additional contribution to the K_{+1} splitting besides the asymmetry splitting. For the (nearly) degenerate rotational states J, K_{+1} this interaction term results in a splitting with magnitude $2\lambda_c C K_{+1} w_{01}^1$. This amounts to $0.002 K_{+1}$ MHz. Here a barrier to internal rotation of $V_1 = 570 \text{ cm}^{-1}$ is taken as deduced for the electronic excited state. In the ground electronic state the splitting will be even less.

It is clear that with the present resolution the K_{+1} splitting due to the interaction of the internal rotation and overall rotation is undetectable in the spectrum of the electronic transition in 1,4-DMN. This is caused by the fact that the symmetry axes of the two methyl groups are nearly perpendicular to the principal c-axis of inertia in this near oblate symmetric top. In similar molecules with comparable barrier heights this splitting can show up in a high resolution laser induced fluorescence spectrum as demonstrated for 1-methylnaphthalene [14]. For lines in the spectrum not split by the asymmetric rotor splitting, the appearance of the splitting linear in the rotational quantum number K

(i.e. K_{+1} for a near oblate symmetric top and K_{-1} for a near prolate symmetric top) gives for a perpendicular band in general the possibility to determine the barrier heights in both electronic states independently. The difference in K -splitting between the transitions $K' = K'' + 1 \leftarrow K''$ and $K' = K'' - 1 \leftarrow K''$ gives directly the barrier to internal rotation in the excited electronic state. In the same way the difference in K -splitting between the transitions $K' \leftarrow K'' = K' + 1$ and $K' \leftarrow K'' = K' - 1$ gives the barrier height in the ground electronic state.

The second interaction term, $-2\lambda_b B P_b(p_1 - p_2)$ couples K_{+1} states with states with $K_{+1} \pm 1$. The energy difference between these states is large compared to the matrix elements. Therefore the contribution to the energy can be calculated by second order perturbation theory. The energy shift for a rotational state characterized by the quantum numbers J and K_{+1} is for $K_{+1} \geq 2$ given by:

$$\Delta E(J, K_{+1}) = \frac{(w_{01}^1 \lambda_b B)^2}{A - B} \left[\frac{J(J+1) - K_{+1}(K_{+1} + 1)}{2K_{+1} + 1} - \frac{J(J+1) - K_{+1}(K_{+1} - 1)}{2K_{+1} - 1} \right] \quad (6.14)$$

Here for simplicity the symmetric rotor energy differences are used. The factor in front is equal to $2 \cdot 10^{-4}$ MHz for a barrier height of 570 cm^{-1} . We again conclude that the effect of this interaction term is too small to show up in the electronic spectrum of 1,4-DMN with the present resolution.

A state with E_i symmetry has in general contributions of both the interaction terms H_{tt} and H_{rt} . The magnitude of the contribution of H_{tt} is $\frac{1}{2} F'(w_{01}^1)^2$. This term is about $7 \cdot 10^{-5}$ MHz in 1,4-DMN with the previous assumptions. The sign of this term is the same for states with E_1 and E_2 symmetry and opposite for states with E_3 and E_4 symmetry. It is clear from table 6.2 that this term in the Hamiltonian splits the two nearly degenerate E_i states and corresponds to the energy difference between geared and anti-geared rotation. The contribution of the term $-2\lambda_c C P_c(p_1 + p_2)$ of H_{rt} equals zero. This is because states with the same E_i symmetry have different J or K_{+1} quantum numbers as seen in table 6.2. The contribution of the second term $-2\lambda_b B P_b(p_1 - p_2)$ of H_{rt} equals zero too. For states with $\sigma_1 = \sigma_2$ the contribution of each rotor is equal in magnitude but with opposite signs, while states with $\sigma_1 = -\sigma_2$ do not interact due to the different symmetry of the Wang functions.

6.5 Summary and conclusion

It has been shown that the $0_0^0 S_1(^1A_1) \leftarrow S_0(^1A_1)$ electronic spectrum of 1,4-DMN can be explained by the simple model of two independent internal rotors attached to an asymmetric rotor frame. The corresponding torsion-rotation wave functions are classified according to the molecular symmetry group G_{36} . There are nine torsion-rotation states connected to every rotational state: a non degenerate A state, a fourfold degenerate G state and two twofold degenerate E_i states. We have fitted the states with G symmetry to an asymmetric rotor Hamiltonian. This results in the effective rotational constants for the upper and lower electronic states listed in table 6.1. Although there is no experimental structure known for 1,4-DMN, a neutron diffraction study on 1,5-DMN [15] allows us to derive a configuration for the 1,4-DMN molecule. The rotational constants calculated from this estimated structure differ by only 0.3 % with the rotational constants derived from the present results. In this

the effective rotational constants are corrected for the internal rotation effect (equation 6.7). This result is well within the 1 % error in the calculated rotational constants, derived from the estimated structure.

The absence of the K_{+1} splitting due to the interaction of overall and internal rotation in our high resolution spectrum makes it impossible to determine both barrier heights separately. However, the results from spin relaxation measurements [5] gives a barrier height of about 770 cm^{-1} in the electronic ground state. With this result and the measured splitting of 40 MHz in the high resolution spectrum the barrier to internal rotation in the electronic excited S_1 state is calculated to be 570 cm^{-1} , with an error of about 10 cm^{-1} .

Acknowledgments

We would like to thank Professor J. Reuss for his stimulating interest. This work is part of the research program of the Stichting voor Fundamenteel Onderzoek der Materie (FOM) and has been made possible by financial support from the Nederlandse Organisatie voor Wetenschappelijk Onderzoek (NWO).

References

- [1] W. Gordy and R.L. Cook, *Microwave Molecular Spectra* (Interscience) 1970
- [2] W.L. Meerts and I. Ozier, *Phys. Rev. Lett.* 41 (1978) 1109
- [3] See, for example, K. Okuyama, T. Hasegawa, M. Ito, and N. Mikami, *J. Phys. Chem.* 88 (1984) 1711
- [4] M. Ebben, R. Spooren, J.J. ter Meulen and W.L. Meerts, *J. Phys. D: Appl. Phys.* 22 (1989) 1549
- [5] K.H. Ladner, D.K. Dalling and D.M. Grant, *J. Phys. Chem.* 80 (1976) 1783
- [6] W.A. Majewski and W.L. Meerts, *J. Mol. Spectrosc.* 104 (1984) 271
- [7] S. Gerstenkorn and P. Luc, *Atlas du spectroscopie d'absorption de la molecule d'iode* (Centre National de la Recherche Scientifique) 1978 ; S. Gerstenkorn and P. Luc, *Rev. Phys. Appl.* 14 (1979) 791
- [8] G. Herzberg, *Molecular spectra and molecular structure, Vol 2* (Van Nostrand Company Inc.) 1966
- [9] J.D. Swalen, and C.C. Costain, *J. Chem Phys.* 31 (1959) 1562
- [10] P. George, C.W. Bock, J.J. Stezowski, T. Hildenbrand, and J.P. Glusker, *J. Phys. Chem.* 92 (1988) 5656
- [11] C.C. Lin, and J.D. Swalen, *Rev. Mod. Phys.* 31 (1959) 841
- [12] P. Bunker, *Molecular symmetry and spectroscopy* (Academic Press) 1979
- [13] S.C. Wang, *Phys. Rev.* 34 (1929) 243
- [14] X.Q. Tan, W.A. Majewski, W.L. Meerts, D.F. Plusquellic and D.W. Pratt, *J. Chem. Phys.* 90 (1989) 2521
- [15] G. Ferraris, D.W. Jones, J. Yerkess and K.D. Bartle, *J. Chem. Soc., Perkin II* (1972) 1628

Samenvatting

De herverdeling van energie in een elektronisch aangeslagen molecuul

In dit proefschrift worden de resultaten beschreven van de experimenten aan middelgrote molekulen als pyrazine, pyrimidine, sym-triazine en naftaleen. De experimentele techniek die hierbij gebruikt werd is de laser geïnduceerde fluorescentie. Door absorptie van een ultraviolet foton wordt een molecuul vanuit de grondtoestand, een singlet S_0 toestand, geëxciteerd naar een elektronisch aangeslagen toestand, de singlet S_1 toestand. Een molecuul kan deze geabsorbeerde energie echter niet vasthouden. Het molecuul valt vanuit de aangeslagen S_1 toestand weer terug naar de grondtoestand S_0 met emissie van een foton. Dit licht dat de molekulen uitzenden na absorptie van licht is de laser geïnduceerde fluorescentie.

In de hier beschreven molekulen blijkt een sterke koppeling te bestaan tussen de aangeslagen singlet S_1 toestand en vibratie toestanden (met dezelfde totale energie) van een andere elektronische toestand, de triplet T_1 toestand. Het effect van deze koppeling is afhankelijk van de dichtheid van deze triplet vibratie toestanden en de sterkte van de koppeling. Wanneer maar weinig triplet toestanden koppelen met de singlet toestand worden er mengtoestanden gevormd met zowel singlet als triplet eigenschappen. Hierdoor zien wij in het spectrum extra lijnen verschijnen. Voorbeelden van een dergelijke koppeling vinden we in de spectra van pyrazine (hoofdstuk 3 en 4), pyrimidine (hoofdstuk 3 en 4) en sym-triazine (hoofdstuk 5).

In het geval dat veel triplet toestanden koppelen met de aangeslagen singlet toestand zijn er geen extra lijnen in het spectrum te zien. De gekoppelde triplet toestanden vormen een soort continuum waarover de elektronische energie van de singlet S_1 toestand verdeeld wordt. De elektronische energie wordt dus binnen het molecuul herverdeeld over de vibratie energie en de elektronische energie van de triplet T_1 toestand. Uiteindelijk wordt ook nu alle geabsorbeerde energie weer uitgezonden door het molecuul. Dit proces is echter voor een triplet toestand vele malen langzamer dan voor een singlet toestand. Daarom worden de triplet toestanden donker genoemd.

We hebben deze processen bestudeerd met behulp van een smalbandige laser en een moleculaire bundel. Door de goede resolutie van deze combinatie hebben we de vibratie en rotatie effecten op deze processen kunnen bestuderen. In hoofdstuk 2 wordt aangetoond dat in het molecuul naftaleen het aantal gekoppelde triplet toestanden erg groot is. Door de molekulen in de bundel vast te vriezen op een koude plaat konden we het licht uit de triplet toestanden detecteren. Gebleken is dat de rotatie van het molecuul geen rol speelt in de singlet-triplet koppeling in naftaleen. Voor pyrimidine en pyrazine werd met dezelfde experimentele methode aangetoond dat een andere koppeling in deze molekulen ook een belangrijke rol speelt: de koppeling tussen de S_1 toestand en vibratie toestanden (met dezelfde totale energie) van de grondtoestand S_0 .

In hoofdstuk 3 en 4 wordt gekeken voor pyrazine en pyrimidine naar de effecten van de vibratie en rotatie van het molecuul op de singlet-triplet koppeling. Hierbij is vooral

gekeken naar het aantal gekoppelde triplet toestanden. Voor pyrimidine blijkt dit aantal goed overeen te stemmen met de theoretische verwachting. In pyrazine daarentegen worden er veel meer toestanden gemeten dan verwacht op grond van een eenvoudige berekening. Dit geeft een indicatie dat in pyrazine een koppeling binnen de triplet toestanden bestaat.

De spectroscopie aan sym-triazine is beschreven in hoofdstuk 5. De spectra tonen aan dat er maar enkele triplet toestanden koppelen. De lijnen in het spektrum vertonen een grote variatie in lijnbreedte. Daarom hebben we ook de levensduur van enkele toestanden gemeten. Het resultaat liet eenduidig zien dat de bredere lijnen in feite groepjes van lijnen zijn.

In hoofdstuk 6 tenslotte wordt de hoge resolutie spectroscopie gebruikt bij de studie naar de interne bewegingen in het molecuul 1,4-dimethylnaftaleen. De twee methyl groepen kunnen min of meer vrij bewegen binnen het molecuul, afhankelijk van de hoeveelheid energie in het molecuul en de elektronische toestand van het molecuul. Met behulp van de laser geïnduceerde fluorescentie techniek werd onderzocht in hoeverre deze twee methyl groepen elkaar beïnvloeden in hun beweging. Binnen de huidige meetnauwkeurigheid werden geen effecten van een interactie tussen de bewegingen van de twee methyl groepen gevonden. Dit resultaat is in goede overeenstemming met de theorie.

Curriculum Vitae

Op 28 december 1960 ben ik geboren te Utrecht. Mijn middelbare school opleiding volgde ik aan het Dominicus College te Nijmegen. Na het behalen van het VWO diploma begon ik met de natuurkunde studie aan de Katholieke Universiteit te Nijmegen. Het kandidaats examen werd behaald in november 1983 en het doctoraal examen in mei 1985. Tijdens de afstudeerperiode was ik werkzaam op de afdeling Vaste Stof Fysika I. Hierna ben ik begonnen met een promotie-onderzoek bij de afdeling Molekuul- en Laserfysika onder begeleiding van Prof. dr. J. Reuss en dr. W.L. Meerts. Resultaten van dit onderzoek staan in dit proefschrift beschreven. Daarnaast werd een bijdrage geleverd aan het onderwijs op de faculteit.

